Coloured Noise in Langevin Simulations of Superparamagnetic Nanoparticles

James McHugh

Doctor of Philosophy

University of York
Physics

October 2016

Abstract

The coloured noise formalism has long formed an important generalisation of the white noise limit assumed in many Langevin equations. The Langevin equation most typically applied to magnetic systems, namely the Landau-Lifshitz-Gilbert (LLG) equation makes use of the white noise approximation. The correct extension of the LLG model to the coloured noise is the Landau-Lifshitz-Miyazaki-Seki pair of Langevin equations. This pair of Langevin equations correctly incorporates a correlated damping term into the equation of motion, constituting a realisation of the Fluctuation-Dissipation theorem for the coloured noise in the magnetic system.

We undertake numerical investigation of the properties of systems of noninteracting magnetic moments evolving under the LLMS model. In particular, we apply the model to superparamagnetic spins. We investigate the escape rate for such spins and find that departure from uncorrelated behaviour occurs as the system time approaches the bath correlation time, and we see that the relevant system time for the superparamagnetic particles is the Larmor precession time at the bottom of the well, leading us to conclude that materials with higher magnetic anisotropy constitute better candidates for the exhibition of non-Markovian properties.

We also model non-Markovian spin dynamics by modifying the commonly used discrete orientation approximation from a Markovian rate equation to a Generalised Master Equation (GME), where the interwell transition rates are promoted to memory kernels. This model makes the qualitative prediction of a frequency-dependent diamagnetic susceptibility, as well as a biexponential decay profile of the magnetisation. The predictions of the GME are compared to the results of LLMS simulations, where we find a similar diamagnetic phase transition and biexponential behaviour.

Contents

Abstract iii

Contents v

List of figures viii

Acknowledgements xi

Declaration xiii

1 Introduction 1

1.1 Magnetism . . . 1

1.2 Types of Magnetism . . . 2

1.3 Superparamagnetism . . . 2

1.4 Stochastic Equations . . . 3

1.5 Coloured Noise . . . 4

2 Langevin & Fokker-Planck Equations 7

2.1 Stochastic Processes . . . 7

2.1.1 Markov Processes . . . 8

2.1.2 Fokker-Planck Equation . . . 8

2.2 Langevin Equations . . . 10

2.2.1 Itô-Stratonovich Dilemma . . . 11

2.2.2 Heun Method . . . 12

2.2.3 Ornstein-Uhlenbeck Noise . . . 13

2.2.4 Separation of Timescales . . . 14

2.2.5 Frequency Spectra of Noise Autocorrelation . . . 15

2.2.6 Fluctuation-Dissipation Theorem . . . 15

2.2.7 Fokker-Planck Equation of the Langevin Equation 18
2.3 Generalized Langevin Equations 20

3 Langevin Spin Dynamics 23
3.1 Landau-Lifshitz-Gilbert 25
3.1.1 Landau-Lifshitz Equation 25
3.1.2 Magnetic Anisotropy 26
3.1.3 Damping 27
3.1.4 Landau-Lifshitz Form of the LLG 28
3.1.5 Thermal Fields 29
3.1.6 Fokker-Planck Equation for the LLG 29
3.1.7 Fokker-Planck Equation: Functional Derivation 31
3.2 Landau-Lifshitz-Miyazaki-Seki 32
3.2.1 Miyazaki-Seki Derivation 32
3.2.2 Spin-only LLMS 34
3.2.3 Mori-Embedding 36
3.3 Simulations 38

4 Debye Susceptibility: The Effect of Coloured Noise 41
4.1 Introduction 41
4.1.1 Linear Response Theory 42
4.1.2 Dispersion & Absorption 44
4.1.3 Kramers-Kronig Relation 45
4.1.4 Fluctuation-Dissipation Theorem 46
4.2 Discrete Orientation Approximation 47
4.2.1 Debye Formulas 48
4.3 Numerical Calculation of AC Susceptibility 50
4.3.1 Statistical Errors 51
4.3.2 Longitudinal Response vs Temperature 53
4.4 AC Susceptibility for non-Markovian Systems 56
4.4.1 Generalised Master Equation 56
4.5 AC Susceptibility in the LLMS 59
4.5.1 Longitudinal Susceptibility vs. Temperature 62
4.5.2 Critical Behaviour 63

4.5.3 Interacting Media 64
4.6 Macrospin Expressions 68
4.6.1 LLMS Fokker-Planck Equation 70
4.6.2 Macrospin Expression for the LLMS 72
4.7 Conclusions 73

5 Thermally-Activated Magnetisation Reversal 75
5.1 Introduction 75
5.1.1 Thermally-Activated Magnetisation Reversal 77
5.1.2 Damping Regimes 78
5.1.2.1 Intermediate-to-High Damping (IHD) 78
5.1.2.2 Very Low Damping (VLD) 79
5.1.2.3 Intermediate Turnover Regime 80
5.2 Escape Time from the LLG 80
5.3 Numerical Simulation 82
5.3.1 System Time τ_s vs. τ_c Characteristic Bath Time 83
5.4 Initial & Switching Conditions 85
5.5 LLMS: Damping Dependence of the Escape Time 88
5.6 Escape time: Temperature Dependence 90
5.7 Angular Variation 93
5.8 Rate Equations for Thermally-Activated Magnetisation Reversal 94
5.8.1 Master Equation 94
5.8.2 Relaxation: Generalised Master Equation 95
5.8.3 Solution from Formal Expression 96
5.8.4 Relaxation 96
5.9 Relaxation: LLMS Simulations 100
5.10 Memory Kernels in the Generalised Master Equation 102
5.10.1 Exponential Waiting Time 102
5.10.2 Biexponential Waiting Time 102
5.11 Conclusions 103

6 Conclusions & Further Work 105
6.1 Non-Markovian Effects in Magnetic Systems 105
6.1.1 System Time & Coloured Noise 105

6.1.2 Superparamagnets & Magnetic Anisotropy 106
6.2 Coloured Noise & Thermal Escape 106
6.3 Generalised Master Equation 107
6.3.1 Frequency-Dependent Diamagnetic Susceptibility 108
6.3.2 Biexponential Decay 108

Abbreviations **111**

Bibliography **111**

List of Figures

3.1 Beahviour of superparamagnetic moments above and below the blocking temperature 24
3.2 Boltzmann Distribution from magnetic Langevin simulations. 38

4.1 Static susceptibility as a Function of reduced barrier height 53
4.2 In-phase Dynamical Susceptibility, χ_1 as a Function of Reduced Barrier Height. 54
4.3 Out-of-phase Dynamical Susceptibility, χ_2 as a Function of Reduced Barrier Height. 55
4.4 Frequency-Dependent Diamagnetic Phase Transition from the GME. 58
4.5 Out-of-phase susceptibility, χ_2 vs Frequency from the GME. 59
4.6 In-Phase Susceptibility vs Frequency from LLMS simulations. 60
4.7 Diamagnetic Phase Transition from LLMS Simulations at low τ_c. 61
4.8 Diamagnetic Phase Transition from LLMS Simulations at higher τ_c. 62
4.9 Out-of-phase susceptibility from LLMS simulations. 63
4.10 χ_1 vs σ from non-Markovian models. 64
4.11 Critical Frequency of Diamagnetic Phase Transition. 65
4.12 Diamagnetic Phase Transition for Interacting Pairs of Spins. 68

5.1 3D Potential Profile for the magnetic escape problem. 78
5.2 Potential energy vs angle for the uniaxial escape problem. 79
5.3 Damping Dependence of Uncorrelated Escape Rate 83
5.4 Escape time with increasing correlation time 84
5.5 Escape Rate for Different Initial Conditions, LLG. 86
5.6 Escape Rate for Different Initial Conditions, LLMS. 88
5.7 Uniaxial escape times with coloured noise. 88

5.8 Escape time for $\Psi = \frac{\pi}{4}$ 90
5.9 Arrhenius behaviour in the LLG 90
5.10 Arrhenius behaviour in the LLMS 91
5.11 Arrhenius behaviour: Comparison of LLG and LLMS models. 92
5.12 Magnetisation profile from the GME for small correlation times. 93
5.13 Individual well populations from the GME for longer correlation times. . . . 98
5.14 Individual well populations from the GME for longer correlation times. . . . 99
5.15 Spin profile from LLMS simulations, small correlation time. 100
5.16 Biexponential behaviour in the LLMS 101

Acknowledgements

I would firstly especially like to thank my supervisor, Professor Roy Chantrell. Without his dedicated support I would never have been able to complete the work undertaken in this thesis, and I am immensely grateful to him for agreeing to be my supervisor.

I would like to thank my family, especially my parents, and all of my friends in Galway, York, London and Leeds, as well as everyone in the Computational Magnetism Group and the the Condensed Matter Group in York.

Declaration

I declare that the research described in this thesis is original work, which I undertook at the University of York, under the supervision of Professor R W Chantrell. This work has not been submitted to any other examining body or for any other degree. Except where stated, all of the work contained within this thesis represents the original contribution of the author.

Chapter 1

Introduction

1.1 MAGNETISM

In principle, the origins of all magnetic phenomena are inherently quantum mechanical. Magnetism provides a direct example of the physical manifestation of the inherent spin of fundamental particles, and of the Pauli exclusion principle, both of which are direct consequences of quantum mechanics. To see how these quantum considerations manifest themselves, we consider a simple two-body system, for example a pair of Hydrogen atoms, featuring a spin degree of freedom

$$\begin{aligned} \Psi(r_1, r_2)_{s_1,s_2} &= \frac{1}{\sqrt{2}}\Big(\psi_1(r_A)\psi_2(r_B) - \psi_2(r_A)\psi_1(r_B)\Big) \\ &\otimes \frac{1}{\sqrt{2}}\Big(|\uparrow\rangle_1|\downarrow\rangle_2 + |\downarrow\rangle_1|\uparrow\rangle_2\Big). \end{aligned} \tag{1.1}$$

The total state of the system is the tensor product of the position-space degrees of freedom and the spin of the Hydrogen nucleus. In general, the ground-state wavefunction may be symmetrical or antisymmetrical with respect to particle interchange. The important point is then, that upon interchanging the labels of the two atoms, the *overall* wavefunction must remain antisymmetric, according to the Pauli principle. The spin part of the wavefunction must compensate for the spatial symmetry of the wavefunction in position space.

Depending on which solution of the Hamiltonian is more energetically favourable, then, we will have two possible states of the system: one in which the atomic spins are aligned, and another in which they are oppositely oriented. It is this very property which is the origin of the exchange interaction in solids, The possibility for the spins to become correlated over multiple spin sites owing to this interaction, which in energetic terms is

extremely strong, is what leads to the formation in some systems systems of a coherent spin direction over the whole sample.

1.2 TYPES OF MAGNETISM

We will briefly mention some of the most common forms of magnetism. *Diamagnetism* is the tendency of a material to be opposed to or repelled by an external magnetic field, and is essentially attributable to the Lorentz force of the magnetic field acting upon the electrons of a material. An important example of diamagnetic behaviour is that exhibited by superconductors, which are said to be perfect or superdiamagnets, under which a superconductor completely expels almost all magnetic flux, leading to a magnetic field which is very close to zero and a susceptibility $\chi_c = -1$.

Ferromagnets are one of the most well-known forms of magnetism. They are materials which consist of numerous aligned magnetic domains with the same spin orientation. Such materials tend to exhibit a macroscopic observable magnetic moment even in the absence of an applied magnetic field, since the presence of a magnetocrystalline anisotropy term causes the spins to preferentially align in a single direction.

Paramagnets are materials in which the constituent atomic magnetic moments tend to align in an applied field, due to the presence of unpaired electrons in the material which are free to do so. An important type of material with a similar behaviour, but on a much larger scale, are the experimentally and technologically relevant *superparamagnetic* particles.

1.3 SUPERPARAMAGNETISM

Superparamagnetic materials consist of nanoscale, single-domain non-interacting magnetic grains, typically dispersed in a non-magnetic medium, with diameters on the order of 10nm. The defining feature of such superparamagnetic materials, is that they are able to sustain a spontaneous magnetic moment across the constituent individual magnetic grains, and it is therefore the case that superparamagnetism is exhibited at temperatures well below the Curie temperature, $T < T_c$, of the grains. [1] [2]

Superparamagnets are integral to many relevant areas of modern technology. Superparamagnetic iron oxide nanoparticles in particular have found applications as nanoscale drug carriers [2] [3]. A particularly promising application of superparamagnetism is in the

medical field, where they form an integral part of the magnetic hyperthermia technique for cancer treatment, which utilises the fact that they can transform electromagnetic energy from an external high-frequency magnetic field into thermodynamical heat, providing an effective method for shrinking cancerous tumours [4] [5] [6].

The properties of magnetic materials have been modeled at a number of different levels, and utilising a variety of distinct approaches, which is in part because the behaviour of magnetic materials varies greatly depending on the time and length-scale we are considering, ranging from the smallest lengthscales where the more fundamental quantum mechanical models are used, providing more fundamental understanding of the physics but coming with a vast simplification of the physics, to first-principles models such as Density Functional Theory (DFT), which solves approximately the ground state properties of a quantum Hamiltonian.

At a larger lengthscale, materials can be modeled using atomistic spin dynamics [7], where we have a large ensemble of atomic magnetic moments interacting via classical forces augmented by a stochastic term which incorporates the action of the thermal bath. At even larger length scales, magnetic properties have been modeled using the continuum micromagnetic approach, this ignores the discrete nature of the underlying atomistic structure of a material and solves for the spatial magnetisation distribution by incorporating magnetic energy terms, such as exchange and Zeeman energy, into the classical Hamiltonian and solving for the magnetisation profile. [8]

1.4 STOCHASTIC EQUATIONS

The superparamagnetic problem is generally approached in a similar fashion to the atomistic case, where we do not typically need to consider interactions between the moments since the spins are usually noninteracting. The incorporation of thermal terms usually results in a *Langevin equation*. This is essentially a classical equation of motion where random thermal forces are included as a type of diffusion process.

Langevin equations are a type of *stochastic differential equation*. Such equations generally, and the Langevin equations in particular form a deep and involved area of study unto themselves, with their formal development and interpretation involving extensive mathematical investigation. Stochastic differential equations have a variety of uses in modeling many real-world systems, including modeling the prices of financial instruments [9], chemical reactions [10], in neurobiology as a means of modeling the firing of individual

neurons [11], in analysing weather patterns [12] and in understanding fMRI data [13], [14].

A key underlying assumption to the implementation of Langevin dynamics is that of the separation of timescales between the system and the thermal bath. The Langevin equation was originally motivated by the need to understand the motion of small particles suspended in a fluid or a gas, which is influenced by the random thermal motion of the surrounding medium. The thermal fluctuations occur on a much shorter timescale than the slow motion of the Brownian particle. [15] This difference in the relevant timescales causes a very large number of particle-gas interactions to occur over the slow timescale of the immersed particle. This results in the *white noise* property for the stochastic term in the differential equation of motion, which essentially amounts to the fact that the stochastic term is completely uncorrelated at different times. However, it is not always possible to assume that this is generally the case. Departure from the white noise limit is generally incorporated by the introduction of a so-called coloured noise..

1.5 COLOURED NOISE

The archetypal example of a coloured noise, and one of the most commonly used and simplest forms, is the Ornstein-Uhlenbeck (OU) process [16] [17]. In contrast to the simple white noise process which is characterised only by its strength, the OU process is described by both the amplitude of the noise and by the characteristic timescale over which the noise is correlated.

Coloured noises have been extensively studied in the context of noisy dynamical flows, and in particular in the context of the Kramers thermal escape problem [18]. An interesting feature of the coloured noise is that increasing correlation time is generally associated with an increase in the escape time of the system. The long-time escape properties are of particular interest to the physics of superparamagnets, where any advancement in our understanding of the escape problem and of the underlying physics is liable to better our understanding of the thermal stability of the spins, and in particular may lead to methods by which we can more easily increase the spin lifetime, or perform manipulation more easily of the spin degree of freedom for just such a bound state.

An important aspect of the incorporation of a coloured noise term into a general Langevin equation is the realisation of the Fluctuation-Dissipation Theorem (FDT) [19] [20]. This amounts to the inclusion of the correct damping term to balance the random thermal forces in equilibrium. Without modifying the damping in this manner, the system

cannot equilibriate. The extension for the case of a magnetic Langevin system has been termed the Landau-Lifshitz-Miyazaki-Seki model. It is an important generalization of the Langevin theoretical approach and is especially timely in relation to recent advances in ultrafast laser processes involving femtosecond laser processes. Following the pioneering work of Beaurepaire et. al. [21] demonstrating ultrafast demagnetization of Ni, more recent work has shown extremely complex and subtle behavior during laser driven processes including thermally driven magnetization switching [22, 23] in which the magnetization is reversed by the action of a thermal pulse in the absence of an applied field. Ultrafast experiments rely on the rapid thermally driven relaxation of the spin system, modelled in refs. [22,23] using a white noise thermostat, however it has been shown [24] that correlated noise can significantly slow down the relaxation processes.

Chapter 2

Langevin & Fokker-Planck Equations

In this chapter we will give a brief introduction to the theory behind the Langevin and Fokker-Planck equations, models which are widely used in physics and are particularly relevant for the study of the properties of superparamagnetic nanoparticles.

2.1 STOCHASTIC PROCESSES

Stochastic processes are an important tool for modelling a wide variety of non-equilibrium statistical processes, and are of particular interest in the study of Langevin equations. A stochastic variable is a quantity X which is defined by the set of possible values x it may have, and the probability distribution to possess a value drawn from that set, $P(X)$. In general the distribution can be continuous or discrete, and adheres to the standard normalisation condition, $\int P(x)dx = 1$. The most general range of stochastic processes are defined with respect to the moments and cumulants of the distribution, although we are generally concerned specifically with the types of processes which are Gaussian, with a continuous probability density [25], [26]

$$P(x) = \frac{1}{2\pi\sigma^2} \exp\Big(- \frac{(x - \mu^2}{2\sigma^2}\Big), \tag{2.1}$$

where μ is the average value and σ is the variance. The moments of a distribution are given as

$$\mu_m = \langle X^n \rangle = \int dx x^m P_x(x). \tag{2.2}$$

The Gaussian distribution is unique in that it is completely specified by its first and

second moments. Gaussian distributions are one of the most commonly used stochastic processes in physical applications, which amounts to assuming that the higher-order cumulants of the relevant process are negligible.

2.1.1 Markov Processes

Markov processes are the subset of stochastic processes which are memory-less in the sense they are local in time. For the one-dimensional process, $(X(t) : t \geq 0)$, we will denote the joint probability distribution as $P(X_1, t_1 : X_2 t_2)$, giving the probability that the process takes the values X_1 at t_1 and X_2 at t_2, while the conditional probability is $P(X_1, t_1|X_2, t_2)$, which is the probability that $X(t_1) = X_1$ given that $X(t_2) = X_2$. A system obeying The *Markov property* follows the constraint that

$$P(X_1, t_1|X_2, t_2 : X_3, t_3) = P(X_1, t_1|X_2, t_2), \tag{2.3}$$

such that the conditional probability to find the process with a certain value at a certain time requires only knowledge of the previous value, but no knowledge is needed of the sequence of transitions taken by the system to reach that state, in other words, it does not depend on the path taken.

2.1.2 Fokker-Planck Equation

The Fokker-Planck equation is the equation for the time-evolution of the probability distribution of a system subject to a stochastic process. It follows for an extremely broad class of processes, in fact any system which satisfies the Markov property. We will make use of the Chapman-Kolmogorov equation, which is the integral form of the Markov property,

$$P(X_3, t_3|X_1, t_1) = \int P(X_3, t_3|X_2, t_2)P(X_2, t_2|X_1, t_1)dx_2. \tag{2.4}$$

Additionally, we assume that the Markov process is time-invariant such that

$$P(X(t_1 + s)) = P(X(t_1)). \tag{2.5}$$

The Fokker-Planck equation follows by taking the integral [27],

$$I = \int_{-\infty}^{\infty} h(Y)\frac{\partial p(Y, t|X)}{\partial t}dY, \tag{2.6}$$

where $h(Y)$ is an arbitrary smooth function with compact support. Rewriting the derivative as the limit,

$$\int_{-\infty}^{\infty} h(Y)\frac{\partial p(Y, t|X)}{\partial t}dY = \lim_{\delta t \to 0}\int_{\infty}^{\infty} h(Y)\Big(\frac{p(Y, t + \Delta t|X) - p(Y, t|X)}{\Delta t}\Big)dY, \tag{2.7}$$

Applying the Chapman-Kolmogorov identity on the right-hand side where Z corresponds to the intermediate state of the stochastic variable,

$$\lim_{\delta t\to 0}\frac{1}{\Delta t}\Big(\int_{\infty}^{\infty}h(Y)\int_{\infty}^{\infty}p(Y,\Delta t|Z)p(Z,t|X)dZdY-\int_{\infty}^{\infty}h(Y)p(Y,t|X)dY\Big), \tag{2.8}$$

Due to the fact that p is a probability density, the integral over all values of the stochastic process is 1, after changing the limits of integration in the first term and allowing T to approach Z in the second term, the right-hand side becomes

$$\lim_{\delta t\to 0}\frac{1}{\Delta t}\Big(\int_{\infty}^{\infty}p(Z,t|X)\int_{\infty}^{\infty}p(Y,\Delta t|Z)(h(Y)-h(Z))dYdZ\Big), \tag{2.9}$$

Since the function $h(Y)$ is smooth we can expand it in a Taylor series around the neighbouring value Z, and the integral becomes

$$\lim_{\delta t\to 0}\frac{1}{\Delta t}\Big(\int_{\infty}^{\infty}p(Z,t|X)\int_{\infty}^{\infty}p(Y,\Delta t|Z)\sum_{n=1}^{\infty}h^{(n)}(Z)\frac{(Y-Z)^2}{n!}\Big)dYdZ. \tag{2.10}$$

This is known as the Kramers-Moyal expansion. Defining the function

$$D^n(Z)=\frac{1}{n!}\frac{1}{\Delta t}\int_{-\infty}^{\infty}(Y-Z)*np(Y,\Delta t|Z)dY, \tag{2.11}$$

so that the integral becomes

$$I=\int_{-\infty}^{\infty}h(Y)\frac{\partial p(Y,t|X)}{\partial t}dY=\int_{-\infty}^{\infty}p(Z,t|X)\sum_{n=1}^{\infty}\sigma^{(n)}(Z)h^{(n)}(Z)dZ, \tag{2.12}$$

by iterated integration of parts and assuming the integrands are equal,

$$\frac{\partial p(X,t)}{\partial t}=\sum_{n=1}^{\infty}-\Big(\frac{\partial}{\partial Z}\Big)[D^{(n)}(Z)p(Z,t|X)]. \tag{2.13}$$

We arrive at the Fokker-Planck by assuming that the higher-order terms in the Kramers-Moyal expansion, $D^{(i)}=0$ for $i\geq 3$, and so we have $D^{(1)}(X)=h(X)$ and $D^{(2)}(X)=\sigma(X)$, the integral becomes to the lowest two orders of the Taylor series

$$\frac{\partial p(X,t)}{\partial t}=\frac{\partial}{\partial X}(h(X)p(X,t))-\frac{\partial^2}{\partial X^2}(\sigma(X)p(X,t)), \tag{2.14}$$

which is the Fokker-Planck equation in the single stochastic variable. For a multidimensional stochastic process, the Fokker-Planck equation is generalised

$$\frac{\partial p(X,t)}{\partial t}=\sum_{i=1}^{N}-\frac{\partial}{\partial X_i}(h(X)p(X,t))-\sum_{i=1}^{N}\sum_{j=1}^{N}\frac{\partial^2}{\partial X_iX_j}(\sigma(X)p(X,t)). \tag{2.15}$$

2.2 LANGEVIN EQUATIONS

Stochastic differential equations in general, and Langevin equations in particular, are invaluable tools used widely in physics and maths, with applications as far ranging as population dynamics, protein kinetics, turbulence, and are widely also used in finance and engineering. Such equations are characterised by the presence of a stochastic term in the expression for the dynamical evolution of the system, a fact which makes their continuity and differentiation properties of particular mathematical interest. [28] [29]

The Langevin equation is a key tool of non-equilibrium statistical mechanics which we will make extensive use of in this work. Under the Langevin approach, the interaction of the slowly-varying system degrees of freedom with a much faster bath are approximated by a stochastic term. The Langevin equation for a system variable x may be written in the form

$$\dot{x} = f(x) + g(x)\eta(t), \tag{2.16}$$

where x is typically some quantity of physical interest, such as the spin of an atomistic magnetic moment or nanoparticle. The derivative is comprised of a deterministic drift component $f(x)$, and a coupling of the dynamical motion to the stochastic process $\eta(t)$ which incorporate the random motion of the thermal bath into the dynamics. The function $g(x)$ couples the variable to the stochastic term, for a general function this results in a *multiplicative* noise, while for the specific case of $g(x)$ constant, the noise is called *additive*.

For a Langevin equation, the stochastic variable $\eta(t)$ is completely defined with reference to it's second moment while the ensemble average is 0,

$$\langle \eta(t) \rangle = 0 \qquad \langle \eta(t)\eta(s) = 2D\delta(t-s), \tag{2.17}$$

hence the process is *Gaussian*, in the sense that it is completely specified by it's second moment, and *stationary* since the joint probability distribution does not change when the process is shifted in time.

The Langevin equation is essentially a consequence of the central limit theorem, according to which the average of any suitably large number of independent, identically-distributed numbers approaches a Gaussian distribution. On the timescale of the resolved subsystem, the effect of the faster bath degrees of freedom approaches a Gaussian due to the number of interactions that occur on the much slower timescale of the system. Knowledge of the detailed dynamics of the fast degrees of freedom is then unnecessary and we

only need knowledge of the variance of the thermal noise, D, which is generally inferred by thermal considerations.

Formally the noise term appearing in the Langevin equation is the derivative of the continuous-time Wiener process, as the integral of the Wiener process over a finite time interval are independent and Gaussian distributed, We may generate an appropriate white noise with the correct autocorrelation function by using the expression

$$\eta = \sqrt{D}\Gamma, \tag{2.18}$$

where Γ are Gaussian-distributed numbers of mean zero and variance 1, which may be generated by a number of different numerical algorithms such as the Box-Muller technique.

2.2.1 Itô-Stratonovich Dilemma

In order to solve for the time-dependence of the system variable $x(t)$ in the Langevin equation it is necessary that we perform integration over the stochastic partial differential equation [30]

$$x(t+\tau) = x(t) + \int_t^{t+\tau} f(x(t'))dt' + \int_t^{t+\tau} g(x(t'))\eta(t')dt', \tag{2.19}$$

It is not sufficient to perform such integration using the standard Riemann integral of a function over a finite interval, owing to the presence of the integral over the white noise tern, which differs in that the end result of such an integration depends crucially on the assumptions made about the interval over which we perform said integration at intermediate steps, a problem which is called the *Itô-Stratonovich dilemma*. We first consider the noise integral

$$W(t) = \int_0^t \eta(t')dt', \tag{2.20}$$

which is the non-stationary Wiener process with moments which are trivially related to the noise autocorrelation, $\langle W(t)\rangle = 0$, $\langle W(t)^2\rangle = 2Dt$. The increments of the Wiener process are Gaussian such that

$$\omega(\tau) = W(t+\tau) - W(t) = \int_t^{t+\tau} \eta(t')dt', \tag{2.21}$$

with $dW = \dot{W}dt = \eta(t)dt$ being the Wiener process. Rewriting the integral in terms of the Wiener process as the Stieltjes integral,

$$x(t+\tau) = x(t) + \int_t^{t+\tau} f(x(t'))dt' + \int_t^{t+\tau} g(x(t'))dW(t'), \tag{2.22}$$

where $dW = \dot{W}t = \eta(t)dt$.

If both the diffusion term $g(x,t)$ and the noise $dW(t)$ were continuous, then in the limit of small Δt, the right-hand side would be $f(x,t)dW(t)dt'$. However, the noise term is by definition discontinuous, and there is an ambiguity in choosing the time at which to evaluate the diffusion function. It is in choosing an intervening time to evaluate the function that we choose an interpretation for the stochastic integral. We may generally write the integral over the Wiener process as

$$A = \int_0^T \mathbf{\Phi}\Big[\omega(\tau'), \tau'\Big] dW(\tau'), \tag{2.23}$$

The Itô interpretation explicitly evaluates this integral as

$$A_I = \lim_{\Delta \to 0} \sum_{i=0}^{N-1} \mathbf{\Phi}\Big[\omega(\tau_i), \tau_i\Big], \Big[\omega(\tau_{i+1}) - \omega(\tau_i)\Big], \tag{2.24}$$

where $\Delta = \max(\tau_{i+1} - \tau_i)$. The multiplicative part of the integral is evaluated at τ_i, while the increment of the Wiener process is independent of this diffusive function. Stratonovich defined the integral as the limit of a different sum as [31]

$$A_S = \lim_{\Delta \to 0} \sum_{i=0}^{N-1} \mathbf{\Phi}\Big[\frac{\omega(\tau_i) + \omega(\tau_{i+1}}{2}, \frac{\tau_i + \tau_{i+1}}{2}\Big]\Big[\omega(\tau_{i+1}) - \omega(\tau_i)\Big]. \tag{2.25}$$

In the Stratonovich interpretation, the Φ function is evaluated in a symmetrical way between the interval (τ_i, τ_{i+1}). We see, then, that the Itô interpretation is "non-anticipating", since the function is evaluated only at the beginning of the interval. This generally leads to the implication that the variable being integrated and the stochastic term are uncorrelated, $\langle x(t)\eta(t)\rangle = 0$. Under the Stratonovich interpretation, this is not the case and $\langle x(t)\eta(t)\rangle \neq 0$. This can be seen as the more realistic physical assumption, since the white noises terms occurring in a Langevin equation are not idealised white noises but are the limit of a physical process with some correlation time. The mathematical process of taking such a limit will generally imply a correlation between the variable x and η.

2.2.2 Heun Method

We will employ the Heun method as the numerical algorithm by which we evaluate stochastic PDE's in the remainder of this work. The Heun method is a predictor-corrector method which invokes the Stratonovich interpretation and so is generally preferable for physical applications. The method first evaluates the integral using a simple Euler step, which is

then fed back into the initial state to make a more accurate integration. The scheme takes the form [32] [33]

$$x(t+\Delta t) = x(t) + \frac{1}{2}\left[\frac{\partial x(t)}{\partial t} + \frac{\partial x_e(t+\Delta t)}{\partial t}\right]\Delta t, \tag{2.26}$$

$$x_e(t+\Delta t) = x(t) + \frac{\partial x(t)}{\partial t}\Delta t. \tag{2.27}$$

When implementing this method in magnetic Langevin equations, the spin-dependent effective fields must be updated for the prediction and correction steps, while the stochastic term for both steps remains the same as we are integrating over the same instance of the Wiener process.. Additionally, the scheme is non-conservative in the spin, which means that the spin magnitude must be renormalised at each step in the simulation. The Heun method also has the advantage that it treats the stochastic and deterministic parts of the stochastic PDE in an essentially symmetric fashion, facilitating the implementation of the algorithm.

2.2.3 Ornstein-Uhlenbeck Noise

The simplest generalisation of the white noise limit to coloured noise is the *Ornstein-Uhlenbeck* process. For the white noise process with autocorrelation function $\langle \xi(t)\xi(s)\rangle = 2D\delta(t-s)$, the corresponding Ornstein-Uhlenbeck process introduces a single timescale over which the noise is exponentially correlated with its values at earlier times. The noise is then itself driven by a Langevin equation [34] [35]

$$\frac{d\xi(t)}{dt} = \frac{1}{\tau_c}\Big(-\xi(t) + \sqrt{2D}\Gamma(t)\Big), \tag{2.28}$$

where $\Gamma(t)$ is drawn from a Gaussian distribution of unit variance, and is again interpreted as the time-derivative of the scalar Wiener process. The solutions to this equation take the form

$$\xi(t) = \frac{\sqrt{2D}}{\tau_c}\int_{-\infty}^{t} dt' K(t-t')\Gamma(t'), \tag{2.29}$$

where $K(t) = e^{-t/\tau_c}$. We may solve for the autocorrelation of this new noise explicitly

$$\langle \xi(t)\xi(s)\rangle = \frac{2D}{\tau_c^2}\int_{-\infty}^{t} dt' \int_{-\infty}^{s} ds' K(t-t')K(s-s')\langle \Gamma(t')\Gamma(s')\rangle. \tag{2.30}$$

As $\Gamma(t)$ is itself a Gaussian process of unit variance, it has an autocorrelation of the form $\langle \Gamma(t)\Gamma(s)\rangle = \delta(t-s)$, inserting this and first performing the integral over t' as this is assumed to be the earlier time, we get

$$\langle \xi(t)\xi(s)\rangle = \frac{2D}{\tau_c^2} e^{-(t+s)/\tau_c}\int_{-\infty}^{s} ds' e^{2s'/\tau_c}, \tag{2.31}$$

upon evaluating the second integral gives us a factor of $\frac{\tau_c}{2}$, finally giving the autocorrelation

$$\langle \xi(t)\xi(s)\rangle = \frac{D}{\tau_c} e^{-(t-s)/\tau_c}, \tag{2.32}$$

Additionally, we may take the zero correlation time limit of this correlation function to see

$$\lim_{\tau_c \to 0} \left(\frac{D}{\tau_c} e^{-(t-s)/\tau_c} \right) = 2D\delta(t-s), \tag{2.33}$$

due to the fact that $\frac{1}{2\tau_c} e^{-t/\tau_c} = \delta(t)$ as τ_c approaches 0. The overall picture for the Ornstein-Uhlenbeck process is then clear. To insert simple correlated noise into a Langevin equation, we replace the noise term by another variable which is itself the solution of a Langevin equation of the form equation 2.28. This Langevin equation is driven by a white noise of the same magnitude as the original white noise. It has an autocorrelation as in equation 2.32, and the zero correlation time limit of this is, again, itself the original delta-correlated white noise.

2.2.4 Separation of Timescales

The important factor in considering whether the white noise approximation is valid is the ratio of the timescales of the system and the bath, which allows us to directly verify whether the timescales are genuinely widely separated. To quantify this we must make some estimate of the timescale of the system dynamics. To illustrate this, we consider the motion of a damped simple 1-D oscillator under the influence of a potential $U(x)$ [36].

$$m\ddot{x} + m\gamma\dot{x} = -\frac{dU(x)}{dx} + \xi(x). \tag{2.34}$$

Dividing through by $m\gamma$ and taking the limit of large γ so the inertial part disappears, this takes the form

$$\dot{x} = \frac{1}{\tau_s}(-\frac{dU(x)}{dx} + \xi(x)), \tag{2.35}$$

where we now have a characteristic system time $\tau_s = \frac{1}{m\gamma}$. Rescaling the time variable $t' = t/\tau_s$, the autocorrelation for the Ornstein-Uhlenbeck noise becomes

$$\langle \xi(t')\xi(t'')\rangle = \frac{\tau_s}{\tau_n} D e^{-(t'-t'')\frac{\tau_s}{\tau_n}}. \tag{2.36}$$

Defining the dimensionless variable $\tau = \tau_n/\tau_s$, this becomes simply

$$\langle \xi(t)\xi(t')\rangle = \frac{D}{\tau} e^{-(t-t')/\tau}. \tag{2.37}$$

We observe that in this simple case as $\tau \to 0$, i.e., $\tau_s > \tau_n$ the uncorrelated white noise behaviour is recovered, while in the limit $\tau \to \infty$ the Ornstein-Uhlenbeck process produces distinct behaviour to the white noise case.

The type of Langevin equation described above originated in the study of Brownian motion, the motion of small particles suspended in a liquid or gas. In such systems, the characteristic frequency of the motion of the suspended particle is assumed to be much lower than that of the particles comprising the bath. This approximation amounts to the assumption of the separation of timescales.

2.2.5 Frequency Spectra of Noise Autocorrelation

The Fourier transform of the white noise autocorrelation, Eq. **??** is given by

$$F(\omega) = \int d\tau \langle \xi(t)\xi(t+\tau)\rangle \exp(i\omega\tau) \tag{2.38}$$

$$= D\int d\tau \delta(\tau)\exp(i\omega\tau) = 2D. \tag{2.39}$$

There is no frequency dependence for the white noise. In contrast, if we take a coloured noise with $\langle \xi(t)\xi(t+\tau)\rangle = \frac{D}{\tau_c}\exp(-\frac{t}{\tau_c})$, with a corresponding Fourier transform

$$F(\omega) = \frac{D\tau^{-2}}{\omega^2 + \tau_c^{-2}}. \tag{2.40}$$

This is a Lorentzian function which preferentially occupies lower frequencies, proportional to the correlation time. Processes such as the Ornstein-Uhlenbeck noise are labelled coloured noise processes, as they do not occupy all frequencies equally, in analogy to the spectrum of visible light.

Hence, we may think of the white noise term used in Langevin equations as the small correlation time limit of a the Ornstein-Uhlenbeck process. Since the white noise approximation relies on the wide separation of the system and bath timescales, it is necessary to explicitly incorporate the effects of coloured noise in the instance that the system is now slow on the timescale of the bath.

2.2.6 Fluctuation-Dissipation Theorem

To see how Langevin equations are implemented in non-equilibrium systems, we will consider one such simple system, and in addition to this we will relate the statistical properties of the system to its equilibrium properties, in a result which is termed the fluctuation-dissipation theorem [36]. We will consider the one-dimensional motion of a spherical

particle in a fluid medium of viscosity η. Newton's equation of motion for the particle is

$$m\frac{dv}{dt} = F_{total}(t), \tag{2.41}$$

and $F_{total}(t)$ is the total force the particle is subjected to at the time t. This force is, in principle, known if all of the positions and momenta of the surrounding medium are known. However, even if such an approach were possible it is generally not feasible to simulate such a large system computationally The force the particle is subjected to is composed of both a frictional component, which opposes the direction of motion of the particle and impedes it with a magnitude that is proportional to the velocity of the particle as well as a fluctuating thermal component. The friction coefficient is related to the viscosity of the medium via Stokes' Law, $\xi = 6\pi\eta a$. The equation of motion for the particle subject to this friction is then

$$m\frac{dv}{dt} = -\xi v. \tag{2.42}$$

This is a simple, linear first-order differential equation with trivial solution

$$v(t) = e^{-\xi/m}v(0) \tag{2.43}$$

A particle immersed in a viscous medium would eventually have its velocity drop to 0 in the long-time limit if the dissipative force were the only force it was subjected to. However, this is not actually the case because the mean square velocity at thermal equilibrium is non-zero, $\langle v^2\rangle_{eq} = k_BT/m$, and so we must consider an extra force in addition to the damping term. The correct term to add to account for the non-zero velocity at equilibrium is the fluctuating thermal term, giving an equation of motion

$$m\frac{dv}{dt} = -\xi v + F(t). \tag{2.44}$$

This is the Langevin equation for the particle. The total force originating from the interaction with the bath has been partitioned into a thermal part and a dissipative response part. The moments of the force dictate that it is a white noise

$$\langle F(t)\rangle = 0, \tag{2.45}$$

$$\langle F(t)F(s)\rangle = 2D\delta(t-s), \tag{2.46}$$

hence there is no net velocity subjected by the medium to the particle, yet the magnitude of the force varies in such a way as to come into equilibrium with the dissipative part.

In the presence of the thermal force, the solution for the particle velocity versus time takes the form

$$v(t) = e^{-\xi t/m} v(0) + \int_0^t dt' e^{-\xi(t-s)/m} F(s)/m, \tag{2.47}$$

We know that at equilibrium, the mean-square velocity is constrained by the temperature, and does not decay to zero. Hence, the parts of the integral on the RHS must meet this criteria when we evaluate the mean-square velocity from this expression. The decaying dissipative part contributes a term $e^{-2\xi t/m} v(0)^2$ which tends to zero at long times. The first noise term contributes

$$2v(0)e^{-\xi t/m} \int_0^t ds e^{-\xi(t-s)/m} F(t)/m. \tag{2.48}$$

This term involves taking an average in the limit of long time of the thermal noise, which is equivalent to the first moment which we have defined to be 0. The final term involving two thermal fields is

$$\int_0^t dt' e^{-\xi(t-t')/m} F(t')/m \int_0^s ds' e^{-\xi(s-s')/m} F(s')/m. \tag{2.49}$$

This term involves the average over time of the product of the noise term, which we may replace with the explicit value of the autocorrelation. Hence, this may be reduced to

$$\int_0^t dt' e^{-\xi(t-t')/m} \int_0^s ds' e^{-\xi(s-s')/m} 2D\delta(t'-s')/m^2. \tag{2.50}$$

Performing the integration over one time dummy variable results in a change of variables, hence the expression for the mean square velocity becomes

$$\langle v(t)^2 \rangle = e^{-2\xi t} v(0)^2 + \frac{D}{\xi m}(1 - e^{-2\xi t/m}). \tag{2.51}$$

In the long-time limit, the exponential terms tend to zero and the rms velocity approaches the equilibrium value, $D/\xi m$. This fact directly leads to the *fluctuation-dissipation theorem*,

$$D = \xi k_B T, \tag{2.52}$$

For the case of a particle in a viscous medium, the fluctuation-dissipation theorem relates the strength of the fluctuating random noise force to the magnitude of the dissipation. This relationship holds more generally for systems described by Langevin equations, and simply amounts to an equilibrium condition, whereby at a specified temperature the dissipative contributions which would drive the system to a completely dead state must be matched in magnitude by the thermal forces which keep the system alive.

2.2.7 Fokker-Planck Equation of the Langevin Equation

The foundation of much of non-equilibrium statistical mechanics is the Liouville equation, and the Fokker-Planck equation for a Langevin equation can be seen as the generalisation of the Liouville equation to a classical particle undergoing a noisy evolution leading to a distribution of possible trajectories for the same initial conditions. For motion in a phase space governed by Hamilton's equations of classical motion,

$$\frac{\partial \mathbf{q}}{\partial t} = \frac{\partial \mathcal{H}(\mathbf{p},\mathbf{q})}{\partial \mathbf{p}} \qquad \frac{\partial \mathbf{p}}{\partial t} = -\frac{\partial \mathcal{H}(\mathbf{p},\mathbf{q})}{\partial \mathbf{q}}, \tag{2.53}$$

where $\mathbf{q}, \mathbf{p}$ are the canonical coordinates and momenta of the system, the values of which span the phase space and thereby completely specify its state. $\mathcal{H}(\mathbf{p},\mathbf{q})$ is the Hamiltonian function, which completely determines the dynamical evolution through Hamilton's equation. [37]

The Liouville equation calculates averages of the classical motion for a probabilistic distribution of values in the phase space, represented as the phase space distribution function $f(\mathbf{p},\mathbf{q},t)$. The time derivative of this probability density takes the form of a conservation law whereby the probability at a phase space coordinate is compensated exactly by the divergence of a probability current, hence

$$\frac{\partial f}{\partial t} = -\frac{\partial}{\partial \mathbf{q}} \cdot \left(\frac{d\mathbf{q}}{dt} f\right) - \frac{\partial}{\partial \mathbf{p}} \cdot \left(\frac{d\mathbf{p}}{dt} f\right), \tag{2.54}$$

and with Hamilton's equations this becomes

$$\frac{\partial f}{\partial t} = -\frac{\partial \mathcal{H}}{\partial \mathbf{p}} \cdot \frac{\partial f}{\partial \mathbf{q}} + \frac{\partial \mathcal{H}}{\partial \mathbf{p}} \cdot \frac{\partial f}{\partial \mathbf{p}} = -Lf, \tag{2.55}$$

where the Liouville operator is defined as $\frac{\partial \mathcal{H}}{\partial \mathbf{p}} \cdot \frac{\partial}{\partial \mathbf{q}} + \frac{\partial \mathcal{H}}{\partial \mathbf{p}} \cdot \frac{\partial}{\partial \mathbf{p}}$, and the probability density at a time t given the distribution at an initial time $f(\mathbf{p},\mathbf{q},t)$ is found from the formal operator solution,

$$f(\mathbf{p},\mathbf{q},t) = e^{-tL} f(\mathbf{p},\mathbf{q},0). \tag{2.56}$$

The Fokker-Planck equation corresponding to a Langevin equation is an extension of the Liouville equation in the sense that that the classical position and conjugate momenta coordinates are now the stochastic variables of the Langevin equation. For a general Langevin equation for a set of stochastic variables $\mathbf{x} = x_i$, we have the generic Langevin equation

$$\frac{dx_i}{dt} = v_i(x_1, x_2, ..) + F_i(t) \rightarrow \frac{d\mathbf{x}}{dt} = \mathbf{v}(\mathbf{x}) + \mathbf{F}(t), \tag{2.57}$$

where F_i is a set of Gaussian white noises with the standard autocorrelation $\langle \mathbf{F}(t)\mathbf{F}(s)\rangle = 2\mathbf{D}\delta(t-s)$. We then look for the probability distribution of the values of $\mathbf{x}$ at time t, $p(\mathbf{x},t)$, for which we must take the average of this distribution over all possible realisations of the noise term. We again have a conserved probability $\int f(\mathbf{x},t) = 1$ at all times, t, and so we anticipate that the derivative in the stochastic case is also given by the divergence of a flux, such that

$$\frac{\partial f}{\partial t} + \frac{\partial}{\partial \mathbf{x}} \cdot \Big(\frac{d\mathbf{x}}{dt}\Big) = 0. \tag{2.58}$$

The time-derivative of the stochastic variables is given by the Langevin equation such that,

$$\frac{\partial f(\mathbf{x},t)}{\partial t} = -\frac{\partial}{\partial \mathbf{x}} \cdot \Big(\mathbf{v}(\mathbf{x}) f(\mathbf{x},t) + \mathbf{F}(t) f(\mathbf{x},t)\Big). \tag{2.59}$$

Writing the noise-free evolution by defining an analogous operator to the Liouville operator,

$$L\Phi = \frac{\partial}{\partial \mathbf{x}}(v(\mathbf{x}) f(\mathbf{x},t)), \tag{2.60}$$

and the noise-free part has an analogous formal solution,

$$f(\mathbf{x},t) = e^{-tL} f(\mathbf{x},0). \tag{2.61}$$

In the presence of the noise term, the derivative is

$$\frac{\partial f}{\partial t} = -Lf - \frac{\partial}{\partial \mathbf{x}} \cdot \mathbf{F}(t) f, \tag{2.62}$$

which upon integration gives

$$f(\mathbf{x},t) = e^{-tL} f(\mathbf{x},0) - \int_0^t ds e^{-(t-s)} \frac{\partial}{\partial \mathbf{x}} \cdot \mathbf{F}(s) f(\mathbf{a},t). \tag{2.63}$$

Putting this expression back into the time derivative of the probability distribution,

$$\frac{\partial}{\partial t} f(\mathbf{x},t) = -Lf(\mathbf{x},t) + \frac{\partial}{\partial \mathbf{x}} \cdot \mathbf{F}(t) f(\mathbf{x},0) + \frac{\partial}{\partial \mathbf{x}} \cdot \mathbf{F}(t) \int_0^t ds e^{-(t-s)L} \frac{\partial}{\partial \mathbf{x}} \cdot \mathbf{F}(s) f(\mathbf{x},t). \tag{2.64}$$

The time evolution now follows from taking the average over the noise. The term proportional to $f(\mathbf{x},0)$ is independent of the noise and so averages to 0. By using the delta-correlated property of the white noise and inserting it into the equation, we have for the resulting noise-averaged distribution function, $\hat{f}$

$$\frac{\partial}{\partial t} \hat{f}(\mathbf{x},t) = -\frac{\partial}{\partial \mathbf{x}} \cdot \mathbf{v}(\mathbf{x}) \hat{f}(\mathbf{x},t) + \frac{\partial}{\partial \mathbf{x}} \cdot \mathbf{D} \cdot \frac{\partial}{\partial \mathbf{x}} \hat{f}(\mathbf{x},t), \tag{2.65}$$

which is the equation for the time-evolution in the absence of the noise term with an additional part that accounts for the average effect of the noise over all trajectories. We

have a drift vector arising from the deterministic dynamical evolution, and a diffusion tensor which is physically related to the random thermal force. An important point to note is that we have performed the integral over the noise term in the diffusive component of this derivation, and hence have implicitly invoked the Stratonovich interpretation. In general the Itô interpretation will give ruse to a different expression for the Fokker-Planck equation. For additive noise the Fokker-Planck under the two interpretations coincide, while the Stratonovich FPE has an additional drift component when compared to the Itô integral for a general multiplicative noise.

We note that, more generally, the Langevin equation for a set of stochastic variables may depend on all of the noise variables such that,

$$\frac{dx_i}{dt} = f(x_i) + g_{i,j}(x)\eta_j(t), \tag{2.66}$$

The Fokker-Planck equation in this case is,

$$\frac{\partial P(x,t)}{\partial t} = -\left[\sum_i \frac{\partial}{\partial x_i} f_i(x) + D\frac{\partial^2}{\partial x_i \partial x_j} g_{i,j}(x)\right] P(x,t). \tag{2.67}$$

2.3 GENERALIZED LANGEVIN EQUATIONS

The Generalized Langevin equation is an extension of the Langevin equation. of particular use in the molecular non-equilibrium dynamics of open systems [38], and in the fractional Langevin equation which may be used to describe systems that exhibit fractional diffusion [39]. It may be derived on extremely general grounds, from the bilinear coupling of a system to a bath of harmonic oscillators. For example, for the problem of a mechanical motion of a particle, the GLE is

$$\dot{q} = -\nabla V(q) - \int_0^t \gamma(t-s)\dot{q}(s) + F(t). \tag{2.68}$$

In fact we may see the GLE as the more accurate approximation to the underlying complex dynamics of the system, with the traditional Langevin equation being the long-time approximation to some more complex memory kernel, applicable in the case that the bath correlation time is much longer than the characteristic time of the system. In particular, the GLE has a similar property to the Langevin equation, by which there is a non-Markovian fluctuation-dissipation theorem between the time-dependent friction and damping terms,

$$\langle F(t)F(s)\rangle = \beta^{-1}\gamma(t-s). \tag{2.69}$$

a result which is also known as Kubo's second fluctuation-dissipation theorem [40]. This statement implies the physical fact that the dissipative and thermal fields balancing each other on a per-frequency basis at equilibrium.

Chapter 3

Langevin Spin Dynamics

For the remainder of this thesis, we will be concerned with the the modelling of superparamagnetism using Langevin equations, and in particular in the case where the timescale of the bath and of the magnetic system are not widely separated. Superparamagnetism may be viewed as single-domain ferromagnetic particles. Their properties are particularly interesting to the magnetic recording industry, where the theoretical basis of all magnetic storage media relies on the use of superparamagnetic grains which have a remanent magentisation on a timescale long enough to facilitate the storage of data. [41]

It is therefore of immense physical and theoretical importance to understand the detailed physics of the superparamagnetic state, especially as it relates to the escape problem over long timescales for such particles, and to understand the theoretical basis underlying the assumptions and approximation employed.

Superparamagnetism occurs when the size of a particle composed of magnetically ordered atoms becomes small enough such that the energy needed to divide into randomly-oriented magnetic subdomains becomes less than the energy required to become a single, large magnetic domain. [42] [43] The overall moment of the ensemble is then represented by a single moment of magnitude

$$\mu_s = \mu_{at} N, \tag{3.1}$$

where μ_{at} is the atomic magnetic moment and N is the number of constituent atomic magnetic moments. Owing to the particularly large size of this superparamagnetic moments, the spin is typically able to exhibit rigidity to thermal effects over much longer timescales than might be expected. This rigidity is evident in the decay profile of the magnetisation, which to a first approximation is given by an Arrhenius law where the

magnetisation decays over a characteristic timescale,

$$M(t) = M_0 e^{-t/\tau}. \tag{3.2}$$

The experimentally-observed properties of strongly depends on the characteristic measuring time, τ_m, of the experimental technique employed to observe the properties of the system, in comparison to the intrinsic time of switching over the energy barrier τ. When the experimental time $\tau_m >> \tau$, the relaxation is much faster than the observation timescales and the nanoparticle reach thermal equilibrium and so the particles are considered to be in the *s*uperparamagnetic regime. In the case there the experimental time is significantly slower than the barrier timescale, $\tau >> \tau_m$, the system relaxes very slowly and the quasistatic ordered magnetisation can be observed. This regime is called the *b*locked regime. [44]

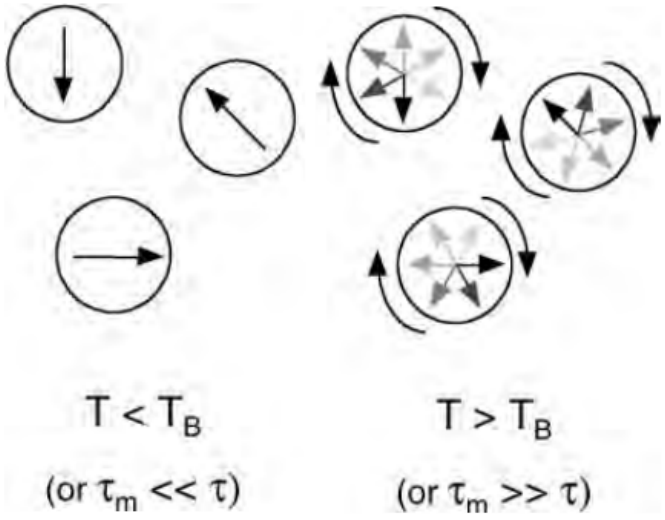

Figure 3.1: Behaviour of superparamagnetic moments above and below the blocking temperature. **Left**: For τ_m much smaller than the relaxation time, a well-defined tate is observed, this is the blocked state. **Right**: For τ_m much larger than the elaxation time, the large fluctuations of the magnetisation over the measurement timescale lead to a measured time-averaged magnetisation of zero. Reproduced from [45]

.

Crucially, the timescale of interwell transition depends on the temperature of the particles, and so we can infer that there is an associated temperature T_B, called the blocking temperature, which divides the system between both regimes and depends on the measure-

ment time of the experiment. The blocking temperature is measurable for and depends on the various different experimental methods, such as AC susceptibility measurements and SQUID magnetometry. [44] The state of the spins above and below the blocking temperature is depicted in Figue 3.1.

We will now detail how the Langevin formalism is applied to general arrays of magnetic moments, and to the problem of superparamagnetism in particular.

3.1 LANDAU-LIFSHITZ-GILBERT

The picture we have for the superparamagnet is then that of a large, single magnetic moment interacting with some thermal bath. The interaction of the superparamagnet with the bath will naturally give rise to both a fluctuating thermal term and a damping. Hence, a Langevin model may be applied to the system. The Langevin equation which is generally used to model superparamagnetic and other systems of spins such as atomic ensembles, is the *Landau-Lifshitz-Gilbert* equation. The equation is not a simple generalisation of the equation for the mechanical problem, and great care must be taken in the construction of both the damping term, and for the the thermal force, as a simple additive noise term will be nonconservative in the spin.

3.1.1 Landau-Lifshitz Equation

The development of the LLG equation started with the work of Landau & Lifshitz [46], [47], who argued that the correct equation of motion for a classical spin vector in an external magnetic field took a simple precessional form

$$\frac{\partial \mathbf{S}}{\partial t} = -\gamma(\mathbf{S} \times \mathbf{H}), \tag{3.3}$$

where $\gamma = 1.76 \times 10^{11} s^{-1} T^{-1}\text{m}$ is the gyromagnetic ratio which gives the ratio of the magnetic moment to the angular momentum, and the vector $\mathbf{S} = \boldsymbol{\mu}/\mu_s$ is a unit vector in the direction of the magnetic moment. The field $\mathbf{H}$ consists of both the externally applied field, and for a superparamagnet we have various effective field terms which are derived from the terms in the Hamiltonian which are proportional to the spin as,

$$\mathbf{H} = -\frac{1}{\mu_s}\frac{\partial \mathcal{H}}{\partial \mathbf{S}}, \tag{3.4}$$

where we call $\mathcal{H}$ the *spin Hamiltonian*, since it only consists of terms pertaining to the magnetic degree of freedom of the system.

In this way much of the physics pertaining to the detailed interaction of the spin with the environemt are incorporated into the Landau-Lifshitz formalism. Typically, the spin Hamiltonian incorporates numerous physical processes, including exchange, anisotropy, dipole-dipole interaction, and various other effects. The typical spin Hamiltonian then takes the form.

$$\mathcal{H} = \mathcal{H}_{exc} + \mathcal{H}_{ani} + \mathcal{H}_{app} + \mathcal{H}_{dd}. \tag{3.5}$$

Many sources for the relevant parameters of the above Hamiltonian are given in density units as they generally arrived at from the assumption of a continuum model of a block material. Such material parameters are simply related to the parameters employed in the Langevin equation by the volume we assume for the nanoparticle. Hence we have a nanoparticle magnetic moment of $\mu_s = M_s V$, where M_s is the spontaneous magnetisation and V is the particle volume. Similarly, the anisotropy term contain a magnetic anisotropy energy density which also trivially gives the desired nanoparticle anisotropy energy as $k_u = K_z V.$, where K_z is the anisotropy energy density and k_u is the energy term used in simulations.

3.1.2 Magnetic Anisotropy

The anisotropy term of the spin Hamiltonian implements the directional dependence of the energy of the magnetic moment. A number of different forms of anisotropy occur in magnetic systems, including the uniaxial form which results in a single preferential direction of alignment, or *easy-axis*, for the spin, and biaxial anisotropy, which may be suitable, for example, im the case of spheroidal nanoparticle where there is an angle between the axis of symmetry of the particle and the easy-axis. [48]

The simplest form of anisotropy, and the one which will generally be considered here, is the uniaxial anisotropy where we have a single preferred direction, the easy axis, $\mathbf{e}$. The uniaxial anisotropy contributes the following term to the spin Hamiltonian,

$$\mathcal{H}_{ani} = -k_u(\mathbf{S} \cdot \mathbf{e})^2, \tag{3.6}$$

where k_u is magnetic energy of the nanoparticle. Performing the derivative with respect to the spin results in a field which is proportional to the projection of the spin onto the easy-axis,

$$\mathbf{H} = -\frac{1}{\mu_s}\frac{\partial}{\partial \mathbf{S}}\mathcal{H} = \frac{2k_u}{\mu_s}(\mathbf{S} \cdot \mathbf{e}). \tag{3.7}$$

We will assume that the z-axis is the easy-axis of the anisotropy in our simulations, such that the components of the contribution to the effective field of the anisotropy takes the simple form,

$$H_z = H_k S_z \tag{3.8}$$

where the anisotropy field magnitude is

$$H_k = \frac{2K_u}{M_s} = \frac{2k_u}{\mu_s}. \tag{3.9}$$

When the spin and the field align in the same direction, there is no precessional motion since the dynamical rate of change is proportional to the cross product of the spin and field. In this way the easy-axis represents the minimum of the spin energy.

3.1.3 Damping

Given the precessional Landau-Lifshitz equation and the physically relevant spin energy terms, we have a purely deterministic formalism for the time-evolution of the spin system. However, the spin-bath interaction will result in dissipation of energy from the system to the bath over time. Hence, it is necessary to incorporate the correct form of damping into the precessional motion. We may arrive at the desired form of damping from the formalism of classical mechanics.

We first express the precessional equations of motion, Eqn. 3.3, as the equations of motion arising from the Euler-Lagrange equation for the corresponding Lagrangian, [49]

$$\frac{d}{dt}\frac{\delta \mathcal{L}[\mathbf{S}, \dot{\mathbf{S}}]}{\delta \dot{\mathbf{S}}} - \frac{\delta \mathcal{L}[\mathbf{S}, \dot{\mathbf{S}}]}{\delta \mathbf{S}} = 0, \tag{3.10}$$

where $\mathcal{L} = \frac{1}{2}(I_1(\Omega_1^2 + \Omega_2^2) + I_3\Omega_3^2) - V(\theta, \phi)$, where Ω_i are the angular velocities and I_i are the moments of inertia [50], and the spin components are taken to be generalised coordinates in analogy with the classical mechanics of particles. The most general method of incorporating damping into classical equations of motion is to introduce a Rayleigh dissipation functional into the Lagrangian or Hamiltonian of the system [51]. Such a dissipation functional takes the form,

$$\boldsymbol{\mathcal{R}} = \frac{1}{2}\sum_{i,j}\int\int \Big[\frac{\partial \mathbf{S}_i(r,t)}{dt} \cdot \boldsymbol{\Lambda}_{i,j}(r,r') \cdot \frac{\partial \mathbf{S}_j(r',t)}{dt}\Big] dr dr', \tag{3.11}$$

where i, j label the spin components, and the equations of motion are now derived from

$$\frac{d}{dt}\frac{\delta \mathcal{L}[\mathbf{S}, \dot{\mathbf{S}}]}{\delta \dot{\mathbf{S}}} - \frac{\delta \mathcal{L}[\mathbf{S}, \dot{\mathbf{S}}]}{\delta \mathbf{S}} + \frac{\delta \mathcal{R}}{\delta \dot{\mathbf{S}}} = 0. \tag{3.12}$$

The dissipation is incorporated via the dissipation tensor, $\mathbf{\Lambda}_{i.j}(r, r')$ which may in general be a nonlocal function. To a first approximation it is satisfactory to assume that this is simply a constant, $\Lambda_{i,j}(r, r') = \Lambda\delta_{i,j}$ in this fashion we arrive at Gilbert's expression for the motion of a damped spin,

$$\frac{d\mathbf{S}}{dt} = \gamma\mathbf{S} \times \Big(\mathbf{H} - \frac{\alpha}{\gamma}\frac{d\mathbf{S}}{dt}\Big). \tag{3.13}$$

Where $\alpha = \Lambda$ [52] [53]. This equation consists of the conservative, precessional part proportional to H and the dissipative spin-dependent field, $-\frac{\alpha}{\gamma}\frac{d\mathbf{S}}{dt}$. The dissipation is then similar to the viscous force proportional to the time derivative of the canonical coordinates for a particle. This equation of motion for a spin with the simple form of damping is called the *Landau-Lifshitz-Gilbert* equation. The LLG equation has a close relationship to other physical systems, such as the motion of vortex filaments and σ-models in particle physics, and is also of interest on a purely mathematical basis due to it's differential geometric properties. [54]

3.1.4 Landau-Lifshitz Form of the LLG

Landau & Lifshitz proposed an alternative phenomenological form of damping by introducing a torque in addition to the precessional motion which pushes the magnetisation in the direction of the applied field. This leads to an equation for the spin [55],

$$\frac{d\mathbf{S}}{dt} = -\gamma(\mathbf{S} \times \mathbf{H}) - \lambda\mathbf{S} \times (\mathbf{S} \times \mathbf{H}). \tag{3.14}$$

It is possible and desirable to equate these two forms of the precessional dynamics, as the Landau-Lifshitz form of the LLG is more suitable for direct numerical simulation. We proceed to multiply the LLG equation in the Gilbert form, Eq. 3.13, across by the cross product of the magnetisation component,

$$\mathbf{S} \times \frac{d\mathbf{S}}{dt} = -\gamma\mathbf{S} \times (\mathbf{S} \times \mathbf{H}). + \alpha\mathbf{S} \times (\mathbf{S} \times \frac{d\mathbf{S}}{dt})) \tag{3.15}$$

From the vector identity, $\mathbf{a} \times \mathbf{b} \times \mathbf{c} = \mathbf{b}(\mathbf{a} \cdot \mathbf{c}) - \mathbf{c}(\mathbf{a} \cdot \mathbf{b})$, and the identity $\frac{d\mathbf{S}}{dt} \cdot \mathbf{S} = 0$, since the spin magnitude is conserved, we arrive at

$$\mathbf{S} \times \frac{d\mathbf{S}}{dt} = -\gamma\mathbf{S} \times (\mathbf{S} \times \mathbf{H}) + \alpha\frac{d\mathbf{S}}{dt}, \tag{3.16}$$

since the spin magnitude $|\mathbf{S}| = 1$ since it is a unit vector. Upon replacing for this expression in Gilbert's equation, Eqn. 3.13, we have

$$\frac{d\mathbf{S}}{dt} = \gamma\mathbf{S} \times \mathbf{H} - \gamma\alpha\mathbf{S} \times (\mathbf{S} \times \mathbf{H}) - \alpha^2\frac{d\mathbf{S}}{dt}, \tag{3.17}$$

which we can trivially re-express by taking the derivative term to the left-hand side, resulting in the Gilbert equation in the Landau-Lifshitz form, [56]

$$\frac{d\mathbf{S}}{dt} = -\frac{\gamma}{1+\alpha^2}(\mathbf{S}\times\mathbf{H}) - \frac{\gamma\alpha}{(1+\alpha^2)}\mathbf{S}\times(\mathbf{S}\times\mathbf{H}). \tag{3.18}$$

3.1.5 Thermal Fields

To incorporate thermal fluctuations into this model, Brown took the equation of motion for the spin with Gilbert damping and modified it to a Langevin equation by augmenting it with a random thermal field which is incorporated in addition to the effective field [57] [58]. The LLG equation then becomes,

$$\frac{d\mathbf{S}}{dt} = -\frac{\gamma}{1+\alpha^2}(\mathbf{S}\times(\mathbf{H}+\mathbf{H}_{th})) - \frac{\gamma\alpha}{(1+\alpha^2)}\mathbf{S}\times(\mathbf{S}\times\mathbf{H}+\mathbf{H}_{th}), \tag{3.19}$$

where the random field $\mathbf{H}_{th}(t)$ is stochastic variable with the white noise properties and $D = \frac{\alpha k_B T}{\gamma\mu_s}$,

$$\langle\mathbf{H}_{th}(t)\rangle = 0, \tag{3.20}$$

$$\langle\mathbf{H}_{th,i}(t)\mathbf{H}_{th,j}(t')\rangle = \frac{2\alpha k_B T}{\gamma\mu_s}\delta_{i,k}\delta(t-t'), \tag{3.21}$$

where i, j label the Cartesian basis vectors. The fact that the thermal contribution is introduced as a fluctuating magnetic field around which the spin precesses automatically leads to conservation of the spin magnitude, while the presence of the same α in the damping and thermal terms is the realisation of the fluctuation-dissipation theorem for the magnetic system.

3.1.6 Fokker-Planck Equation for the LLG

An important consequence of the LLG Langevin equation is that it enables us to derive the Fokker-Planck equation for the probability distribution of the spin orientation. To do this we compare the LLG to the generic Langevin equation, and separate the terms so that we have a deterministic drift vector, $f(\mathbf{S})$, and the the thermal diffusion tensor proportional to the white noise, $g_{i,j}(\mathbf{S})\eta_i((t)$. For the LLG equation of the form,

$$\frac{d\mathbf{S}}{dt} = -\frac{\gamma}{1+\alpha^2}\big[\mathbf{S}\times(\mathbf{H}+\boldsymbol{\eta})\big] - \alpha\frac{\gamma}{1+\alpha^2}\big[\mathbf{S}\times\big[\mathbf{S}\times(\mathbf{H}+\boldsymbol{\eta})\big]\big]. \tag{3.22}$$

We then define the following vector,

$$A_i(\mathbf{S},t) = -\frac{\gamma}{1+\alpha^2}\Big[(\mathbf{S}\times\mathbf{H})_i + \alpha(\mathbf{S}\times(\mathbf{S}\times\mathbf{H}))_i\Big] \tag{3.23}$$

, and the tensor

$$B_{ik}(\mathbf{S},t) = \frac{\gamma}{1+\alpha^2}\Big[-\sum_j \epsilon_{ijk}S_j + \alpha(\delta_{ik}S^2 - S_iS_k)\Big]. \tag{3.24}$$

Then the Fokker-Planck equation for the LLG takes the form.

$$\frac{\partial P}{\partial t} = -\sum_i \frac{\partial}{\partial S_i}\left[A_i + q\sum_{jk} B_{jk}\frac{\partial B_{ik}}{\partial S_j}\right]P + \sum_{ij}\frac{\partial^2}{\partial S_i \partial S_j}\left[q\sum_k B_{ik}B_{jk}\right]P, \tag{3.25}$$

Where the unknown constant q has yet to be determined. The second part of the drift term may be evaluated by noting that

$$\sum_j \frac{\partial B_{jk}}{\partial S_j} = -\frac{2\alpha\gamma}{1+\alpha^2}, \tag{3.26}$$

Hence

$$\sum_k B_{ik}(\sum_j \frac{\partial B_{jk}}{\partial S_j}) = 0, \tag{3.27}$$

and so this part is identically zero and disappears. The diffusive term is evaluated by again using the identity Eqn. 3.26,

$$-q\sum_{jk} B_{ik}B_{jk}\frac{\partial}{\partial S_j} = q\frac{\alpha^2\gamma^2}{(1+\alpha^2)^2}S^2\left[S\times\left[S\times\frac{\partial}{\partial S}\right]\right]_i. \tag{3.28}$$

which may be simplified by identifying the Néel time, which is the characteristic diffusion time in the absence of a potential, a fact that can be seen simply by setting the potential terms to 0 in the Langevin and Fokker-Planck equations.

$$\frac{1}{\tau_N} = \frac{2q\alpha^2\gamma^2}{(1+\alpha^2)^2} \tag{3.29}$$

The constant q is then found by identifying the stationary distribution in the absence of a potential with the equilibrium distribution, $P_0(S) \propto e^{-\beta\mathcal{H}(S)}$. this makes the Néel time

$$\frac{1}{\tau_N} = \frac{2\alpha\gamma}{(1+\alpha^2)}\frac{k_BT}{\mu_s}. \tag{3.30}$$

This equilibrium condition also relates the coefficient of the correlation function to the diffusion coefficient. The final expression for the Fokker-Planck equation is then

$$\frac{\partial P(S,t)}{\partial t} = -\frac{\partial}{\partial S}\left[-\frac{\gamma}{1+\alpha^2}(S\times H) + \alpha(S\times S\times H) + \frac{1}{2\tau_N}(S\times S\times\frac{\partial}{\partial S})\right]P(S,t). \tag{3.31}$$

3.1.7 Fokker-Planck Equation: Functional Derivation

We note that we can also arrive at this expression via functional techniques. We may use the LLG in the *K*ubo form, in which the thermal field appears only in the precessional part and not in the damping. While the Langevin equations are different, the FPE is identical [59], as we will see.

$$\frac{dS}{dt} = -\frac{\gamma}{(1+\alpha^2)}\Big[S \times (H+\eta)\Big] - -\frac{\gamma\alpha}{(1+\alpha^2)}\Big[S \times (S \times H)\Big]. \tag{3.32}$$

The probability distribution for the noise is

$$F\Big[\eta(t)\Big] = \frac{1}{Z_\eta}\exp\Big[-\frac{1}{D}\int_{-\infty}^{\infty} d\tau \eta^2(\tau)\Big], \tag{3.33}$$

where $Z_\eta = \int D\eta F$ is the noise partition function and $D\eta$ denotes the measure in the functional integration over all realisations of the noise field η. The average of any functional of the noise may be expressed by reference to the noise distribution in a similar manner to the expected value of a continuous random variable as

$$\langle A[\eta]\rangle_\eta = \int D\eta A[\eta]F[\eta], \tag{3.34}$$

Since $\frac{\delta\eta_i(s)}{\delta\eta_j(s)} = \delta_{ij}\delta(t-s)$ we may trivially arrive at the correlation function for the noise. If we define the distribution function for the spin with reference to an occupation function as follows

$$f(S,t) = \langle \pi(S,t)\rangle_\eta, \tag{3.35}$$

where the occupation is

$$\pi(S,t) = \delta(S - \overrightarrow{s}), \tag{3.36}$$

hence we average this function over all possible realisations of the noise function. Since $\dot{\pi} = -\frac{\partial\pi}{\partial S}\cdot s$ we may then relate the expression for the distribution to the equation of motion,

$$\frac{\partial f}{\partial t} = \frac{1}{1+\alpha^2}\frac{\partial}{\partial S}\Big[(S\times H) + S\times(S\times H)\Big]P(S,t) + S\times\langle\eta(t)\pi(t,[\eta])\rangle_\eta. \tag{3.37}$$

The standard Fokker-Planck expression is then recovered by calculating the expectation as

$$\langle\eta(t)\pi(t,[\eta])\rangle_\eta = -\frac{D}{1+\alpha^2}S\times\frac{\partial f}{\partial S}. \tag{3.38}$$

3.2 LANDAU-LIFSHITZ-MIYAZAKI-SEKI

The Landau-Lifshitz-Miyazaki-Seki equation is the correct implementation of coloured noise into the magnetisation dynamics. In fact, it is the generalised master equation for the magnetic system when the memory kernel is chosen as $K(t) = e^{-t/\tau_c}$ [60]

3.2.1 Miyazaki-Seki Derivation

The original Miyazaki-Seki derivation assumes a single classical spin, which interacts with some thermally fluctuating isotropic medium, in the presence of an externally applied magnetic field, in this case assumed to lie along the z-axis.

The local magnetic field exerted upon the spin is initially taken to be

$$H = H_0 + \boldsymbol{\eta} \tag{3.39}$$

where $\boldsymbol{\eta}$ is the local thermally fluctuating part of the field, and the field H_0 consists of both the external applied magnetic field and the mean local magnetic field induced by the external field, $H_0 = (1+\chi')H_{ext}$, where the term proportional to χ' is the field induced by the average magnetisation of the surrounding medium. The fluctuating thermal magnetic field is then assumed to have a single characteristic relaxation time,

$$\frac{d}{dt}\boldsymbol{\eta} = -\frac{1}{\tau_c}\boldsymbol{\eta} + \mathbf{R}, \tag{3.40}$$

with the white noise taken to have autocorrelation

$$\langle R_i(t)R_j(s)\rangle = \frac{2}{\tau_c}\chi k_B T \delta_{ij}\delta(t-s), \tag{3.41}$$

where i, j label the Cartesian basis coordinates. χ is the susceptibility of the local magnetic field induced by the spin at the site. This expression for the thermal field has an Ornstein-Uhlenbeck Fokker-Planck equation, since $\frac{d\boldsymbol{\eta}}{dt} = f(\boldsymbol{\eta}) + g(\boldsymbol{\eta})\mathbf{R}(t)$, where $f(\boldsymbol{\eta}) = -\frac{1}{\tau_c}$ and $g(\boldsymbol{\eta}) = 1$. The corresponding Fokker-Planck equation is

$$\frac{\partial P(\boldsymbol{\eta},t)}{\partial t} = \frac{1}{\tau_c}\Big[\frac{\partial}{\partial \boldsymbol{\eta}}\cdot\boldsymbol{\eta}\Big]P(\boldsymbol{\eta},t) + \frac{k_B T\chi}{\tau_c}\Big[\frac{\partial}{\partial\boldsymbol{\eta}}\cdot\frac{\partial}{\partial\boldsymbol{\eta}}\Big]P(\boldsymbol{\eta},t). \tag{3.42}$$

The FPE is subject to the stationarity condition that

$$P_{st}(\boldsymbol{\eta}) = \exp\,(-\frac{1}{2\chi k_B T}\boldsymbol{\eta}^2), \tag{3.43}$$

where the energy required to produced the magnetic field is $\frac{\boldsymbol{\eta}^2}{2\chi}$.

The above FPE for the Ornstein-Uhlenbeck field alone is then amended to account for the spin-fie;d interaction by considering the energy between the spin and the magnetic field. The energy induced by the field and the deviation of the spin from it's equilibrium value due to the field interaction is given by

$$U(S,\eta) = \frac{1}{2\chi}\eta^2 - \eta \cdot S \tag{3.44}$$

The time-evolution of the joint probability distribution is then taken to be

$$\frac{\partial}{\partial t}P(S,\eta,t) = -\frac{\partial}{\partial S}\cdot \dot{S}P(S,\eta,t) - -\frac{\partial}{\partial \eta}\cdot \dot{\eta}P(S,\eta,t), \tag{3.45}$$

where the probability flux in each variable is related to it's time-evolution. The first term is the flow due to the spin which is given simply by the precession around the corresponding local magnetic field. The second term, which is the flow in the space of the magnetic field has a contribution due to the potential energy interaction between the field and the spin and a diffusional part corresponding to the driving random field.

$$\dot{\eta}P(S,\eta,t) = -\xi\frac{\partial U}{\partial \eta}P(S,\eta,t) - \frac{k_B T\chi}{\tau_c}\frac{\partial}{\partial \eta}P(S,\eta,t), \tag{3.46}$$

where ξ is a mobility which is taken to be $\xi = \frac{\chi}{\tau_c}$. As

$$\frac{\partial U}{\partial \eta} = \frac{\eta}{\chi} - S. \tag{3.47}$$

then the Fokker-Planck equation for the combined spin-field system is given by

$$\begin{aligned}\frac{\partial}{\partial t}P(S,\eta,t) &= \frac{\partial}{\partial S}\cdot\Big[\gamma S\times(H+\eta)\Big]P(S,\eta,t)\\ &+ \frac{1}{\tau_c}\frac{\partial}{\partial \eta}\cdot\Big[\eta-\chi S\Big]P(S,\eta,t)\\ &+ \frac{k_B T\chi}{\tau_c}\frac{\partial}{\partial \eta}\cdot\left[\frac{\partial}{\partial \eta}\right]P(S,\eta,t).\end{aligned} \tag{3.48}$$

Corresponding to this Fokker-Planck equation is a pair of Langevin equations in the variables S and η, with the diffusion term occurring in the field part of the Langevin equation giving rise to the Gaussian driving white noise for the pair of equations.

$$\frac{d}{dt}S = S\times\big(H+\eta\big), \tag{3.49}$$

$$\frac{d}{dt}\eta = -\frac{1}{\tau_c}(\eta-\chi S) + R, \tag{3.50}$$

with the fluctuation-dissipation of the field R given by Eqn. 3.41.

3.2.2 Spin-only LLMS

To arrive at an expression for the LLMS in terms of the spin-only, we may solve for the noise in a similar way as we did for the Ornstein-Uhlenbeck noise given above [60],

$$\frac{d\eta}{dt} = -\frac{1}{\tau_c}\Big(\eta(t) - \chi S(t)\Big) + R, \tag{3.51}$$

where we note that in comparison we have the additional term coupling to the spin. We will write the noise autocorrelation in the form $\langle R(t)R(t')\rangle = 2\frac{\chi k_B T}{\tau_c}\delta(t-t')$. and so $D = \frac{\chi k_B T}{\mu_s}$. We then have

$$\eta(t) = \frac{\chi}{\tau_c}\int_{-\infty}^{t} dt' K(t-t')S(t') + \sqrt{\frac{2D}{\tau_c}}\int_{-\infty}^{t} dt' K(t-t')\Gamma(t), \tag{3.52}$$

where we still have both a damping and a thermally-driven term. Following [24], we integrate the first term by parts to arrive at

$$\eta(t) = \sqrt{\frac{2D}{\tau_c}}\int_{-\infty}^{t} dt' K(t-t')\Gamma(t) - \chi\int_{-\infty}^{t} dt' K(t-t')\frac{dS(t')}{dt'}, \tag{3.53}$$

and by inserting this into the precessional equation for the spin, we get the spin-only form for the LLMS equation

$$\frac{dS}{dt} = \gamma S(t) \times \Big(H + \bar{\eta} - \chi\int_{-\infty}^{t} dt' K(t-t')\frac{dS(t')}{dt'}\Big), \tag{3.54}$$

where we now label the thermal fluctuations by $\bar{\eta}(t)$.

$$\bar{\eta}(t) = \sqrt{\frac{2D}{\tau_c}}\int_{-\infty}^{t} dt' K(t-t')\Gamma(t'). \tag{3.55}$$

Proceeding in the same way as for the Ornstein-Uhlenbeck noise, the autocorrelation for this thermal field is

$$\langle\bar{\eta}(t)\bar{\eta}(t')\rangle = DK(t-t') = \frac{\chi k_B T}{\mu_s}K(t-t') = \frac{\beta^{-1}}{\mu_s}\chi K(t-t'), \tag{3.56}$$

Recognising $\chi K(t-t')$ as the damping term, we see that this is a representation of the Fluctuation-Dissipation theorem for the coloured noise, where the additional factor of μ_s arises from the spin normalisation. Taking the zero correlation time limit,

$$\lim_{\tau_c\to 0}\langle\bar{\eta}(t)\bar{\eta}(t')\rangle = 2D\tau_c\delta(t-t'). \tag{3.57}$$

We note that the LLMS thus derived from the physical consideration of the spin-field interaction is not immediately comparable with the typical expression for the Ornstein-Uhlenbeck coloured noise, owing to the fact that the $1/\tau_c$ term has been implicitly absorbed

in the white noise term. If we rescale the driving noise such that $Q(t) = \tau_c R(t)$, we then have a pair of Langevin equations

$$\frac{dS}{dt} = \gamma(S \times (H + \eta)), \tag{3.58}$$

while the noise evolves as,

$$\frac{d\eta}{dt} = -\frac{1}{\tau_c}\Big(\eta(t) - \chi S(t) + Q\Big). \tag{3.59}$$

The autocorrelation of the white noise is

$$\langle Q(t)Q(t')\rangle = \frac{2\chi\tau_c k_B T}{\mu_s}\delta(t-t') = 2D\delta(t-t'), \tag{3.60}$$

with $D = \frac{\chi\tau_c k_B T}{\mu_s}$, while the limit of the autocorrelation of the thermal term in the spin-only expression is now,

$$\lim_{\tau_c\to 0}\langle \bar{Q}(t)\bar{Q}(t')\rangle = \frac{D}{\tau_c}\delta(t-t'), \tag{3.61}$$

which is directly comparable to the Ornstein-Uhlenbeck form of the coloured noise. The expression of the LLMS in terms of the bath variable Q has the additional benefit that $[Q] = T$ and so we can interpret Q as the thermal magnetic field contribution to the evolution of the bath field.

Finally, we may see that the limit of the LLMS equation for vanishing correlation time is the LLG equation. For small correlation times we can then take the Taylor expansion about the time t in t', so that the damping term becomes,

$$\int_{-\infty}^{t} K(t-t')\frac{d\mathbf{S}(t')}{dt'}dt' = \Big[\int_{-\infty}^{t} K(t')dt'\Big]\frac{d\mathbf{S}(\mathbf{t})}{dt} + ... \tag{3.62}$$

Hence the spin and memory kernel decouple in the small correlation time limit, and the Langevin equation becomes

$$\frac{dS}{dt} = \gamma S(t) \times \Big(H + \bar{\eta} - \Big[\chi\int_{-\infty}^{t} dt' K(t-t')\Big]\frac{dS(t)}{dt}\Big), \tag{3.63}$$

After performing the integration over t', the damping is

$$\chi\int_{-\infty}^{t} dt' e^{-(t-t')/\tau_c} = \chi\tau_c. \tag{3.64}$$

and by direct comparison of the damping terms in this expression and in Gilbert's equation we have the relationship of the phenomenological damping to the LLMS parameters $\alpha = \chi\gamma\tau_c$. We note also that this expression can be seen if we identify the driving

white noise in the bath field of the LLMS with the thermal magnetic fields of the LLG.

$$\begin{aligned}\langle Q(t)Q(t')\rangle &= \frac{2\chi\tau_c k_B T}{\mu_s}\delta(t-t') \\ &= \frac{2\alpha k_B T}{\gamma\mu_s}\delta(t-t') \\ &= \langle H_{th}(t)H_{th}(t')\rangle\end{aligned} \tag{3.65}$$

under the assumption that $\alpha = \gamma\chi\tau_c$.

3.2.3 Mori-Embedding

Finally, we note that the above procedure of reducing the full LLMS equation to the spin-only LLMS is a specific instance of the Mori-embedding procedure, for writing an effective Langevin equation for a resolved set of variables from some full set of variables [61] [62].

If we define a general phase space X over a vector field f, which is partitioned into two parts as

$$X = X_1 \times X_2 \tag{3.66}$$

$B(X)$ is the space of observables on the phase space, X, and $\phi : \mathcal{R} \to B(X)$ denotes a path on the space of observables describing the time-evolution of an observable subject to the condition that $\phi_0 = \phi(0)$. The time-derivative is defined as

$$\dot{\phi} = L\phi \tag{3.67}$$

where L is the Liouville operator associated to the vector space f. Typically, the Mori-Zwanzig procedure may describe the reduction of the dynamics on some very large phase space to a much smaller restricted space, but in the case of the LLMS we eliminate only the magnetic field's degrees of freedom. We define the projection operator on the space of observables as

$$P : B(X) \to B(X) \tag{3.68}$$

The projection operator has the property that for any element of the full space, $\psi \in B(X)$, the projection $P\psi(x_1, x_2)$ depends only on the restricted space x_1, and the standard projection operator property that $P^2 = P$. The Mori-Zwanzig procedure gives the corresponding equations of motion for the projected observable on the restricted subspace. We define in addition to the project on operator it's complement $Q = \mathbb{I} - P$, with $P + Q = \mathbb{I}$. The projected equation of motion is

$$P\dot{\phi} = PL\phi \tag{3.69}$$

$$= PLP\phi + PLQ\phi \tag{3.70}$$

with a similar expression for the complement

$$Q\dot{\phi} = QLP\phi + QLQ\phi \tag{3.71}$$

If we write $\eta = Q\phi$, this equation is

$$\dot{\eta} = QL\eta + QLP\phi \tag{3.72}$$

which has solution

$$\eta(t) = e^{tQL}\eta(t) + \int_0^t e^{(t-s)QL}QLP\phi(s)ds \tag{3.73}$$

which is

$$Q\phi(t) = e^{tQL}Q\phi(t) + \int_0^t e^{(t-s)QL}QLP\phi(s)ds \tag{3.74}$$

Replacing for $Q\phi$ in the time evolution of our resolved variable, we then have,

$$\begin{aligned} P\dot{\phi}(t) &= PLP\phi(t) + PL\left[e^{tQL}Q\phi(0)\int_0^t e^{(t-s)QL}QLP\phi(s)\right] && (3.75)\\ &= PLP\phi(t) + PL\int_0^t e^{(t-s)QL}QLP\phi(s) + PLe^{tQL}Q\phi(0) && (3.76)\end{aligned}$$

Finally, if we write the projected operator as $\xi = P\phi$, the equation of motion for the restricted dynamics becomes

$$\xi(t) = PL\xi(t) + PL\int_0^t e^{(t-s)QL}QL\xi(s) + PLe^{tQL}Q\phi(0) \tag{3.77}$$

with the general result that the reduced dynamics take the form of a Markovian, deterministic part, a memory function over the previous dynamics of the resolved variable, and the noise whose precise time-evolution depends on some unknown, typically microscopic degrees of freedom.

3.3 SIMULATIONS

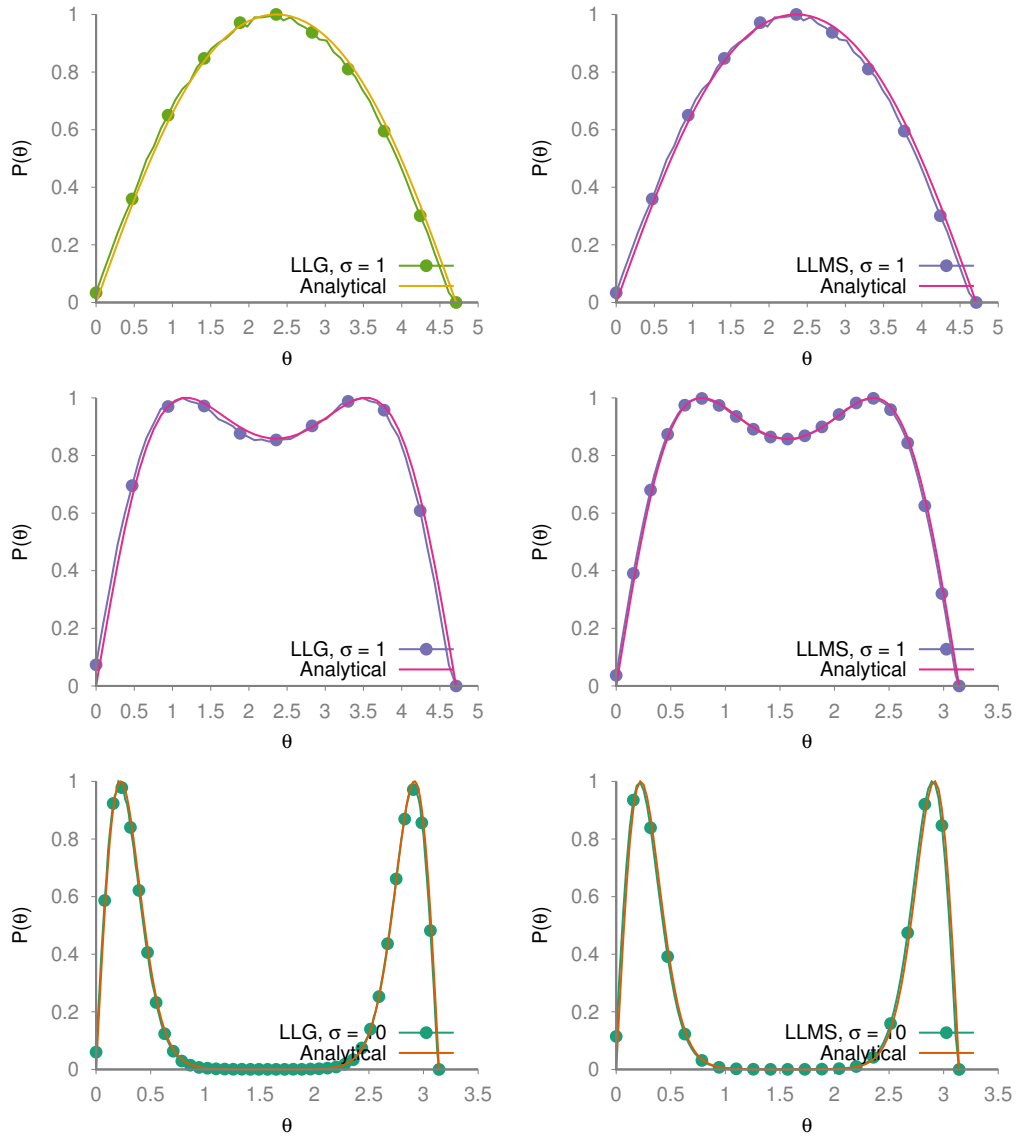

Figure 3.2: $P(\theta)$ vs θ, from numerical simulations at various σ, using **Left**: the LLG Langevin equation and **Right** the LLMS Langevin equation with $\tau_c \gamma H_k = 2$.

To verify both the physical validity of the Langevin models outlined in this chapter, and to verify that our own implementation thereof is accurate and consistent with the analytical theory, we perform some initial simulations for a superparamagnetic moment at different temperatures. For a moment with only magnetic anisotropy and no external field, the

Hamiltonian of the system is simply

$$E(\theta) = -k_u sin^2(\theta) \tag{3.78}$$

The correct probability distribution for the spin at equilibrium is then

$$P(\theta) \propto \sin(\theta) e^{-E(\theta)/k_B T} = \sin\theta \exp(\frac{-k_u sin^2\theta}{k_B T}). \tag{3.79}$$

where θ is the angle between the spin and the easy-axis and the factor of $\sin\theta$ arises from normalising the probability distribution on the sphere.

We perform numerical integration of the LLG and the LLMS employing the Heun scheme. For the LLG, the thermal magnetic field at timestep i is generated from

$$H_{th}(t_i) = \sqrt{\frac{2\alpha k_B T}{\gamma \mu_s \Delta t}} \Gamma_i \tag{3.80}$$

and similarly, the random field for the LLMS noise is

$$R(t_i) = \sqrt{\frac{2\chi k_B T}{\tau_c \Delta t}} \Gamma_i \tag{3.81}$$

where the numbers Γ_i are drawn from a random Gaussian distribution using the Box-Muller technique.

For the integration of the LLMS equation, it is often more numerically stable to integrate the equation by re-expressing it in terms of a new noise variable, $\bar{\boldsymbol{\eta}} = \boldsymbol{\eta} - \chi \mathbf{S}$

$$\frac{d\mathbf{S}}{dt} = \gamma \mathbf{S} \times (\mathbf{H} + \hat{\boldsymbol{\eta}}) \tag{3.82}$$

$$\frac{d\hat{\boldsymbol{\eta}}}{dt} = -\chi\gamma \mathbf{S} \times (\mathbf{H} + \hat{\boldsymbol{\eta}}) - \frac{1}{\tau_c}\hat{\boldsymbol{\eta}} + \mathbf{R} \tag{3.83}$$

To calculate the Boltzmann distribution ,we initialise the spin along the easy-axis direction, then allow the spin to evolve for 10^8 steps after equilibriation and evaluate the probability distribution by recording the number of steps the spin spends at each angle to the easy-axis. We vary the value of the reduced barrier height parameter, $\sigma = \frac{k_u}{k_B T}$, by varying the temperature of the bath. The results of the calculations are presented in Figure 3.2, showing good agreement between the Boltzmann distribution and the results of the simulations. This confirms our implementation of the LLG algorithm and verifies that the LLMS reproduces the correct behaviour at equilibrium, as anticipated from the representation of the fluctuation-dissipation for the system, and as seen in previous work using the equation [24].

Chapter 4

Debye Susceptibility: The Effect of Coloured Noise

4.1 INTRODUCTION

The magnetic susceptibility of a material, whether a fine magnetic particle or a more complex array of magnetic moments such as a ferromagnet, is one of the most important measures of its magnetic properties. The AC susceptibility is a complex-valued proportionality function relating the induced AC magnetic moment exhibited by a material in response to an applied AC magnetic field.

A chief advantage of AC susceptibility experiments is that they may yield information regarding a material which the static DC susceptibility, that is, the susceptibility in a *constant* applied field, does not, owing to the dynamical nature of the response. It may give us insight into a variety of systems including superparamagnets as well as spin glasses, superspin glasses, quasi 2D ferromagnets and various other systems. In particular, the dynamical susceptibility has implications for the relaxational and absorption properties of a system as well as the phase, where for a ferromagnetic system the susceptibility will diverge near the Curie temperature of the phase transition. Importantly, it is also related to the magnetic correlation function through the Fluctuation-Dissipation theorem. [63] [64]

In AC susceptibility experiments, an AC magnetic field is applied to the sample and measurements are taken of the resulting magnetic moment. In general the response of the magnetic moment may be linear or nonlinear, depending on the strength of the externally applied field. We will generally be concerned with the linear response regime, for which

the Fourier transform of the magnetisation in the presence of a weak applied field is

$$\mathbf{M}(\omega) = \frac{d\mathbf{M}}{d\mathbf{H}} \cdot \mathbf{H}_0 \sin(\omega t) = \boldsymbol{\chi}(\omega) \cdot \mathbf{H}_0 \sin(\omega t), \tag{4.1}$$

Hence the susceptibility is the slope of the $M(H)$ curve. By trivially rearranging Eq. 4.1, we see that we may also think of it as the proportionality constant between the Fourier expansion coefficient of the magnetisation $\mathbf{M}(\omega)$ and the corresponding Fourier coefficient of the applied magnetic field, $\mathbf{H}(\omega) = \mathbf{H_0} \cos(\omega t)$,

$$\boldsymbol{\chi}(\omega) = \mathbf{M}(\omega)/\mathbf{H}(\omega). \tag{4.2}$$

The static limit of this dynamical quantity, $\boldsymbol{\chi}(0) = \mathbf{M}(0)/\mathbf{H}(0)$, is the DC magnetic susceptibility.

In the context of superparamagnetism the dynamical susceptibility is particularly interesting. In the noninteracting Néel theory, the blocking temperature is related to the measurement time of the experiment, τ_m, via

$$T_B = \frac{\Delta E}{\ln(\tau_0/\tau_m)k_B}, \tag{4.3}$$

where ΔE is the energy barrier and τ_0 is the attempt frequency. The measurement time is of the order of $1 - 100$s for DC measurements, and is the inverse of the measurement frequency for AC measurements. For superparamagnets, the AC susceptibility gives experimental insight into the behaviour for different values of the measurement time τ_m by varying the measurement frequency.

In the following we shall investigate the complex susceptibility of superparamagnetic particles using two models, via direct numerical simulation of the Landau-Lifshitz-Gilbert Langevin equation, and the related phenomenological rate equation known as the discrete orientation model which is the low temperature approximation to the full Langevin dynamics, as well as the effect of correlations on the susceptibility spectrum in their respective non-Markovian extensions.

4.1.1 Linear Response Theory

The response of a generic magnetic moment to an AC applied field falls into two regimes, with the response being linear for smaller applied fields, while at larger fields it enters the nonlinear regime. We are only interested in the smaller applied fields in this work, in which case the response of the moment is amenable to treatment via the linear response

theory [40] [65], according to which the relationship between the input to a system, $f(t)$, which may in general be some perturbing force, and the output $x(t)$, is expressed not just in terms of the current value of the applied force but as a weighted integral over previous values of the input function

$$x(t) = \int_{-\infty}^{t} dt' F(t-t')h(t') + \ldots, \tag{4.4}$$

where $F(t-t')$ is the *linear response function*. The linear response is simply the lowest-order term in the full Volterra expansion for the response, and in the case of large applied force these terms cannot be ignored as higher-order terms must be taken into account.

Supposing now that we have a single-domain superparamagnetic particle under the influence of an oscillating external magnetic field, where at $t = 0$ the field is first applied to the particle, inducing a magnetic moment, $m(t)$. The response function of the moment to the applied field is $\chi(t)$, a complex function corresponding to in and out of phase components [66]. The magnetic field as a function of time is $H(t)$, such that the infinitesimal change in the spin over an infinitesimal time, δt,

$$\delta m(t) \propto H(t')\delta t' a(t-t'). \tag{4.5}$$

If we assume the AC field is applied along the z-axis, such that $\mathbf{H} = (0, 0, H_z \cos(\omega t)$, then the projection of the magnetic moment on to the magnetisation axis, m_z, at a time t is the integral over such infinitesimal changes to the moment in response to the external field

$$m_z(t) = \int_0^t \frac{dH_z(t')}{dt} a(t-t')dt', \tag{4.6}$$

which may be evaluated using integration by parts

$$m_z(t) = H_z(t')a(t-t')\Big|_{t'=0}^{t} - \int_0^t H_z(t')\frac{d}{dt'}a(t-t')dt', \tag{4.7}$$

If we assume the condition that the magnetic field vanishes for $t < 0$ initially such that $H(0) = 0$, and that there is no instantaneous response so that $a(0) = 0$, then the first term disappears and the expression for the response in the linear regime becomes

$$m_z(t) = \int_0^t H_z(t-t')\frac{da(t')}{dt'}dt'. \tag{4.8}$$

Now assuming that the external magnetic field takes the form $H(t) = H_z cos(\omega t)$ such that the x and y components of the field are 0. Then the z-component of the spin vs time takes the form

$$m_z = \int_0^t H_z \cos(\omega(t-t'))\frac{da(t')}{dt'}dt'. \tag{4.9}$$

which is

$$m_z(t) = H_z \cos(\omega t) \int_0^t \cos(\omega(t')) \frac{da(t')}{dt'} dt + H_z \sin(\omega t) \int_0^t \sin(\omega(t')) \frac{da(t')}{dt'} dt, \qquad (4.10)$$

after a large amount of time has elapsed such that $t' \to \infty$, the derivatives of the response function are negligibly small and the expression for the spin becomes

$$m_z(t) = H_z \chi_1(\omega) \cos(\omega t) + H_z \chi_2(\omega) \sin(\omega t), \qquad (4.11)$$

where the susceptibilities are defined as

$$\chi_1(\omega) = \int_0^\infty \frac{da(t')}{dt'} \cos(\omega t') dt', \qquad (4.12)$$

$$\chi_2(\omega) = \int_0^\infty \frac{da(t')}{dt'} \sin(\omega t') dt'. \qquad (4.13)$$

The complex susceptibility is defined by the in and out of phase components such that

$$\chi(\omega) = \chi_1(\omega) + i\chi_2(\omega). \qquad (4.14)$$

Comparing this definition of the susceptibility to the expression for the magnetisation vs time, we see that we can evaluate the susceptibility numerically for a specified frequency by evaluating the component of the Fourier transform of the spin response of the corresponding frequency.

4.1.2 Dispersion & Absorption

Using complex notation, the spin and field may be written as

$$H(t) = Re\Big[H_0 e^{i\omega t}\Big] \qquad m(t) = Re\Big[m(\omega) e^{i\omega t}\Big]. \qquad (4.15)$$

As we have seen, in the linear regime the frequency-dependent Fourier transform component takes the form $m(\omega) = \chi(\omega)h(\omega) = (\chi_1(\omega) + i\chi_2(\omega))h$. The in and out of phase components of the susceptibility in that they are closely related to the dispersion and absorption of the magnetic system. Taking the time derivative of the spin [67]

$$\frac{dm}{dt} = Re[i\omega m(\omega) e^{i\omega t}], \qquad (4.16)$$

and then expressing the spin as

$$\begin{aligned} m(t) &= Re[(\chi_1(\omega t) - i\chi_2(\omega t)] H_0 e^{i\omega t} \qquad (4.17) \\ &= Re[\chi_1(\omega t) - i\chi_2] H_0 (\cos(\omega t) + i \sin(\omega t)) \\ &= H_0(\chi_1(\omega) \cos(\omega t) + \chi_2(\omega) \sin(\omega t)). \end{aligned}$$

The total power absorbed by the system over a field cycle $T = 2\pi n$ is

$$\begin{aligned} P &= \frac{1}{T}\int_0^T H(t)\frac{dm}{dt}dt \qquad (4.18)\\ &= \frac{1}{T}\int_0^T \Big(\frac{H_0 e^{i\omega t} + H_0^* e^{-i\omega t}}{2}\Big)\Big(\frac{im(\omega)e^{i\omega t} - i\omega m^*(\omega)e^{-i\omega t}}{2}\Big)\\ &= \frac{1}{4T}T[i\omega H_0^* m(\omega) - i\omega H_0 m^*(\omega)]\\ &= \frac{1}{2}Re[-i\omega H_0 m^*(\omega)]\\ &= \frac{\omega}{2}Re[-iH_0(\chi_1(\omega)+\chi_2(\omega))H_0^*]\\ &= \frac{\omega|h|^2}{2}Re(-i\chi_1(\omega)+\chi_2(\omega))\\ &= \frac{\omega|h|^2}{2}\chi_2(\omega). \end{aligned}$$

Hence we see that the out of phase component is related to the total power absorbed by the magnetic system due to interaction with the field. Similarly, a Debye relaxation process with a single relaxation time is related to the in-phase susceptibility through the Casimir-Du Pre equations [68],

$$\chi(\omega) = \frac{\chi_T - \chi_S}{1 + i\omega\tau} + \chi_S, \qquad (4.19)$$

where $\chi_{T,S}$ are the isothermal and adiabatic susceptibilities, respectively, defined as

$$\chi_S = \Big(\frac{\partial M}{\partial H}\Big)_S = \chi_1(\omega), \qquad (4.20)$$

$$\chi_T = \Big(\frac{\partial M}{\partial H}\Big)_T = \chi_1(0). \qquad (4.21)$$

4.1.3 Kramers-Kronig Relation

The Kramers-Kronig relation connects the real and the imaginary parts of any complex function which is analytic in the upper-half of the complex plane. For the susceptibilities, it takes the form [69]

$$\chi_1(\omega) - \chi(\infty) = \frac{1}{\pi}\mathcal{P}\int_\infty^\infty \frac{\chi_2(\omega')}{\omega' - \omega}d\omega', \qquad (4.22)$$

$$\chi_2(\omega) = -\frac{1}{\pi}\mathcal{P}\int_\infty^\infty \frac{\chi_1(\omega') - \chi_\infty}{\omega' - \omega}d\omega'. \qquad (4.23)$$

where $\mathcal{P}$ denotes the principal value of the integral, which gives us a physical relationship between the absorption and dispersion. These relations imply that knowledge of the dissipative part of the response completely specifies the reactive response and vice versa. In general this is not sufficient for reconstructing physical response since it requires

knowledge of the susceptibility over the entire range $(-\infty, \infty)$, although for many systems it is sufficient to assume that the spectrum is symmetric around $\omega = 0$, such that the positive-frequency components imply the values for negative frequencies.

4.1.4 Fluctuation-Dissipation Theorem

The Fluctuation-Dissipation theorem for an ensemble of spins is reflected in the relationship between the spin-spin correlation function and the dissipative part of the response function. The magnetic correlation function is the spatial and temporal Fourier transform of the spin-spin autocorrelation, and is a quantity which is experimentally accessible via neutron scattering experiments. For a general system it takes the form

$$S^{ij}(q,\omega) = \frac{1}{2\pi}\int dt e^{-i\omega t}\langle S^i(-q,0)\cdot S^j(q,t)\rangle, \tag{4.24}$$

where the spatial Fourier transform is defined as

$$S^i(q,t) = \frac{1}{\sqrt{N}}\sum_i e^{-iq\cdot r_n} S_n^\alpha(t), \tag{4.25}$$

where $i,j = x,y,z$ label different Cartesian directions and the sum n is over discrete spin sites. The magnetic correlation function may be simplified to

$$S^\alpha(q,t) = \frac{1}{\sqrt{2\pi}}\sum_i \int dt e^{-i\omega t} e^{-iq\cdot r_i}\langle S_0^\alpha(t)\cdot S_i^\beta(t)\rangle. \tag{4.26}$$

The Fluctuation-Dissipation theorem is then seen in the relationship between the out of phase susceptibility and the symmetric spin-spin correlation function,

$$S^{ij}(q,\omega) = \frac{1}{\pi}\frac{1}{g^2\mu_B^2}\frac{k_BT}{\omega}\bar{\chi}^{ij}(q,\omega), \tag{4.27}$$

where $\bar{\chi}$ is the symmetric tensor of absorption, which is defined in terms of the out-of-phase susceptibility as

$$\bar{\chi}_{ij}(q,\omega) = \frac{1}{2}\Big(\chi_2^{ij} + \chi_2^{ij}(q,\omega)\Big), \tag{4.28}$$

The most important implication of the Fluctuation-Dissipation theorem in the context of our numerical simulations is that it relates the average power absorbed by the spin system in its interaction with the bath to the complex part of the susceptibility and to the spin-spin correlation function as,

$$P_{avg}(q,\omega) = \omega\chi_2^{\alpha\alpha}(q,\omega) = \frac{\pi g^2\mu_B^2}{k_BT}\omega^2 S^{\alpha\alpha}(q,\omega). \tag{4.29}$$

Hence in general we anticipate that the out-of-phase susceptibility should be a positive quantity for all frequencies whether we are implementing a Markovian or non-Markovian model. While the non-Markovian extensions to the models considered may alter the detailed dynamical and relaxational properties of the spin-bath system, we anticipate that the thermodynamic equilibrium properties should be the same.

4.2 DISCRETE ORIENTATION APPROXIMATION

The *discrete orientation approximation* is an approximation to the full dynamics of superparamagnetic relaxation, valid in the case that the constraining energy barriers are large in comparison to the thermal energy scale, $\sigma > 1$, but is less than some critical value such that interwell transitions would be inhibited altogether. [70] In this case, the magnetisation $\mathbf{M}$ does not assume a continuous angular distribution but is instead restricted only to certain stable orientations which correspond to local minima of the spin Hamiltonian.

In this case, we assume the system may be modelled according to a rate equation, according to which the spin occupies the labelled energy minima with probability n_i, where each integer i corresponds to a given fixed orientation. Transitions between these minima occur according to characteristic rates determined by the energy barriers of the system. The rate of change of the population in a given orientation then assumes a rate equation of the form,

$$\dot{n}_i = \sum_{j \neq i} (\kappa_{ji} n_i - \kappa_{ji} n_j), \tag{4.30}$$

where κ_{ij} is the transition probability or escape rate out of orientation i into the orientation j, with individual well populations evolving at a rate that is proportional to the population in each well and the fixed transition rate between the wells, which is determined thermodynamically. The dynamics is then specified by N such rate equations for the N stable orientations. As the total probability of the spin occupying any well is always subject to the normalisation condition $\sum_{i=0}^{N} n_i = 1$, the sum of the individual rates must then balance out, $\sum_{i=0}^{N} \dot{n}_i = 0$, hence there is a redundancy in the description and we need only consider $N - 1$ rate equations as the time-evolution of the other populations will always imply the Nth.

For a uniaxial single-domain particle with magnetic field applied parallel to its easy axis, the free energy, [71], is

$$E/KV = 1 - 2hx - x^2, \tag{4.31}$$

with K the anisotropy constant, V the particle volume, and the reduced field $h = H/H_K$ where $H = H(t)$ is the time dependent applied magnetic field, and $H_K = 2K/M_s$ is the anisotropy field. Further, M_s is the saturation magnetization of the particle, and $x = \cos\vartheta$, where ϑ is the angle spanned by the magnetization vector and the applied field.

At $|h| < 1$ the system has two local minima located at $x = \pm 1$, and thermally activated transitions between these two minima take place with rates $\kappa_{12} = \kappa_{1\to 2}$ and $\kappa_{21} = \kappa_{2\to 1}$. Neglecting all intrawell processes [72–74], the thermally activated dynamics of the system are then given by the discrete orientation rate equation. [71, 75] for the occupation probabilities n_1 and n_2, Hence, there are only two stable orientations corresponding to the easy-axis directions. The rate equations are then

$$\dot{n}_i = -\kappa_{12} n_1 + \kappa_{21} n_2 \qquad \dot{n}_2 = \kappa_{12} n_1 - \kappa_{21} n_2. \tag{4.32}$$

Utllising the probability normalisation, $n_2 = 1 - n_1$, they become

$$\dot{n}_1 = -(\kappa_{21} + \kappa_{21}) n_1 + \kappa_{21} \qquad \dot{n}_2 = -(\kappa_{21} + \kappa_{21}) n_2 + \kappa_{12}. \tag{4.33}$$

The total magnetisation, given as the difference in the population of the two wells, follows from the individual rate equations, and in fact completely specifies the behaviour as only one rate equation is necessary for such a system. The magnetisation evolves as

$$\frac{dm}{dt} = \frac{d(n_1 - n_2)}{dt} = -(\kappa_{12} + \kappa_{21}) m(t) + (\kappa_{21} - \kappa_{12}). \tag{4.34}$$

Then the population of both wells and the overall magnetisation $m = n_1 - n_2$, approach their equilibrium value with a simple exponential rate, $e^{-(\kappa_{12}+\kappa_{21})t} = e^{-\Gamma t}$, with the reversal characterised by the escape frequency $\Gamma = \kappa_{12} + \kappa_{21}$, implying a reversal time $\tau = \Gamma^{-1}$. The model is also applicable to the case of a transverse applied field, where the escape time and rate are related as $\tau = (2\Gamma)^{-1}$, and for more complex potentials, such as biaxial anisotropy with two saddle points [70].

For the uniaxial spin energy the transition rates are implied by the energetics at the well which lie parallel and anti-parallel to the applied field, thus $\kappa_{12} = f_0 \exp[-\sigma(1+h)^2]$, and $\kappa_{21} = f_0 \exp[-\sigma(1-h)^2]$ where f_0 is the prefactor, usually taken to be a constant [70, 76] and $\sigma = KV/k_B T$ where k_B is the Boltzmann constant and T the ambient temperature.

4.2.1 Debye Formulas

The Debye formulas determine the initial AC response of a general two level, equilibrium system to an applied AC perturbation. The general theory is immediately applicable to

the dynamic magnetic susceptibility [77] [78]. The Debye formulas may be derived from the Markovian master equation, where we make the assumption of an oscillatory AC-field applied along the z-axis, of the form

$$h(t) = h_0 \cos \omega t, \tag{4.35}$$

where $0 < h_0 \ll 1$ is a small field amplitude, and ω is the frequency of oscillation of the field. This field enters the master equation via the transition rates, κ_{ij}, with the corresponding susceptibility being derived by solving the magnetisation as a function of time. We first expand the expressions for the individual transition rates to first order in h_0,

$$\begin{aligned} \kappa_{12} &= f_0 \exp\left[-\sigma(1+h)^2\right] = f_0 \exp\left[-\sigma(1+2h_0\cos(\omega t))\right] \\ \kappa_{21} &= f_0 \exp\left[-\sigma(1-h)^2\right] = f_0 \exp\left[-\sigma(1-2h_0\cos(\omega t))\right]. \end{aligned} \tag{4.36}$$

We then calculate the relevant rates occurring in Eq. 4.57 for the total magnetisation,

$$\begin{aligned} \kappa_{12}+\kappa_{21} &= f_0 \exp\left[-\sigma(1+2h_0 cos(\omega t))\right] + f_0 \exp\left[-\sigma(1-2h_0 cos(\omega t))\right] \\ &= f_0 e^{-\sigma}\Big[\exp\left(2h_0\cos(\omega t)\right) + \exp\left(-2h_0\cos(\omega t)\right)\Big] \\ &= f_0 e^{-\sigma}\Big[1+2h_0\cos(\omega t) + 1 - 2h_0\cos(\omega t)\Big] = 2f_0 e^{-\sigma}, \end{aligned} \tag{4.37}$$

where we have expanded the exponential factors to the first order in h_0, and we will henceforth define $\Gamma = 2f_0 e^{-\sigma}$.

Similarly, the difference of the rates found in Eq. 4.57 is evaluated as

$$\begin{aligned} \kappa_{12}+\kappa_{21} &= f_0 \exp\left[-\sigma(1+2h_0 cos(\omega t))\right] - f_0 \exp\left[-\sigma(1-2h_0 cos(\omega t))\right] \\ &= f_0 e^{-\sigma}\Big[\exp\left(2h_0\cos(\omega t)\right) - \exp\left(-2h_0\cos(\omega t)\right)\Big] \\ &= f_0 e^{-\sigma}\Big[1+2h_0\cos(\omega t) - 1 + 2h_0\cos(\omega t)\Big] = 2\Gamma h_0\cos(\omega t). \end{aligned} \tag{4.38}$$

The magnetisation in the presence of the oscillating field then evolves according to

$$\frac{dm}{dt} = -\Gamma m(t) + 2\Gamma h_0 \cos(\omega t). \tag{4.39}$$

Hence we have a simple first-order differential equation for the total magnetisation. This is solved by the choice of integrating factor, $e^{-\Gamma t}$, yielding for the formal solution of magnetisation vs time,

$$m(t) = \frac{2h_0\Gamma^2}{\Gamma^2+\omega^2}\cos(\omega t) + \frac{2h_0\Gamma\omega}{\Gamma^2+\omega^2}\sin(\omega) + Ce^{-\Gamma t} + O(h_0^2), \tag{4.40}$$

and as we are interested in the long-time behaviour, we ignore the exponential term and the time-evolution of the magnetisation in the steady state is

$$m(t) = h_0\Big[2q\frac{\Gamma^2}{\omega^2+\Gamma^2}\cos(\omega t) + 2q\frac{\omega\Gamma}{\omega^2+\Gamma^2}\sin(\omega t)\Big] = h_0(\chi_1\cos\omega t + \chi_2\sin\omega t) + O(h_0^2), \tag{4.41}$$

where we identify the in-phase and out-of-phase components of the magnetic response with their corresponding Debye susceptibilities,

$$\chi_1(\omega) = 2\sigma\frac{\Gamma^2}{\omega^2+\Gamma^2} \tag{4.42}$$

$$\chi_2(\omega) = 2\sigma\frac{\omega\Gamma}{\omega^2+\Gamma^2} \tag{4.43}$$

It should be noted that we use only $O(h_0)$ terms of the relaxation rates whose precise form is thus irrelevant. For this reason Debye susceptibilities, Eq. 4.42 and Eq. 4.43, are quite general and hold also for other physical quantities, such as electric susceptibility [77].

The Debye formulas are thus derived from the assumption of a Markovian master equation. It is interesting, then, to consider the effects of the non-Markovian extension of such rate equations on these well-understood Debye formulas. This provides an important generalization of the Debye formulas and a point of comparison with the non-Markovian LLMS model.

4.3 NUMERICAL CALCULATION OF AC SUSCEPTIBILITY

In order to calculate the susceptibility from numerical Langevin equations we could, naively, thermalise the spins in zero magnetic field before evolving them in the presence of a magnetic field with some arbitrary complicated time profile, and calculate the susceptibility as the ratio of the Fourier transforms of the field and spin according to Eq. 4.2, However, such a problem is ill-posed problem in the Hadamard sense, which means that we need data with extremely small statistical error in order to obtain dependable information on the spectrum of the susceptibility, $\chi(\omega)$.

However, it is both computationally cheaper and more convenient to calculate the response on a component by component basis for an applied field with a single well-defined frequency of oscillation,

$$H_z = h_0\cos(\omega t). \tag{4.44}$$

The system is first initialised along the positive z-axis, $S_z = 1$, and is simulated until equilibrium. a magnetic field with a magnitude that oscillates at a single well-defined

frequency is then applied to the equilibriated system, and the real and complex components of the susceptibility are calculated via the Sine and Cosine Fourier transform of the magnetic response, respectively,

$$\chi_1(\omega) = \frac{1}{h_0}\frac{1}{N}\sum_{i=1}^{N}\langle S_z\rangle \cos(\omega t), \tag{4.45}$$

$$\chi_2(\omega) = \frac{1}{h_0}\frac{1}{N}\sum_{i=1}^{N}\langle S_z\rangle \sin(\omega t), \tag{4.46}$$

where N is the total number of steps taken in calculating the susceptibility, and $\langle S_z\rangle$ is the average z-component of the magnetisation for the ensemble of spins. It is important that the total number of steps is taken such that the spin is subjected to an integer number of field cycles, $N = 2\pi N_c/\omega\Delta t$, and we generally use a value of $N \geq 1000$.

To ensure that the response is in the linear regime the calculations are repeated for various values of the field amplitude, h_0, and when the obtained values do not depend on the amplitude, we are in the linear regime. We choose values of h_0 which are as large as possible while still remaining within the linear response regime, in order to minimise statistical errors. The simulation is then repeated sufficiently many times so as to resolve all of the salient features of the magnetic response.

4.3.1 Statistical Errors

When computing the dynamic response, statistical errors occur in the calculated quantities as we are averaging stochastic data for a finite number of isolated spins at a finite number of time intervals, resulting in a set of statistically independent measurements of the computation, N_m, calculated over a cycle of the oscillating field. We may see the correct way to reduce such systematic errors by following ref [79]. Generically such measurements over a single field cycle can be expressed as

$$Q_n = \int_n dt f[m_1(t), ..., m_N(t)]g(t), \tag{4.47}$$

where N is the number of spins being simulated, and $g(t)$ is a sinusoidal function of time. In the case that g is taken as the cosine or sine of the oscillating field amplitude, we have the sine and cosine Fourier transform giving rise to the in and out of phase components of the susceptibility. The exact result is then the average of the N_m outcomes,

$$q = \frac{1}{N_m}\sum_{n=1}^{N_m} Q_n. \tag{4.48}$$

To increase the accuracy of such ensemble averages we might initially consider to increase the number of spins in the ensemble or increase the number of field oscillations over which the average is computed. The lth order cumulants of the quantities q and Q have the relationship

$$\kappa_l(q) = N_m^{-(l-1)}\kappa_l(Q). \tag{4.49}$$

For large numbers of measurements the q distribution becomes Gaussian to a good approximation due to the central limit theorem. Hence the result of a measurement lies in the interval $(q + \sqrt{\kappa_2(q)}, q - \sqrt{\kappa_2(q)})$, and the statistical error of the measurement is $2\sqrt{\kappa_2(q)}$. The relative fluctuation is then simply given as

$$\frac{\delta q}{q} = \frac{\sqrt{\kappa_2(q)}}{q} = \frac{1}{\sqrt{N_m}}\frac{\delta Q}{Q} = \frac{1}{\sqrt{N_m}}\frac{\sqrt{\kappa_2(Q)}}{Q}. \tag{4.50}$$

The above considerations imply that to increase accuracy and decrease the relative fluctuation $\frac{\delta q}{q}$, it is not efficient to simply increase the number of measurements either by increasing the total time of the computation or the number of spins in the simulation, as in both cases the error only decreases by a factor of $\sqrt{N_m}$.

The expression for the field-cycle averaged values is similar to the calculation of thermal equilibrium quantities only over some arbitrary timescale rather than one which is related to the cycles of the external field. For such an equilibrium system we have the relationship

$$\frac{\partial}{\partial H}\langle m_z\rangle = \frac{1}{k_B T}[\langle m_z^2\rangle - \langle m_z\rangle^2], \tag{4.51}$$

which holds regardless of the magnitude of the external field H. The total magnetization in the field direction is then the time-average of the moment per spin,

$$M_{z,n} = \int_n dt \frac{m_z(t)}{t_m N}, \tag{4.52}$$

then the statistical error in the spin magnitude calculation is

$$\frac{\delta M_z}{M_z} = \frac{1}{\sqrt{t_m N}}\frac{\sqrt{k_B T \partial M_z/\partial H}}{M_z} \tag{4.53}$$

which again implies that enlarging either the time or the number of spins is inefficient to increase accuracy. However, the quantity $\sqrt{k_B T \partial M_z/\partial H}$ and hence the statistical error decreases with increasing H for very general functional dependence of the spin on the applied field. Hence, to increase accuracy of calculations of the susceptibility, we will apply the largest probing field possible without departing from the linear response regime such that $m \propto \chi H$. This procedure optimizes calculations by reducing the quantity $\delta M/M$.

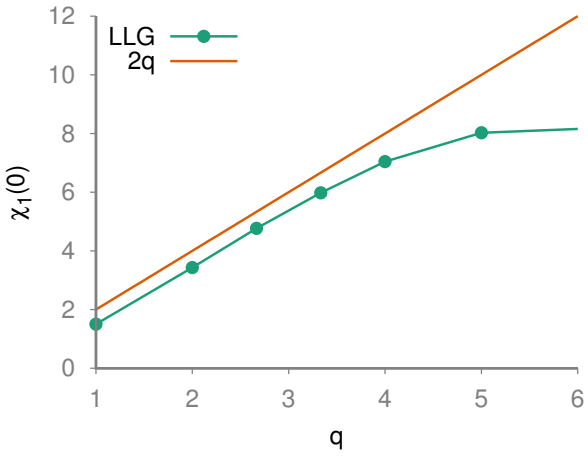

Figure 4.1: Static susceptibility vs reduced barrier height as predicted by the Debye equations, and from numerical simulations for a Co nanoparticle utilising the Landau-Lifshitz-Gilbert model.

4.3.2 Longitudinal Response vs Temperature

To verify that our procedure for calculating the susceptibilities is adequate, we first calculate the temperature-dependence of the susceptibility of a superparamagnetic particle using the LLG-Langevin equation, allowing us to compare the predictions of the discrete orientation model to the numerical evaluation of the susceptibilities.

We consider an ensemble of non-interacting nanoparticles represented as single-domain magnetic moments, with material parameters chosen so as to be comparable to a Co nanoparticle. The external constant bias field is taken to be 0 for all spins in the sample, while the anisotropy axes are assumed to be parallel for all spins in the ensemble, with the oscillating field again taken to be parallel to the anisotropy axis, allowing us to investigate the linear parallel susceptibility of the spins.

The material parameters are taken such that for a particle with a volume of $V = 8 \times 10^{-24} m^3$ and anisotropy energy density $K_e = 4.2 \times 10^5 J/m$, the anisotropy is then $k_u = 3.36 \times 10^{-18} J$ with a magnetic moment of $\mu_s = 1.12 \times 10^{-17} J/T$. The temperature and damping parameters are taken such that $\sigma = 2$ and $\alpha = 0.5$. An ensemble of $10,000$ spins were used for the simulations.

Figure 4.1 depicts the variation of the static ($\chi_1(0) = \chi_0$) component of the Debye susceptibility, and the static magnetic susceptibility for the Co nanoparticle calculated from numerical simulations of the LLG equation, for values of the reduced barrier height

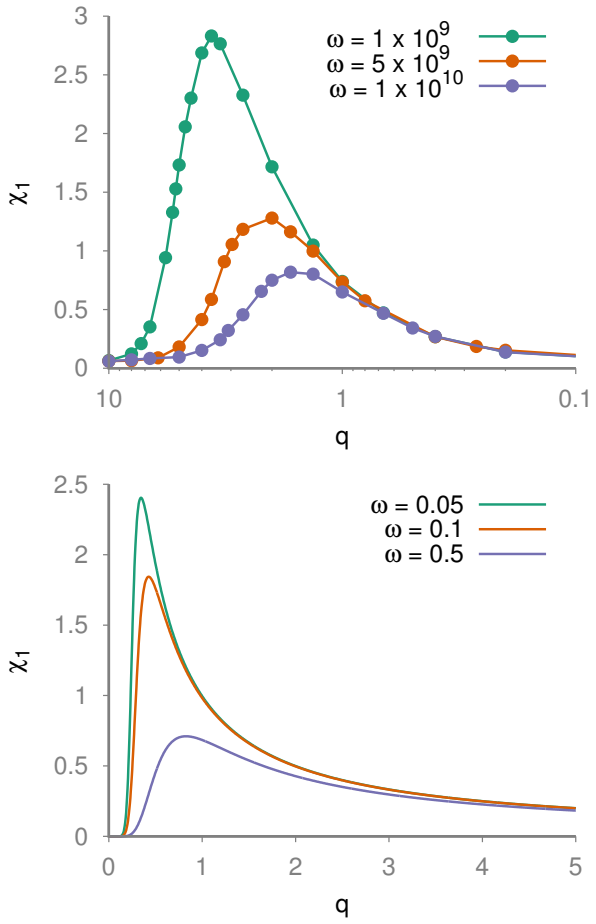

Figure 4.2: χ_1 vs σ from **Top**: LLG simulations for a Co nanoparticle and **Bottom**: Debye susceptibility from the analytical master equation.

$\sigma > 1$, such that the spin energy is confined to stable easy-axis directions of the anisotropy, allowing direct comparison of the models. The Debye equations predict a simple linear dependence $\chi_0 = 2\sigma$ of the static susceptibility. For $\sigma < 4$ the numerical simulations reproduce such a dependence. At higher σ, transitions between the stable orientations are inhibited altogether, such that the spin is restricted to a single direction, giving a constant magnetisation and hence χ_0 for increasing σ.

In Figure 4.2, we compare the barrier height dependence of the in-phase component of the response. The numerical simulations are compared to Debye susceptibilities for a system with a transition rate of $\Gamma = 1s^{-1}$. The response breaks down into two regimes, corresponding to $T > T_B$ and $T < T_B$. At low temperatures, the longitudinal relaxation time, $\tau_{||}$, is much larger than the dynamical measurement time, which is simply related to the field frequency, $\tau_m = 2\pi/\omega$. Hence, overbarrier transitions between the wells occur

with vanishingly small probability, even for a large number of field cycles, and the response at low T is then almost entirely due to rotation of the moments near the bottom of the well. The intrawell modes are very fast, so that the spin adjusts almost instantaneously to the field, leading to a small and mostly in-phase response to the field.

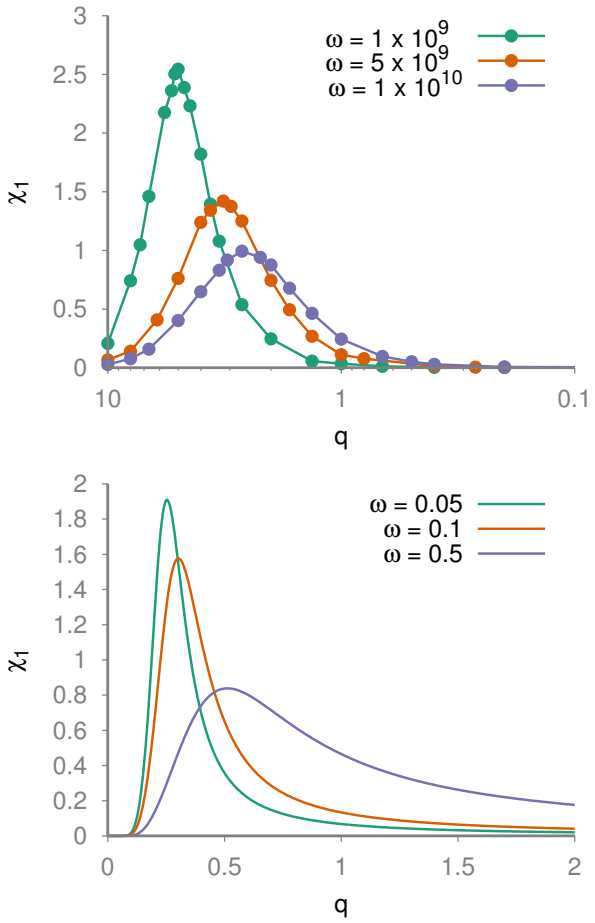

Figure 4.3: χ_2 vs σ from **Top**: LLG simulations for a Co nanoparticle and **Bottom**: Debye susceptibility from the analytical master equation.

As T increases, the spins start to be able to overcome the barrier with some small probability over the course of a number of field cycles at an ω-dependent value of the temperature. This leads to a sharp increase in the response, however the thermally-activated response is not very large at these temperatures, which implies a larger lag between the spin and the field and hence much of the response is out of phase in this region. As T continues to increase the overbarrier rotations occur more frequently, and the in-phase response increases dramatically. This continues until the overbarrier process occurs at a much higher frequency than the frequency of the oscillating field, resulting in a

frequency-dependent peak in the response which corresponds to the blocking temperature, T_B, for the particles. In the limit of very high temperatures, the response tends to 0 as the thermal dynamics start to dominate over the response to the field.

We can see that both models reproduce this qualitative behaviour, with the characteristic peak of the in-phase response becoming larger and shifting to lower temperatures as the frequency of the field decreases, and both models predicting that the in-phase response converges and diminishes in the limit of higher temperatures. The qualitative dependence for the out of phase component, $\chi_2(\omega)$, shown in Figure 4.3 is also similar with the larger out-of-phase response occurring at intermediate temperatures. Overall, it is evident that the Debye model is readily comparable to the simulations of the stochastic LLG equation.

4.4 AC SUSCEPTIBILITY FOR NON-MARKOVIAN SYSTEMS

Having considered the response in the Markovian case for both the full Langevin dynamics and the discrete orientation approximation, we may now extend both models by allowing the dynamics to depend not just on the present state of the system but also on its recent history.

4.4.1 Generalised Master Equation

The standard extension of the Master Equation formalism given in Equation 4.30, to incorporate non-Markovian behaviour is the *Generalized Master Equation*, under which the simple transition rates are promoted to integro-differential expressions over recent well populations, using a set of memory kernels,

$$\dot{\mathbf{P}}_i(t) = \mathbf{A}_{ij}\mathbf{P}_j \rightarrow \dot{\mathbf{P}}(t) = \int_0^t \mathbf{M}(t-s)\mathbf{P}(s), \tag{4.54}$$

where $\mathbf{P}$ is a vector of state populations, $\mathbf{A}$ is a matrix of their transition rates, κ_{ij}, and $\mathbf{M}(t)$ is an $i \times j$ matrix of memory kernel functions. Rate equations of this form have been widely applied in both the context of open quantum systems, where the vector $\mathbf{P}$ is composed of probability amplitudes, and in classical statistical mechanical problems, such as transport and relaxation phenomena, in superradiance and laser processes [80], and in the context of continuous-time random walks. The non-Markovian extension to the discrete orientation model is then most generally expressed as

$$\dot{n}_i = \Big[\sum_{j \neq i} \int_0^\infty M_{ij}(t-s) n_i(s) ds - \int_0^\infty M_{ji}(t-s) n_j(s) ds \Big]. \tag{4.55}$$

We will make the simplifying assumption that the the form of the memory is generic between wells, with the individual rates again determined by the energetics of the system. The set of memory kernels are then drastically simplified such that

$$M_{ij}(t-s) = \kappa_{ij}(s)K(t-s), \tag{4.56}$$

where now we need only consider the single memory kernel $K(t)$. In the context of the discrete orientation model,

$$\frac{dm}{dt} = -\int_0^t K(t-s)[\kappa_{12}(s)+\kappa_{21}(s)]m(s)ds + \int_0^t K(t-s)[\kappa_{12}(s)-\kappa_{21}(s)]ds, \tag{4.57}$$

where we now have an integro-differential expression for the rate of change of the magnetisation.

We will now assume that the memory kernel $K(t)$ is completely specified by a single characteristic correlation time, and has the exponential form [60, 81]

$$K(t) = \frac{e^{-t/\Theta}}{\Theta} \to \delta(t) \text{ as } \Theta \to 0, \tag{4.58}$$

where Θ is the memory time. We stress here that this time is not necessarily the same as the quantity that appears in the coloured noise expression.

We may now utilise the Generalized Master Equation approach to evaluate the Debye susceptibilities for such a damped system by applying the oscillatory field. The transition rates, to first order in h_0, again take the form of Eqs 4.38 and 4.39, and the time-evolution of the magnetisation is now composed of two convolution integrals

$$\frac{dm}{dt} = -\Gamma\int_0^t K(t-s)m(s)ds + 2\Gamma h_0\int_0^t K(t-s)\cos(\omega s)ds, \tag{4.59}$$

which is readily solved by first taking the Laplace transform.

$$rm(r) - m_0 = -\Gamma\bar{K}(r)m(r) + 2\Gamma h_0\bar{K}(r)\bar{\cos}(\omega t), \tag{4.60}$$

where have made use of the convolution theorem, r is the frequency-space variable and the notation $\bar{f} = \mathcal{L}[f(t)](r)$ denotes the application of the Laplace transform to the function $f(t)$. For simplicity we will assume the initial magnetisation $m_0 = 0$, as we are interested in the long-time, steady-state result, which is in fact independent of the initial magnetisation. Applying the Laplace transform to the constituent functions,

$$\mathcal{L}[K(t)](r) = \frac{1}{1+r\Theta} \qquad \mathcal{L}[\cos(\omega t)](r) = \frac{r}{r^2+\omega^2}. \tag{4.61}$$

We arrive at the expression for the Laplace transform of the magnetisation,

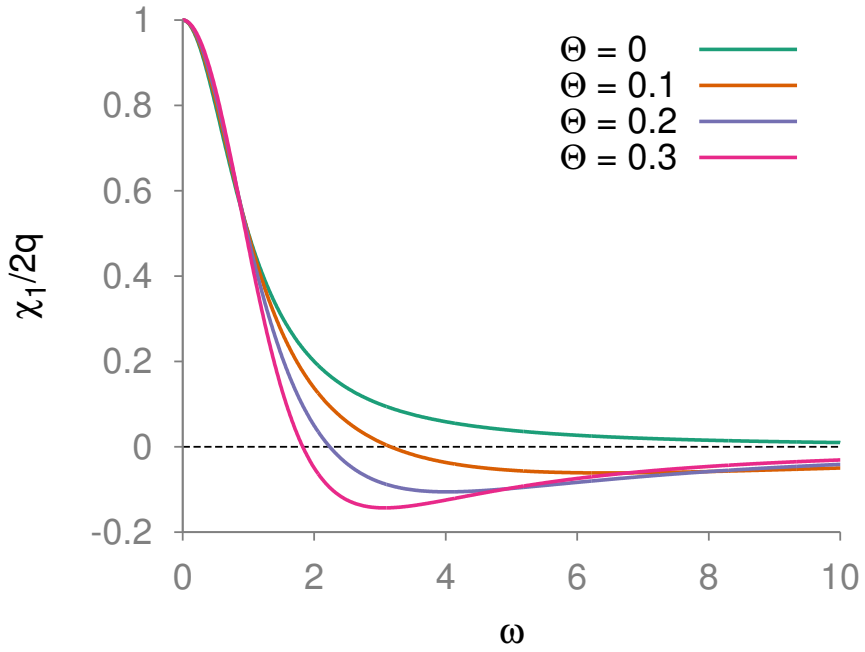

Figure 4.4: The in-phase component of the AC susceptibility versus the frequency ω of the probing field. The rate is assumed to be $\Gamma = 1$ Hz. For non-zero correlation time, there is a frequency dependent phase transition to diamagnetic behaviour.

$$m(r) = \left[\frac{2\Gamma h_0}{\Gamma + r + r^2\Theta}\right]\left[\frac{r}{r^2+\omega^2}\right]. \tag{4.62}$$

By taking the inverse Laplace transform we arrive at the long time, steady state solution in which the exponentially decaying components of the response tend to zero, which has the form

$$m(t) = \frac{\Gamma - \Theta\omega^2}{\Gamma^2 - 2\Gamma\Theta\omega^2 + \Theta^2\omega^4 + \omega^2}\cos(\omega t) + \frac{\Gamma\omega}{\Gamma^2 - 2\Gamma\Theta\omega^2 + \Theta^2\omega^4 + \omega^2}\sin(\omega t), \tag{4.63}$$

which is similar to the ordinary master equation, with susceptibilities modified due to the non-zero correlation time of the states. The in-phase and out-of-phase susceptibilities become,

$$\chi_1(\omega) = 8\sigma\tilde{n}_{\uparrow\uparrow}\frac{\Gamma(\Gamma - \omega^2\Theta)}{\omega^2 + (\Gamma - \omega^2\Theta)^2}, \tag{4.64}$$

$$\chi_2(\omega) = 8\sigma\tilde{n}_{\uparrow\uparrow}\frac{\omega\Gamma}{\omega^2 + (\Gamma - \omega^2\Theta)^2}. \tag{4.65}$$

The in-phase susceptibility, $\chi_1(\omega)$, is plotted in Fig. 4.4. The most salient feature of the in-phase component is the fact that it becomes negative at sufficiently large frequencies for any $\Theta > 0$, passes through a local minimum, and only then rapidly approaches its

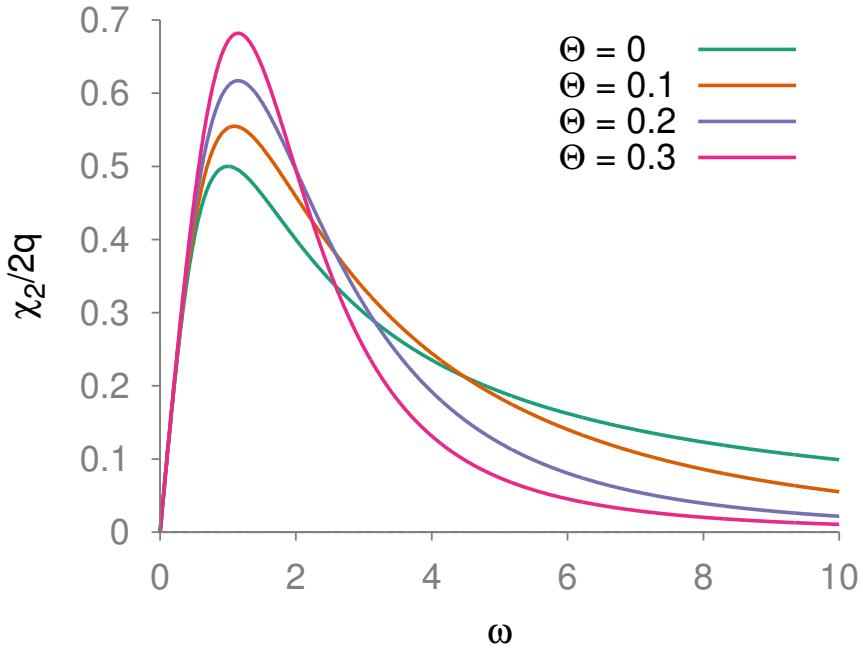

Figure 4.5: The out-of-phase components of the ac susceptibility, χ_2, versus the frequency ω of the probing field. The rate $\Gamma = 1$ Hz

asymptotic zero value from below. This means that the particle is paramagnetic at low frequencies, but diamagnetic at high frequencies. In the diamagnetic phase of the response the particle is apparently slowed down by the medium in which it finds itself, and cannot follow the rapidly oscillating field. One can therefore expect to find the frequency induced diamagnetism in particles suspended in viscous fluids. However, the effect has previously been observed experimentally in single crystals by Rhyee *et al.* [82] Theoretically the effect can be so strong that it would render the magnetic permeability negative [83].

The out-of-phase component, $\chi_2(\omega)$, is shown in Figure 4.5. It is interesting in that its peak grows significantly higher and narrower with increasing memory time, which implies that memory enhances energy losses and heating of the sample in a narrow frequency interval. This behavior is required from particles used to treat cancer by magnetic particle hyperthermia [84].

4.5 AC SUSCEPTIBILITY IN THE LLMS

The LLMS pair of Langevin equations provide an alternative way to introduce memory into our model of superparamagnetic spins via the frequency-dependent damping and noise

spectrum. We evaluate the in and out of phase components using the same method as in the LLG. In these simulations we choose the spin-bath coupling $\chi = \alpha/\tau_c\gamma$, such that $\alpha = 0.5$ in the corresponding uncorrelated system where $\tau = \tau_c\gamma H_k << 1$.

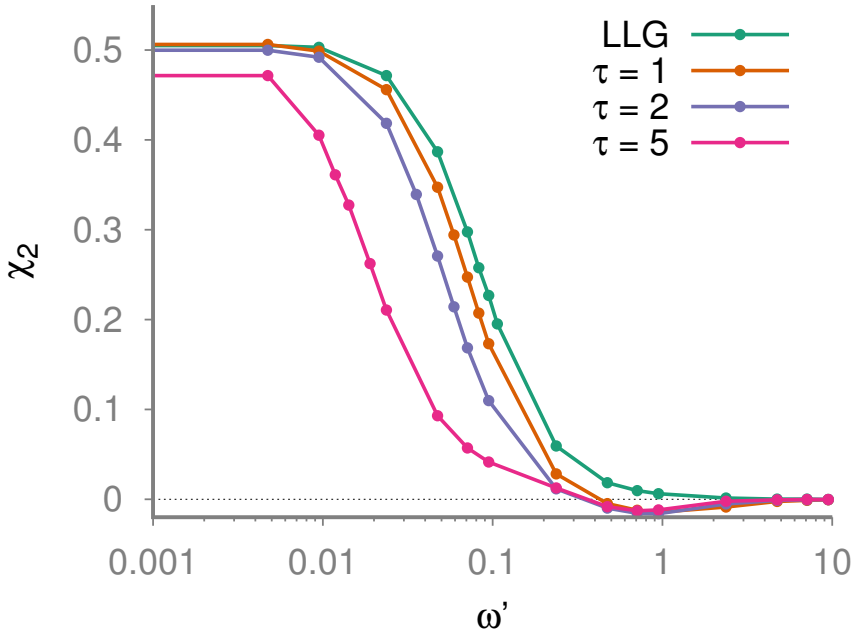

Figure 4.6: The variation of the real part of the susceptibility with the frequency, normalised by the Larmor frequency, $(\omega' = \omega/\gamma H_k)$ for various values of $\tau = (\gamma H_k)^{-1}\Theta$.

Figure 4.6 depicts the variation of the in-phase component of the magnetic response vs frequency calculated from LLMS simulations for various values of the correlation time. The LLG and LLMS simulations converge on the same value of $\chi_1(0) = \chi_0$ for the static susceptibility as frequency decreases. For low frequencies there is only a weak dependence of χ_1 on τ. However,for intermediate frequencies there is a monotonic decrease of χ_1 with τ. The effect of the correlation time is to decrease the in-phase response of the spin across the range of frequencies for $\omega' < 1$. This is a qualitatively similar behaviour to the change in the response in the non-Markovian extension of the master equation, where we again attribute the decrease in the response to the delay of the spin response to the oscillation of the magnetic field magnitude.

Figure 4.7 shows the variation of χ_1 at higher values of $\omega' > 1$, for values of the correlation time $\tau = 0.1, 0.2, 0.3$. This shows that the susceptibility in the LLMS becomes negative for a similar range of frequencies to the analytical prediction of the master equa-

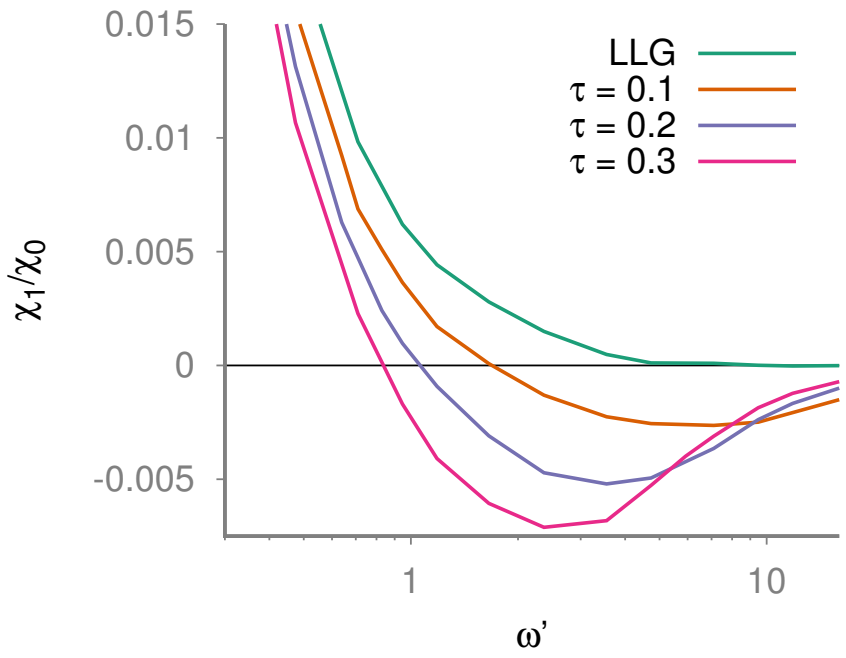

Figure 4.7: The variation of the real part of the susceptibility with the frequency, normalised by the Larmor frequency, ($\omega' = \omega/\gamma H_k$) for various values of $\tau = (\gamma H_k)^{-1}\Theta$, in the vicinity of the diamagnetic phase transition, for $\tau = 0.1, 0.2, 0.3$

tion and confirming that the negative susceptibility arises from a phase change induced by the slowing down of the response of the particle by the medium. For both models we note that with increasing correlation time, the transition to diamagnetic behaviour occurs at lower frequencies. In both cases, at low frequencies the timescale of the field oscillation is much longer than the correlation time, hence the field is less able to "resolve" the effects of the memory kernel.

We also note a qualitative similarity in the cross-over in the variation of χ_1 with frequency, in agreement with the analytical predictions, an indication that the different models imply similar physics. Figure 4.8 shows the variation of the susceptibility for higher values of the correlation time.

Finally, Figure 4.9, shows the variation of χ_2 with frequency. The behaviour is similar to the master equation for $\tau < 1$, with the magnitude of the peak increasing implying increased heating of the sample. At higher correlation times, the magnitude of the peak decreases implying that it then becomes more difficult to heat the sample, while still shifting the peak to lower frequencies. We note that as we increase the magnitude of the correlation time, the transition rate between the wells, Γ from the LLMS simulations

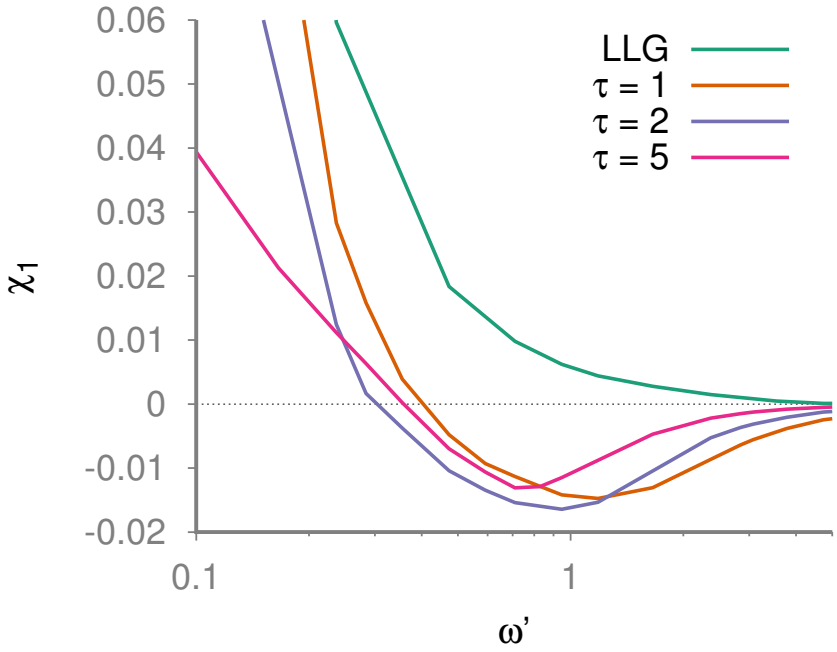

Figure 4.8: The variation of the real part of the susceptibility with the frequency, normalised by the Larmor frequency, $\omega' = \omega/\gamma H_k$) for various values of $\tau = (\gamma H_k)^{-1}\Theta$, in the vicinity of the diamagnetic phase transition, for $\tau = 1, 2, 5$.

tends to decrease, while for the master equation it is explicitly held constant. We attribute the difference between the two models to this fact, in that at long correlation times the decreasing escape rate will cause the peak to decrease more than the increasing correlations causes it to increase.

4.5.1 Longitudinal Susceptibility vs. Temperature

As an additional point of comparison between the LLMS and the generalised master equation, we present the variation of the real part of the susceptibility with the inverse barrier parameter, σ, in Figure 4.10. This gives us additional physical intuition regarding the diamagnetic susceptibility, where we see that both models predict similar high temperature behaviour. The picture for $\sigma < 1$ is then very similar to the Markovian case, where the spin is easily able to follow the direction of the oscillating field, and the response decreases as the increasing effect of temperature causes the spin to randomise. There is again a peak in the susceptibility, and if we interpret this as the blocking temperature we can see that both models predict an increase in the blocking temperature as the correlation time

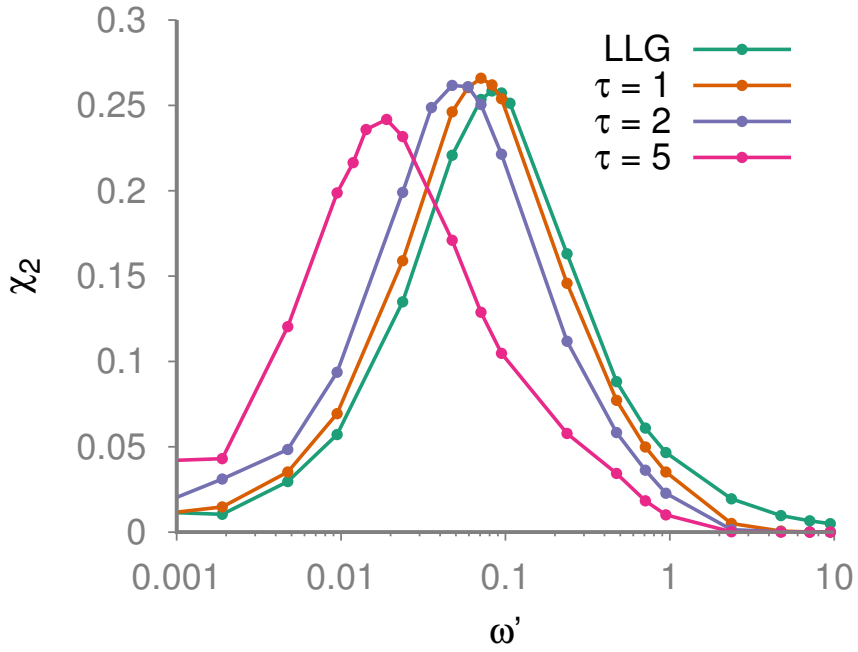

Figure 4.9: The variation of the imaginary part of the susceptibility with the frequency, normalised by the Larmor frequency, $\omega' = \omega/\gamma H_k$) for various values of $\tau = (\gamma H_k)^{-1}\Theta$.

increases.

Finally, an interesting point to note is that, for $\Theta > \Gamma/4$ in the master equation, the susceptibility may be negative across the entire temperature range, as evidenced by the $\Theta = 0.5$ curve in Figure 4.10. We do not see such behaviour in the LLMS. We again attribute this distinction to the fact that the escape rate decreases for any fixed χ in the LLMS, a property which we generally expect rate processes to adhere to for increasing correlation time, [85], while the fixed master equation rate allows the correlation time to exceed the escape time.

4.5.2 Critical Behaviour

We finally consider the critical frequency for the transition to diamagnetic behaviour. From Equ. 4.64 the transition to diamagnetic behavior occurs at the frequency $\omega_c^2 = \Gamma/\Theta \propto \tau^{-1}$ and so we estimate that

$$\Theta = f_0 \exp -(KV/kT)/\omega_c^2, \tag{4.66}$$

relating the measurable critical frequency to the correlation time Θ. In Figure 5.13 we show the correlation time dependence as exhibited by the LLMS and see that the low-τ

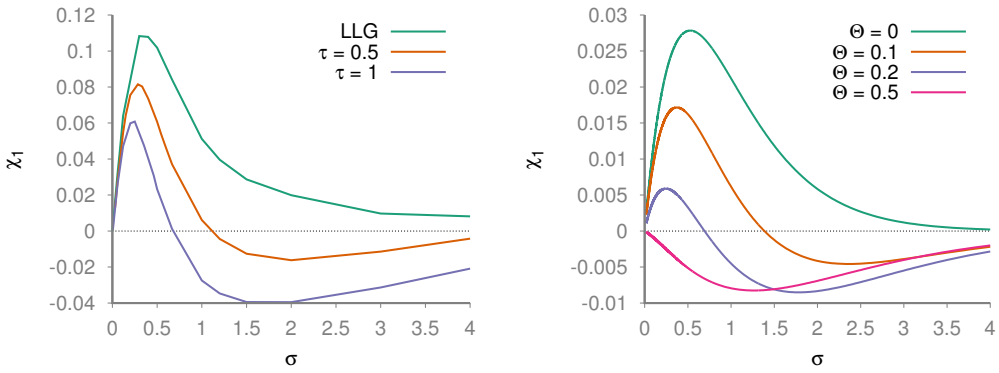

Figure 4.10: The in-phase susceptibility, χ_1 vs σ for $\omega' = 1$, **Left:** from LLMS simulations and **Right:** from the generalised master equation.

behaviour coincides qualitatively with the master equation. Overall, the behavior predicted by the LLMS approach shows non-monotonic behavior with an increase for large Θ. We anticipate that this departure is again due to the assumption of a fixed transition rate, Γ, between the wells in the master equation expression.

4.5.3 Interacting Media

So far we have only considered noninteracting ensembles of superparamagnetic spins. It is possible to consider an exactly solvable model system of two identical superparamagnetic particles with parallel easy axes [71,86]. The particles interact with each other via dipolar coupling, giving rise to two metastable magnetically ordered states and a magnetically neutral state, $\uparrow\uparrow$, $\uparrow\downarrow + \downarrow\uparrow$, and $\downarrow\downarrow$. The mutual coupling is determined by the bond angle, β, between the easy axes and is ferromagnetic if β is zero, $\beta = 0$, and antiferromagetic if $\beta = \pi/2$. The thermally driven dynamics of the particle pair, at the *small* applied fields of interest to the linear response regime, are described by the three level master equation [71]

$$\dot{n}_1 = -(2\kappa_{12} + \kappa_{21})n_1 - \kappa_{21}n_3 + \kappa_{21}, \tag{4.67}$$

$$\dot{n}_3 = -\kappa_{23}n_1 - (2\kappa_{32} + \kappa_{23})n_3 + \kappa_{23}, \tag{4.68}$$

where again we made use of the probability conservation $n_1 + n_2 + n_3 = 1$. The two particle occupation probabilities are $n_1 = n_{\uparrow\uparrow}$, $n_2 = n_{\uparrow\downarrow+\downarrow\uparrow}$, and $n_3 = n_{\downarrow\downarrow}$. n_2 corresponds to the demagnetized state, and the reduced magnetization is again the difference of the oppositely-oriented magnetised states, $m = 2(n_1 - n_3)$. The rates of the thermally

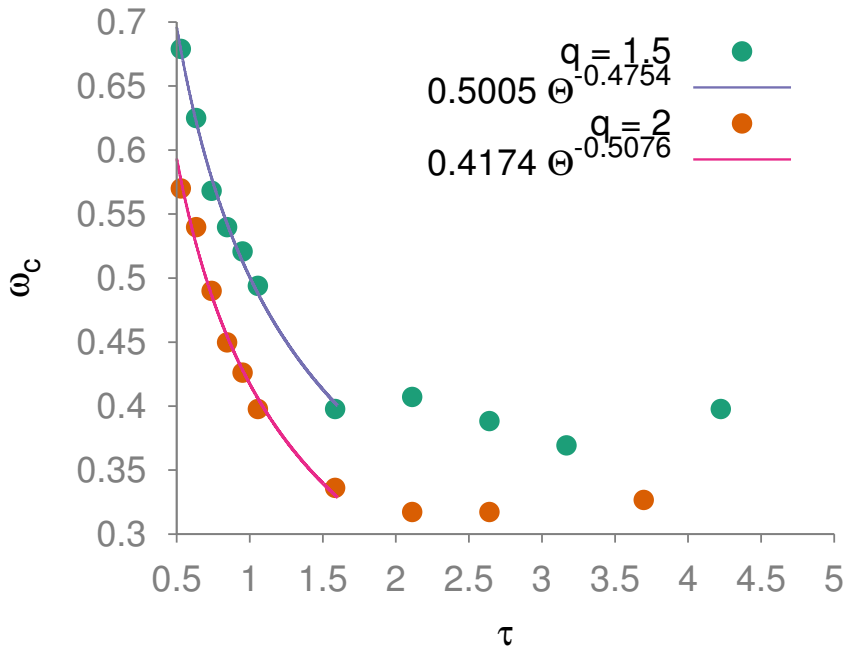

Figure 4.11: Estimated critical frequency, ω_c of diamagnetic phase transition vs correlation time and numerical fit for low Θ. The τ-dependence compares favourably to the prediction of the master equation, $\omega_c \propto \Theta^{-1}$ in this regime. The prefactor is similarly comparable to $\sqrt{e^{-q}}$ at low Θ.

activated transitions between the individual minima, $\kappa_{ij} = \kappa_{i\to j}$, are given by the formula

$$\kappa_{ij} = f_0 e^{-\sigma Q_{ij}}, \tag{4.69}$$

where the transition amplitudes are again derived from the energetics of the system.

$$Q_{12} = h_c^2 + \varepsilon\rho + 2h(2 - h_c), \tag{4.70}$$

$$Q_{21} = h_c^2 - 2hh_c, \tag{4.71}$$

$$Q_{23} = h_c^2 + 2hh_c, \tag{4.72}$$

$$Q_{32} = h_c^2 + \varepsilon\rho - 2h(2 - h_c). \tag{4.73}$$

Where we have the dipolar strength, ρ which varies with the distance between the pair of interacting spins as $\rho = M_s^2 V/2KR^3$, where R is the distance between the particles, the critical applied field h_c which and a normalisation factor ϵ. For ferromagnetic spins the bond angle $\beta = 0$, then the critical field $h_c^2 = (1-\rho)(1-3\rho)$ and $\varepsilon = 8$, while for antiferromagnetic coupling, $\beta = \pi/2$ we have $h_c^2 = (1-\rho)(1+3\rho)$ and $\varepsilon = -4$.

The rate of change of the magnetisation is then

$$\frac{dm}{dt} = \frac{d}{dt}(n_1 - n_3) = -(2\kappa_{12} + \kappa_{21} - \kappa_{23})n_1 - (\kappa_{21} - 2\kappa_{32} + \kappa_{23})n_3 + (\kappa_{21} - \kappa_{23}) \quad (4.74)$$

The individual rates occurring in Eq. 4.74 are then explicitly solved to first order in the applied field, h_0, as

$$\begin{aligned}
\kappa_{12} &= f_0 e^{-\sigma(h_c^2+\epsilon\rho)}\Big(1 - 2h_0\cos(\omega t)(2 - h_c)\Big), && (4.75)\\
\kappa_{21} &= f_0 e^{-\sigma h_c^2}\Big(1 + 2qh_c h_0\cos(\omega t)\Big) && (4.76)\\
\kappa_{23} &= f_0 e^{-\sigma h_c^2}\Big(1 - 2qh_c h_0\cos(\omega t)\Big), && (4.77)\\
\kappa_{32} &= f_0 e^{-\sigma(h_c^2+\epsilon\rho)}\Big(1 + 2h_0\cos(\omega t)(2 - h_c)\Big). && (4.78)
\end{aligned}$$

Upon inserting the rates into the time derivative of the magnetisation, Eq. 4.74 and introducing the rate now as $\Gamma = 2f_0 e^{-\sigma(h_c^2+\epsilon\rho)}$, may be reduced to an expression in terms of the overall magnetisation due to the fact that the expansion is first order in the transition rates, as

$$\frac{dm}{dt} = -\Gamma m(t) + 2\Gamma h_0\cos(\omega t), \quad (4.79)$$

which has the same form as the problem in the absence of interactions and hence implies the same magnetisation and susceptibilities, only with the rate Γ modified due to the interaction of the spin pair.

Introducing now memory into Eq. 4.74 by again promoting the transition amplitudes to memory kernels, the individual equations become,

$$\begin{aligned}
\dot{n}_1 &= -(2\kappa_{12} + \kappa_{21})n_1 - \kappa_{21}n_3 + \kappa_{21} && (4.80)\\
\rightarrow &- \int_0^t K(t-s)[(2\kappa_{12}(s) + \kappa_{21}(s))]n_1(s)\\
&- \int_0^t K(t-s)\kappa_{21}(s)n_3(s)\\
&+ \int_0^t K(t-s)\kappa_{21}(s),
\end{aligned}$$

$$\begin{aligned}
\dot{n}_3 &= -\kappa_{23}n_1 - (2\kappa_{32} + \kappa_{23})n_3 + \kappa_{23} && (4.81)\\
\rightarrow &- \int_0^t K(t-s)\kappa_{23}(s)n_1(s)\\
&- \int_0^t K(t-s)[(2\kappa_{32}(s) + \kappa_{23}(s))]n_3(s)\\
&+ \int_0^t K(t-s)\kappa_{23}(s),
\end{aligned}$$

and implying magnetisation evolves as

$$\begin{aligned} \dot{m} = & - \int_0^t K(t-s)\Big[2\kappa_{12}(s) + \kappa_{21}(s) - \kappa_{23}(s)\Big] n_1(s) ds \\ & - \int_0^t K(t-s)\Big[\kappa_{21}(s) - 2\kappa_{32}(s) - \kappa_{23}(s)\Big] n_3(s) ds \\ & + \int_0^t K(t-s)\Big[\kappa_{21}(s) - \kappa_{23}(s)\Big] ds \\ & = -\Gamma \int_0^t K(t-s) m(s) ds + 2\Gamma h_0 \int_0^t K(t-s)\cos(\omega s) ds, \end{aligned} \tag{4.82}$$

which is again identical to the noninteracting case with the modified Γ, a result which also follows from the uncorrelated form as the memory kernel simply multiplies all of the rates occurring in the rate equations for both the individual wells and the overall magnetisation.

We then obtain again the formulas (9) and (10), but with $\Gamma = 2f_0 e^{-\sigma(h_c^2+\varepsilon\rho)}$. The prefactor is however altered from simply $2q$ to become

$$\tilde{n}_{\uparrow\uparrow} = \lim_{t\to\infty} n_1(t) = \frac{1}{2(1+e^{-\varepsilon\rho})} \tag{4.83}$$

in zero field. The formal equivalence results for interacting and noninteracting spins follows from the fact that in the first order of h_0 Eq. (11) and (12) yield a single rate equation for the reduced magnetization m. This property follows from the symmetry of the interacting system, and is preserved also if a mean field theory is employed. However, it could not hold for more complex, strongly coupled particle assemblies whose response is thus not of the Debye type [87].

We may note that ferromagnetic coupling with $\varepsilon > 0$ reduces the rate Γ and facilitates the onset of the diamagnetic state, while antiferromagnetic coupling, which favors the creation of magnetically neutral demagnetized states, has the opposite effect.

In Figure 4.12 we depict the susceptibility found from numerical simulation of the Miyazaki-Seki equation with pairs of weakly interacting ferromagnetically and antiferromagnetically coupled spins, unnormalised in this case by the static susceptibility χ_0 so as to allow ready comparison between the magnitude of the effects. The simulations are performed by evolving pairs of spins with an explicit ferromagnetic coupling term in the spin Hamiltonian given by

$$\mathcal{H}_J = -J(S_i \cdot S_j). \tag{4.84}$$

As in the noninteracting case the ensemble of particles are brought into equilibrium, and the susceptibility is then evaluated in the usual fashion. For weak ferromagnetic

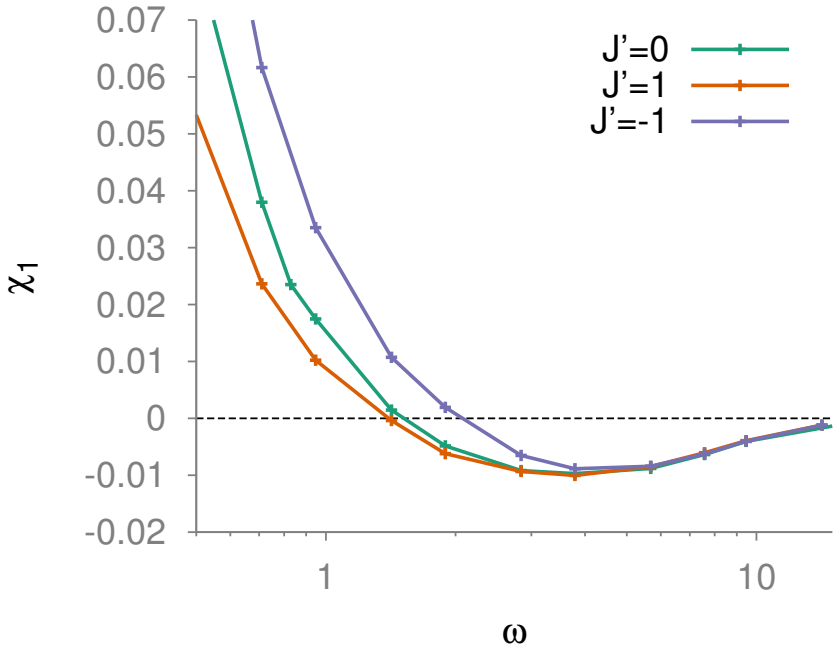

Figure 4.12: χ_1 vs ω' with exchange coupled pairs of nanoparticles.

coupling $J' = J/\sigma <\approx 1$ the diamagnetic response increases slightly for intermediate frequencies, and similarly decreases for antiferromagnetic coupling $J' = -1$, in both cases coinciding with the noninteracting case for very high frequencies. At larger ferromagnetic and antiferromagnetic couplings the diamagnetic effect decreases. We note that the interwell transition rate decreases with increasing ferromagnetic coupling, so we generally anticipate that the memory effect ought to become weaker as the characteristic time of the system becomes longer and longer relative to the memory, similar to the high σ behaviour.

4.6 MACROSPIN EXPRESSIONS

We may also arrive at the functional form for the LLG susceptibilities analytically, by considering the macrospin expression for the time-evolution of the magnetisation, which leads to the Landau-Lifshitz-Bloch (LLB) equation. We define the average of the spin components over an ensemble of spins,

$$\mathbf{m} = \langle \frac{\boldsymbol{\mu}}{\mu_s} \rangle = \langle \mathbf{S} \rangle = \int d^3N \mathbf{N} f(\mathbf{N}, t). \tag{4.85}$$

where $f(\mathbf{N}, t)$ is the probability distribution dictated by the LLG Fokker-Planck equation, and $\mathbf{N}$ is a unit vector denoting the spin orientation. The equation of motion for the

macrospin is [88],

$$\frac{d\mathbf{m}}{dt} = \gamma \mathbf{m} \times \mathbf{H} - \Lambda_N \mathbf{m} - \gamma\alpha \mathbf{S} \times (\mathbf{S} \times \mathbf{H}). \tag{4.86}$$

Importantly, this expression is not closed, in that it is not given in terms of the macrospin only and contains terms proportional to the second moment of the spin distribution, $\langle S_i S_j \rangle$.

Assuming we have a distribution of spins subject to an applied field, then the distribution function in the macrospin expression is explicitly

$$f(\mathbf{N}) = \frac{\exp \boldsymbol{\xi}_0 \cdot \mathbf{N}}{\mathcal{Z}(\boldsymbol{\xi}_0)}, \tag{4.87}$$

where $\boldsymbol{\xi} = \frac{\mu_s \mathbf{H}}{k_B T}$, then we may eliminate the second moment from the macrospin equation of motion by solving for $\langle S_i S_j \rangle$, yielding

$$\frac{d\mathbf{m}}{dt} = \gamma \mathbf{m} \times \mathbf{H} - \Lambda_N \Big(1 - \frac{\mathbf{m} \cdot \boldsymbol{\xi}_0}{|\boldsymbol{\xi}\mathbf{m}|}\Big)\mathbf{m} - \gamma\alpha \Big(1 - \frac{\mathbf{m}}{\boldsymbol{\xi}}\Big) \frac{(\mathbf{m} \times (\mathbf{m} \times \mathbf{H})}{\mathbf{m}^2}. \tag{4.88}$$

For small deviations from equilibrium, then $\boldsymbol{\xi} \approx \boldsymbol{\xi}_0$ he applied magnetic field is $\mathbf{H} = \frac{k_B T \boldsymbol{\xi}_0}{\mu_s}$, and the magnetisation, $\mathbf{m} \approx \mathbf{m}_0 = B(\boldsymbol{\xi}_0)\frac{\boldsymbol{\xi}_0}{\boldsymbol{\xi}_0}$, where $B(\boldsymbol{\xi}) = \coth(\boldsymbol{\xi}) - 1/\boldsymbol{\xi}$ is the Langevin function, then we have the relationship

$$\mathbf{m} - \mathbf{m}_0 \approx B'(\boldsymbol{\xi}_0)(\boldsymbol{\xi}_0 - \boldsymbol{\xi}). \tag{4.89}$$

where B' is the derivative of the Langevin function with respect to the spin. The longitudinal part of the equation is simplified as

$$\Lambda_N \Big(1 - \frac{\mathbf{m} \cdot \boldsymbol{\xi}_0}{|\boldsymbol{\xi}\mathbf{m}|}\Big) = \Gamma_1 \Big(1 - \frac{\mathbf{m} \cdot \mathbf{m}_0}{\mathbf{m}^2}\mathbf{m}\Big), \tag{4.90}$$

where the longitudinal rate is $\Gamma_1 = \frac{\Lambda_N}{\xi B'} B$ and the transverse term becomes

$$\frac{\gamma\alpha k_B T}{\mu_s}\Big(1 - \frac{\mathbf{m}}{\boldsymbol{\xi}}\Big)\frac{\boldsymbol{\xi}_0}{B(\boldsymbol{\xi}_0)}\frac{(\mathbf{m} \times (\mathbf{m} \times \mathbf{m}_0)}{\mathbf{m}^2} = \Gamma_2 \frac{(\mathbf{m} \times (\mathbf{m} \times \mathbf{m}_0)}{\mathbf{m}^2} \tag{4.91}$$

where $\Gamma_2 = \frac{\Lambda_N}{2}(\frac{\xi_0}{B(\xi_0)} - 1)$. The LLB equation is then

$$\frac{d\mathbf{m}}{dt} = \gamma \mathbf{m} \times \mathbf{H} - \Gamma_1 \Big(1 - \frac{\mathbf{m} \cdot \mathbf{m}_0}{\mathbf{m}^2}\Big)\mathbf{m} - \Gamma_2 \frac{(\mathbf{m} \times (\mathbf{m} \times \mathbf{m}_0)}{\mathbf{m}^2}. \tag{4.92}$$

This is the Landau-Lifshitz-Bloch equation for the ensemble of noninteracting paramagnetic. We may derive an expression for the susceptibility of a macrospin evolving according to the LLB equation. We assume that the applied field has only a z-component of the form $H_z = H_0 \cos(\omega t)$. The equilibrium magnetisation then varies as

$$\mathbf{m}_{0,z} = B'(\boldsymbol{\xi}_0)\cos(\omega t), \tag{4.93}$$

with the x and y components identically zero. We then solve for the time evolution of the z-component of the magnetisation,

$$\frac{dm_z}{dt} = \gamma m_z \times H - \Gamma_1\Big(1 - \frac{\mathbf{m}\cdot\mathbf{m}_0}{\mathbf{m}^2}\Big)m_z - \Gamma_2\frac{(m_z \times (m_z \times m_0)}{m^2}. \tag{4.94}$$

Both terms involving $m \times m_0$ are 0 due to the assumption that the applied field lies along the z direction. we then have

$$\frac{dm_z}{dt} = -\Gamma_1\Big(1 - \frac{m\cdot m_0}{m^2}\Big)m_z. \tag{4.95}$$

Assuming the spin lies only along the z-direction, this simplifies to

$$\frac{dm_z}{dt} = -\Gamma_1\Big(m_z - m_0\Big) = -\Gamma_1\Big(m_z - B'(\xi_0)\cos(\omega t)\Big), \tag{4.96}$$

which we recognise has a similar form to the master equation expression. The magnetisation as a function of time is

$$m_z(t) = B'\Big(\frac{\Gamma^2}{\Gamma^2+\omega^2}\cos(\omega t) + \frac{\Gamma\omega}{\Gamma^2+\omega^2}\sin(\omega t)\Big). \tag{4.97}$$

Hence we identify the in and out of phase components of the magnetic susceptibility for the ensemble of paramagnets evolving according to the LLG as

$$\chi_1(\omega) = B'\frac{\Gamma^2}{\Gamma^2+\omega^2} = \frac{\mu_s}{k_BT}\frac{dB}{dH}\frac{\Gamma^2}{\Gamma^2+\omega^2}. \tag{4.98}$$

and

$$\chi_2(\omega) = B'\frac{\Gamma\omega}{\Gamma^2+\omega^2} = \frac{\mu_s}{k_BT}\frac{dB}{dH}\frac{\Gamma\omega}{\Gamma^2+\omega^2}/ \tag{4.99}$$

4.6.1 LLMS Fokker-Planck Equation

A similar macrospin expression exists for the LLMS, in the restricted cases for which there is an analytical expression of the Fokker-Planck equation in terms of the spin only. The full Fokker-Planck equation for the LLMS is in terms of two variables, spin and the thermal field. If we assume the narrowing limit such that $\gamma\sqrt{k_BT\chi}\tau_c << 1$, while still holding that the spin system is correlated, such that $\tau_c\gamma H_k > 1$, [60], additionally it is assumed that we are in the high temperature limit, then the spin-bath coupling is rather weak, and the fluctuating field remains first-order in $\chi k_BT/\tau_c$, and the noise and spin variables are decoupled, $\langle R(t)R(t')S(t')\rangle \approx \langle R(t)R(t')\rangle\langle S(t')\rangle$. In this case, the spin changes slowly over the timescale of the thermal noise.

In this limit, we may then perform a change of coordinates, into a frame that is rotating with the Larmor frequency in some fixed applied external field, γH. The spin and the noise terms in the corotating frame are,

$$\mathbf{S}_c(t) = \mathbf{U}(t) \cdot \mathbf{S}(t) \qquad \boldsymbol{\eta}_c(t) = \mathbf{U}(t) \cdot \boldsymbol{\eta}(t). \tag{4.100}$$

where the transformation matrix is the exponential of the infinitesimal generator,

$$\mathbf{U}(t) = \exp(-\boldsymbol{\Omega} t) = \begin{pmatrix} \cos(\gamma H t) & -\sin(\gamma H t) & 0 \\ \sin(\gamma H t) & \cos(\gamma H t) & 0 \\ 0 & 0 & 1 \end{pmatrix} \tag{4.101}$$

and the generator is

$$\boldsymbol{\Omega} = \begin{pmatrix} 0 & \gamma H & 0 \\ -\gamma H & 0 & 0 \\ 0 & 0 & 0 \end{pmatrix} / \tag{4.102}$$

For an arbitrary vector $\mathbf{A}$, we have that $\boldsymbol{\Omega} \cdot \mathbf{A} = \gamma(\mathbf{A} \times \mathbf{H})$. The spin term in the Miyazaki-Seki Langevin equation becomes, in the transformed coordinates,

$$\begin{aligned} \frac{d\mathbf{S}_c}{dt} &= \frac{d}{dt}\Big(\exp(-\boldsymbol{\Omega} t) \cdot \mathbf{S}(t) \Big) = -\boldsymbol{\Omega} \cdot \mathbf{S}_c(t) + \mathbf{U}(t) \cdot \frac{d\mathbf{S}}{dt} \\ &= \gamma \mathbf{S}_c \times \boldsymbol{\eta}_c. \end{aligned} \tag{4.103}$$

where the rotating term is compensated for by the change in coordinates. Similarly, a rotational term is introduced into the time derivative of the noise field, which then becomes

$$\frac{d\boldsymbol{\eta}_c}{dt} - \gamma \boldsymbol{\eta} \times \mathbf{H} - \frac{1}{\tau_c}(\boldsymbol{\eta}_c - \chi \mathbf{S}_c) + \mathbf{R}_c. \tag{4.104}$$

where $\mathbf{R}_c(t) = \mathbf{U}(t) \cdot \mathbf{R}(t)$ is the Wiener process in the corotating frame, which has the same FDT as the non-transformed case.

We again formally solve for the magnetic field in the corotating frame as we did in the original frame, with the field being given as

$$\boldsymbol{\eta}_c(t) = \frac{\chi}{\tau_c} \int_{-\infty}^{t} ds \boldsymbol{\Psi}(t-s) \cdot \boldsymbol{\eta}_c(t) + \bar{\mathbf{R}}_c(t). \tag{4.105}$$

where

$$\boldsymbol{\Psi}(t) = \exp\Big(-(\boldsymbol{\Omega} + \frac{1}{\tau_c}) \cdot \mathbf{S} \Big). \tag{4.106}$$

$$\bar{\mathbf{R}}_c(t) = \int_{-\infty}^{t} ds \boldsymbol{\Psi}(t-s) \cdot \mathbf{R}_c(t). \tag{4.107}$$

Implying a fluctuation-dissipation theorem for the bath field

$$\langle \bar{\mathbf{R}}_c(t)\bar{\mathbf{R}}_c(s)\rangle = \mathbf{\Psi}(t-s)/ \tag{4.108}$$

Owing to the weak spin-bath coupling, it is now valid to assume that τ_c *is short compared to the characteristic timescale of the spin.* It is then valid to assume the spin and memory kernel decouple, such that

$$\int_{-\infty}^{t} ds\mathbf{\Psi}(t-s)\cdot\mathbf{S}_c(t) = \Big[\int_{-\infty}^{t} ds\mathbf{\Psi}(t-s)\Big]\cdot\mathbf{S}_c(t) = \mathbf{\Gamma}\cdot\mathbf{S}_c(t). \tag{4.109}$$

The elements of the matrix Γ are then evaluated by explicitly taking the integral over time as

$$\mathbf{\Gamma} = \begin{pmatrix} \frac{\tau_c}{1+(\tau_c\gamma H)^2} & -\frac{\tau_c^2\gamma H}{1+(\tau_c\gamma H)^2} & 0 \\ \frac{\tau_c^2\gamma H}{1+(\tau_c\gamma H)^2} & \frac{\tau_c}{1+(\tau_c\gamma H)^2} & 0 \\ 0 & 0 & \tau_c \end{pmatrix}. \tag{4.110}$$

The equation of motion for the spin in the corotating frame is then

$$\frac{d\mathbf{S}_c}{dt} = \gamma\mathbf{S}_c\times\Big[\frac{\chi}{\tau_c}\Gamma\cdot S_c + \bar{\eta}_c\Big], \tag{4.111}$$

where the FDT for the bath field is now also approximated to lowest order as

$$\langle\bar{\boldsymbol{\eta}}_c(t)\bar{\boldsymbol{\eta}}_c(s)\rangle = 2\mathbf{\Gamma}\delta(t-s). \tag{4.112}$$

In the original frame of reference the equation of motion for the spin is

$$\frac{d\mathbf{S}}{dt} = \gamma S\times\Big(\mathbf{H}+\bar{\eta}+\frac{\chi}{\tau_c}\Gamma\cdot S\Big). \tag{4.113}$$

The Fokker-Planck equation for this Langevin equation is,

$$\begin{aligned}\frac{df}{dt} = &- \frac{\partial}{\partial\mathbf{N}}\Big(\gamma(1+\delta)[\mathbf{N}\times\mathbf{H}] + \gamma\bar{\eta}_2(\mathbf{N}\cdot\mathbf{H})[\mathbf{N}\times\mathbf{H}] \\ &- \bar{\eta}_1[\mathbf{N}\times[\mathbf{N}\times\mathbf{H}]]\Big)f \\ &- \frac{\partial}{\partial\mathbf{N}}\Big(D\Big[\mathbf{N}\times\Big[\mathbf{N}\times\frac{\partial}{\partial\mathbf{N}}\Big]\Big)f\end{aligned} \tag{4.114}$$

where $\delta = \bar{\eta}_2/(\beta\mu_0)$, $\bar{\eta}_2 = \bar{\eta}_1\tau_c$, $\bar{\eta}_1 = \gamma\alpha/\kappa$, $D = \Lambda_N/(2\kappa)$ and $\kappa = 1+(\gamma\tau_c H_k)^2$.

4.6.2 Macrospin Expression for the LLMS

The Fokker-Planck for the low damping case has a similar form to the LLG, and the corresponding macrospin expression takes the form

$$\frac{d\mathbf{m}}{dt} = \gamma'[\mathbf{m}\times\mathbf{H}] - \mathbf{\Lambda}\cdot\mathbf{m} - \bar{\mathbf{\Gamma}}_2\frac{[\mathbf{m}\times[\mathbf{m}\times\mathbf{m}_0]}{\mathbf{m}^2}], \tag{4.115}$$

where

$$\mathbf{\Lambda} = \bar{\mathbf{\Gamma}}_1\Big(1 - \frac{\mathbf{m}\cdot\mathbf{m}_0}{\mathbf{m}^2}\Big)\mathcal{I} + \begin{pmatrix} \Lambda_N & 0 & 0 \\ 0 & \Lambda_N & 0 \\ 0 & 0 & 0 \end{pmatrix}, \tag{4.116}$$

where $\bar{\Gamma}_1 = \Gamma_1/\kappa$ and $\bar{\Gamma}_2 = \Gamma_2/\kappa$.

The overall effect of the correlations is to introduce coupling of the longitudinal relaxation to the transverse components. However, for the longitudinal susceptibility there is no coupling since the applied field, anisotropy and magnetisation lie along the same axis. The susceptibility is then functionally rhe same as the LLG macrospin, with the renormalised constants,

$$\chi_1(\omega) = B'\frac{\bar{\Gamma}_1^2}{\bar{\Gamma}_1^2+\omega^2} = \frac{\mu_s}{k_BT}\frac{dB}{dH}\frac{\bar{\Gamma}_1^2}{\bar{\Gamma}_1^2+\omega^2}, \tag{4.117}$$

and

$$\chi_2(\omega) = B'\frac{\bar{\Gamma}_1\omega}{\bar{\Gamma}_1^2+\omega^2} = \frac{\mu_s}{k_BT}\frac{dB}{dH}\frac{\bar{\Gamma}_1^2\omega}{\bar{\Gamma}_1^2+\omega^2}. \tag{4.118}$$

A susceptibility of this form will always be positive as it is the same functionally as the LLG susceptibility. We note that the results from both LLMS and the GME predict positive susceptibility at high temperatures, $\sigma < 1$, which is the condition under which the approximation to the LLMS Fokker-Planck equation was calculated and so the analytical considerations from the macrospin expressions do qualitatively coincide with our observed numerical results. The overall implication of this analysis, as well as the low-σ behaviour from both the GME and LLMS models is that the diamagnetic susceptibiltiy is a characteristic property of magnetic moments which are in the superparamagnetic regime, and is not readily exhibited for the paramagnetic $\sigma < 1$ case.

4.7 CONCLUSIONS

We have presented analytical and numerical studies of the frequency-dependent susceptibility of magnetic nanoparticles. From both the analytical and numerical models, we see a consistent qualitative prediction that there is a frequency-induced diamagnetic response above a critical frequency which is a function of the correlation time. In both models, this effect may be enhanced by the presence of interparticle interactions. leading to the possibility that interaction effects may be considered as a memory effect.

The effects of heat-bath correlations are not easy to investigate experimentally. Our prediction of frequency-induced diamagnetic behavior represents an important prediction

of a clear experimentally accessible signature of heat-bath correlations, with Equ. 4.66 giving a direct relationship between the correlation time and the critical frequency for diamagnetic behaviour. Measurements of the correlation time would generate new understanding of the properties of thermal baths and their interaction with spin systems and would be especially important in the understanding of ultrafast magnetization processes as pointed out in ref. [24]

Chapter 5

Thermally-Activated Magnetisation Reversal

5.1 INTRODUCTION

The problem of escape from a metastable state occurs across a wide range of distinct physical phenomena. Study of the problem has contributed to and received major contributions from fields as diverse as chemical kinetic reaction-rate theory, the theory of diffusion in solids, electrical transport in semiconductors, and the dynamics of nonlinear optics, in addition to many other fields. The unifying concept for many of these treatments is that of the escape process as being induced by random forces in a manner similar to Brownian motion, and, as we have seen, to the LLG treatment of magnetic spins. These relatively weak random forces induce excitation over the characteristic energy barrier of the system on a certain, relatively long timescale, wherein the system spends the majority of the time in some local minimum, punctuated by rare barrier-crossing events to a neighbouring local minimum of the problem. The energy barrier of the problem arises from the physical Hamiltonian of the system, and so is reflected in the forces acting on the particle via the external potential energy profile.

The classical treatment of such escape problems starts with Arrhenius' treatment of chemical reaction-rate data, from which he observed that the rate varies logarithmically with the inverse temperature, $\beta = (k_B T)^{-1}$. This observation lead to the transition state theory model of the escape problem, giving rise to the simple exponential Arrhenius

behaviour for the rate

$$\Gamma_{TST} = Ae^{-E_B/k_BT}, \tag{5.1}$$

where E_B is the barrier height, the threshold energy for activation over the barrier. This is the probability per unit time of the bound particle possessing sufficient energy to surmount the internal barrier. The prefactor modifies the overall escape probability by accounting for the frequency per unit time at which the bound particle is in a position to attempt to escape the well, and hence is frequently termed the *attempt frequency* [89].

Arrhenius was motivated by the study of chemical reaction rates, and developed the analogy between a chemical reaction and a one-dimensional particle escape problem, where the reaction state is analogous to the position at the bottom of one potential well, x_A, and product state corresponding to the global potential minimum, x_B, which the reaction proceeding from x_A to x_B via the saddle point, x_C which is the intermediate transition state of the problem.

In a one-dimensional well, the Transition-State theory (TST), which essentially treats the problem as if it were at all points at equilibrium, predicts that this prefactor is simply the frequency of oscillation of the bound particle at the bottom of the well,

$$A = \frac{\omega_A}{2\pi}. \tag{5.2}$$

The chief disadvantage of the TST approach to the escape problem is that it predicts dynamical escape in the absence of any coupling to the bath, where the escape time does not tend towards infinity with decreasing coupling but rather tends toward a constant rate. The low damping behaviour may be corrected for by including a damping-proportional correcton factor to the TST transition rate as

$$\Gamma = \Lambda\Gamma_{TST} = \Lambda\frac{\omega_A}{2\pi}e^{-E_B/k_BT}. \tag{5.3}$$

These nonequilibrium effects may be incorporated in the rate calculation by accounting for the dynamical coupling to the bath which introduces such nonequilibrium effects into the rate and correctly accounts for coupling to the bath and the weak damping behaviour of the transition rate. Such an extension is the simple TST may be accounted for by explicitly treating the problem from the Langevin equation,

$$p = m\dot{x} \qquad \dot{p}(t) + \beta p(t) + \frac{dV}{dx} = F(t), \tag{5.4}$$

where $\beta p(t)$ is the systematic frictional drag force and the driving thermal force $F(t)$ has the appropriate statistics as dictated by the Fluctuation-Dissipation theorem, and the

corresponding Klein-Kramers Fokker-Planck equation

$$\frac{\partial p}{\partial t} = -\frac{p}{m}\frac{\partial p}{\partial t} + \frac{\partial V}{\partial x} + \beta\frac{\partial}{\partial p}\Big(Wp + mk_BT\frac{\partial W}{\partial p}\Big). \tag{5.5}$$

5.1.1 Thermally-Activated Magnetisation Reversal

The general theory of thermally-activated Kramer's escape is of particular interest in the context of fine single-domain superparamagnetic spins, wherein the constraining potential of the escape problem is provided by the magnetic anisotropy of the particle. This is the physical property which all magnetic recording devices take advantage of, where the confinement of the spins by the anisotropy over long timescales leads to suitable media for the storage of information. In the Arrhenius form, the relaxation time is

$$\tau \propto f_0^{-1} e^{vK/(k_BT)} = f_0^{-1} \exp\frac{\Delta E_{cr}}{k_BT}. \tag{5.6}$$

In comparison to the Kramers escape expression, we see that the attempt frequency is the frequency of Larmor gyromagnetic precession at the bottom of the well, and the spins must overcome the anisotropic confining potential which is proportional to the volume of the particle.

According to the Arrhenius law, we may engineer the escape time to be large enough so that the escape time becomes very long by either increasing the volume of the particle and thus increasing the magnetic anisotropy energy, or decreasing the temperature of the particles. Thus, there is an approximate minimum particle radius or volume above which the magnetic moment appears to be completely stable on the timescales of interest for information storage. The reversal time, τ_R, for the magnetic system is defined similarly to the mechanical problem, that is, it is the average time for the spin to liberate itself from one minimum of the potential due to interaction with the thermal fluctuations of the heat bath.

The spin Hamiltonian for the moment experiencing both an external applied field and an in-built anisotropy takes the general form.

$$\mathcal{H} = -d_z S_z^2 - \mu_s \overrightarrow{B} \cdot S. \tag{5.7}$$

For the full three-dimensional problem, where there may be an arbitrary angle between the externally applied field and the easy-axis of the anisotropy, the free energy takes the explicit form

$$V(\theta,\phi) = \sigma\beta^{-1}\Big(\sin^2\theta - 2h(\cos\psi\cos\theta + \sin\psi\sin\theta\cos\phi)\Big), \tag{5.8}$$

where θ, ϕ are the spin components in spherical coordinates, where $\theta = \cos^{-1}(S_z)$ and $\phi = \tan^{-1}(\frac{S_y}{S_x})$ since the spin magnitude $|S| = \sqrt{S_x^2 + S_y^2 + S_z^2} = 1$ is assumed to be fixed. ϕ is the angle between the applied field and the easy axis. The potential has a bistable character under the condition than the critical applied field value, $h < h_c(\psi) = ((cos^{2/3}\psi + sin^{2/3}\psi)^{-3/2}$ for applied fields below this value, in which case there is a local and global minimum in the north and south polar regions, with an equatorial saddle point between the two regions. An example of the sort of potential profile is show in Figure 5.1.

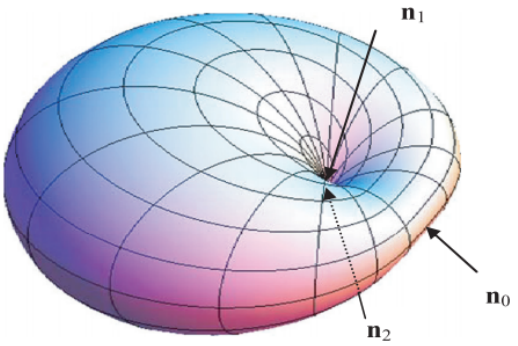

Figure 5.1: 3D Potential Profile for $\psi = \frac{\pi}{2}$ and $h = 0.5$. Figure taken from ref [48].

For the uniaxial problem, the applied field lies along the direction of the easy axis such that $\psi = 0$, the free energy becomes

$$E = -d_z sin^2(\theta) + b_z cos(\theta), \tag{5.9}$$

where d_z is the positive magnetic anisotropy constant and the easy-axis for the anisotropy is taken to lie along the z-axis. Such a potential energy is a function only of the angle between the moment and the z-axis.. With suitably chosen parameters, such that $h = (\mu_S B_z)/(2k_u) < 1$ and $\sigma = k_u/(k_B T) > 1$, there is an energy barrier ΔE of the form

$$\Delta E = d_z(1 - h)^2. \tag{5.10}$$

The uniaxial potential as a function of θ is show in Figure 5.2.

5.1.2 Damping Regimes

Intermediate-to-High Damping (IHD)

in the IHD regime the spin distribution is approximately the Boltzmann distribution almost everywhere within the well. The distribution only departs from the Boltzmann

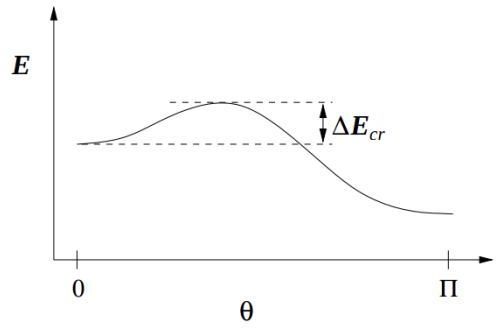

Figure 5.2: Potential energy vs angle for the uniaxial escape problem. Figure taken from ref [90].

behaviour in a very small region near the barrier saddle point due to the motion of particles across the barrier and into the opposite minima. However, the barrier is sufficiently limited in spatial extent that it may be represented entirely in the potential profile as an inverted parabola.

Very Low Damping (VLD)

The very low damping regimes involves particularly complex analysis. For the single-domain ferromagnetic case, it has been treated extensively by Coffey, Kalmykov and collaborators, [91] [48], [92].

In the high damping regime, the moderate to high value of the friction ensures that the energy of a spin undergoing precessional motion deep within a well is much smaller than the barrier energy, with all spins quickly thermalising around the minimum of the corresponding potential, before escaping through the action of the random thermal force eventually giving the spin sufficient energy to escape. In contrast, in the low-damping regime, the damping may become so small that the energy of the particles may exceed the barrier energy purely through the librational motion at the bottom of the well, while the energy lost along an escape trajectory decreases with the decreasing damping. In the Kramers TST formalism the escape rate in the low damping is greatly overestimated as the particles are assumed to be injected and initialised at the source point already having sufficient energy to surpass the barrier, hence erroneously tending towards a constant escape rate at small damping, the TST may only be applied if **the energy dissipated during a period of oscillation is greater than the thermal energy**.

The net result of this is that the assumption the spins approach the barrier region with

the Boltzmann distribution is completely invalid, the barrier region extends far beyond the saddle point. The motion of the particles is now completely undissipative, with the motion of a particle inside the well being almost entirely guided by the dynamical motion and is very nearly Newtonian. The first two terms of the FPE vanish. The escape occurs when the energy of the particle due to the precessional dynamical motion exceeds the energy barrier, and escape occurs when the large amplitude almost conservative precessional motion of the particle trajectory is along the critical path of the problem, which is the energy requires to just escape the well. The low damping regime is inherently tied to the concept of large oscillations of the spin within the well.

Intermediate Turnover Regime

The turnover regime is an approximately critically damped regime, in which neither the escape directly via thermal bath energy nor the energy controlled diffusion dominate. The Liouville term in the FPE does not disappear in this regime, which means you cannot simply average out the phase dependence of the distribution function. This is ultimately accounted for by constructing from the FPE an expression for the distribution function in the barrier region with the energy and action as independent variables.

5.2 ESCAPE TIME FROM THE LLG

The LLG in spherical coordinates takes the form.

$$\frac{\partial p(N,t)}{\partial t} + \frac{\partial J_\phi}{\partial \phi} + \frac{\partial J_\theta}{\partial \theta} = 0, \tag{5.11}$$

which we note is the same form as the ordinary Cartesian coordinates, this follows from the fact that the spherical coordinates similarly span the space available to the spin, so the gradient takes the same functional form. We have then simply to evaluate the probability currents in the transformed coordinates. using the relationship

$$\mathbf{N} \times \frac{\partial V}{\partial \mathbf{N}} = -\mathbf{e}_\phi \frac{\partial V}{\partial \theta} + \frac{\mathbf{e}_\phi}{\sin(\theta)} \frac{\partial V}{\partial \phi}, \tag{5.12}$$

the currents become,

$$J_\theta(N,t) = -\frac{\alpha\gamma}{(1+\alpha^2 M_s)} \Big(\frac{\partial V}{\partial \theta} - \frac{1}{\alpha \sin\theta} \frac{\partial V}{\partial \phi} \Big) P(N,t) + \frac{1}{2\tau_N} \frac{\partial P}{\partial \theta}, \tag{5.13}$$

$$J_\phi(\phi,t) = -\frac{\alpha\gamma}{(1+\alpha^2 M_s)} \Big(\frac{1}{\alpha} \frac{\partial V}{\partial \theta} + \frac{1}{\sin\theta} \frac{\partial V}{\partial \phi} \Big) P(N,t) + \frac{1}{2\tau_N \sin\theta} \frac{\partial P}{\partial \phi}. \tag{5.14}$$

In the particular case of an axially-symmetric potential, the Fokker-Planck equation takes a much simpler form, allowing us to evaluate the switching rate between wells explicitly, resulting in an expression for the escape time which is valid for all values of the damping parameter, α, whereas in the Klein-Kramers case the problem is always in terms of two variables, the position and momentum and only has a one-dimensional form depending on the damping regime. In comparison, for the magnetic relaxation problem, the three regimes only appear in the nonaxially symmetric case and the FPE becomes truly two-dimensional.

In the quasi-stationary case, the probability flux per unit time is approximately zero, hence we have $\cdot p = 0$ and the axial current term may be taken as 0, $\partial J/\partial\phi = 0$, since the potential is only a function of θ. The total current through any point along the coordinate θ is then a fixed flow, such that

$$J = 2\pi J_\theta \sin\theta \tag{5.15}$$

we then have

$$\frac{\partial P}{\partial \theta} + \frac{\partial V}{\partial \theta} P = e^{-V} \frac{\partial}{\partial \theta}(e^V P) = -\frac{2\tau_N}{\pi \sin\theta}. \tag{5.16}$$

The probability as a function of θ is then

$$P(\theta) = -\frac{\tau_N J}{\pi} e^{-V(\theta)} \int_{\theta_!}^{\theta_m} \frac{e^{V(\theta')}}{\sin\theta'} d\theta'. \tag{5.17}$$

The total number of particles inside the well follows as the integral of the probability that a particle is inside the well, where we define θ_m as the boundary angle denoting that a particle resides in the well, hence [57],

$$N_i = 2\pi \int_{\theta_i}^{\theta_0} P \sin\theta d\theta = -2\tau_N J \int_{\theta_i}^{\theta_0} e^{-V(\theta)} \sin\theta \int_{\theta_0}^{\theta} \frac{e^{V(\theta)}}{\sin\theta} d\theta' d\theta. \tag{5.18}$$

The escape rate from the well then follows as the ratio of the number of particles in the well to the flux out of the well, simply giving us

$$\tau(\theta_i) = N_i/J = -2\tau_N \int_{\theta_i}^{\theta_0} e^{-V(\theta)} \sin\theta \int_{\theta_0}^{\theta} \frac{e^{V(\theta)}}{\sin\theta} d\theta' d\theta, \tag{5.19}$$

which becomes

$$\tau(\theta_i) = 2\tau_N \int_{\theta_I}^{\theta_0} \frac{e^{V(\theta')}}{\sin\theta'} \int_{\theta'}^{\theta_I} e^{-V(\theta)} \sin\theta d\theta' d\theta. \tag{5.20}$$

after integration by parts. The rate may then be evaluated by making the assumption that the particles are tightly bound within the well, which follows in the high barrier limit, so that the integral over θ need only be taken over a very small range of angles near the

minimum. The inner integral is then analytically solvable using the method of steepest descents, [57] [70],

$$\int e^{-V(\theta)} \sin\theta d\theta \approx \int_0^\infty \theta \exp\Big(- (V(0) + V''_{\theta\theta}(0)\frac{\theta^2}{2})\Big) = \frac{e^{-V(0)}}{V''_{\theta\theta}(0)}, \tag{5.21}$$

where we take the integral to infinity since we have already made the assumption that the particles are located near the centre of the well. Since we are near the barrier we may approximate the exact potential by taking the Taylor series for the potential,

$$V(\theta) \approx V(\theta_0) - |V''_{\theta\theta}|(\theta - \theta_0)^2/2. \tag{5.22}$$

And so the outer integral is evaluated as

$$\int e^{-V(\theta)} \sin\theta d\theta \approx \frac{\sqrt{\pi} e^{-V(\theta_0)}}{\sin\theta_0 \sqrt{2|V''_{\theta\theta}|(\theta_0)}}. \tag{5.23}$$

In the high-barrier limit, the escape time for the uniaxial case is then

$$\tau = \frac{\tau_N}{V''_{\theta\theta}(0)} \frac{\sqrt{2\pi}}{\sqrt{|V''_{\theta\theta}(\theta_0)|}} \frac{e^{V(\theta_0)-V(0)}}{\sin\theta_0}. \tag{5.24}$$

By using the potential corresponding to an applied field and an anisotropy term, the escape time becomes for a superparamagnetic in the uniaxial case,

$$\tau = \frac{\tau_N \sqrt{\pi}}{\sigma^{3/2}(1-h^2)} \Big((1+h) e^{-\sigma(1+h)^2} + (1-h) e^{-\sigma(1-h)^2} \Big), \tag{5.25}$$

and in the limit of no applied field,

$$\tau = \frac{\tau_N \sqrt{\pi} e^{\sigma}}{2\sigma^{3/2}}. \tag{5.26}$$

5.3 NUMERICAL SIMULATION

To investigate the thermally-activated escape time numerically, we initialise an ensemble of spins in the local minimum of the potential, which is antiparallel to the applied field. The spin is then time-evolved according to the relevant Langevin equation, LLMS or LLG, until the particle is considered to have escaped the well when some switching condition is considered to have been met, for example, $S_z < m_0 = 0$. This is then iterated until an ensemble average has been taken, and the average of this escape time for each individual particle is then taken as the escape time for the ensemble.

Figure 5.3 depicts the damping dependence of the escape time as predicted by the one-dimensional TST and from numerical simulations using this method and the LLG and

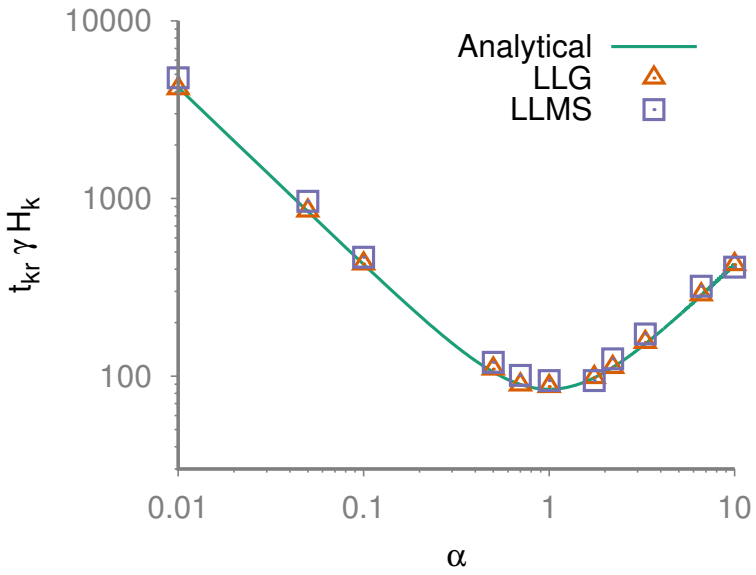

Figure 5.3: Analytical prediction for escape time and results of numerical simulations using the LLG and the LLMS for small correlation times, $\sigma = 7.5$.

the LLMS Langevin equations. The results of our simulations show excellent agreement with the analytical expression, showing the characteristic $\frac{\alpha}{1+\alpha^2}$ dependence for both the LLG and the uncorrelated LLMS. These results serve as an important validation, both of the implementation of the LLG Langevin equation, and demonstrates that the LLMS for small correlation times converges on the behaviour of the LLG.

5.3.1 System Time τ_s vs. τ_c Characteristic Bath Time

For the uniaxial escape problem the external field in the LLMS will consist of an external applied part and an anisotropy

$$H = H_a + H_0 \tag{5.27}$$

the magnitude of the anisotropy field depends on the orientation of the spin and is given by $H_a = \frac{2k_u}{\mu_s}\overrightarrow{S_z} \cdot \overrightarrow{z} = H_k\overrightarrow{S_z} \cdot \overrightarrow{z}$ where $\overrightarrow{z}$ is the direction of easy magnetisation and k_u is the anisotropy energy. We will assume the uniaxial case, where the external field is applied along the same direction as the easy axis, both fields only have components in the z-direction.

To get an idea of the order of magnitude of the system time of a spin bound to an energy minimum by such an anisotropy potential, we note that the anisotropy field varies

with the projection of the spin on to the easy-axis as

$$H_a = H_k(S_z \cdot z)\overrightarrow{z} = H_k \cos(\theta)\overrightarrow{z}, \tag{5.28}$$

Therefore, the *largest field magnitude* and consequently the fastest timescale of the problem is set by the value for which the anisotropy is at its largest, which is when the spin and the easy-axis precisely coalign. For any other orientation, the field will be smaller and the timescale of oscillation hence slower. Taking then a constant external applied field of this maximum magnitude, H_k, for a spin with at an arbitrary angle to the z-axis, the spin-only Langevin equation in the correlated case becomes

$$\frac{dS}{dt} = \gamma S(t) \times \left(H_k \overrightarrow{z} + \bar{\eta} - \chi \int_{-\infty}^{t} dt' K(t-t') \frac{dS(t')}{dt'}\right), \tag{5.29}$$

if we define the system time for the spin as $\tau_s = (\gamma H_k)^{-1}$ then

$$\frac{dS}{dt} = \frac{1}{\tau_s} S(t) \times \left(\overrightarrow{z} + H_k^{-1}\bar{\eta} - H_k^{-1}\chi \int_{-\infty}^{t} dt' K(t-t') \frac{dS(t')}{dt'}\right) \tag{5.30}$$

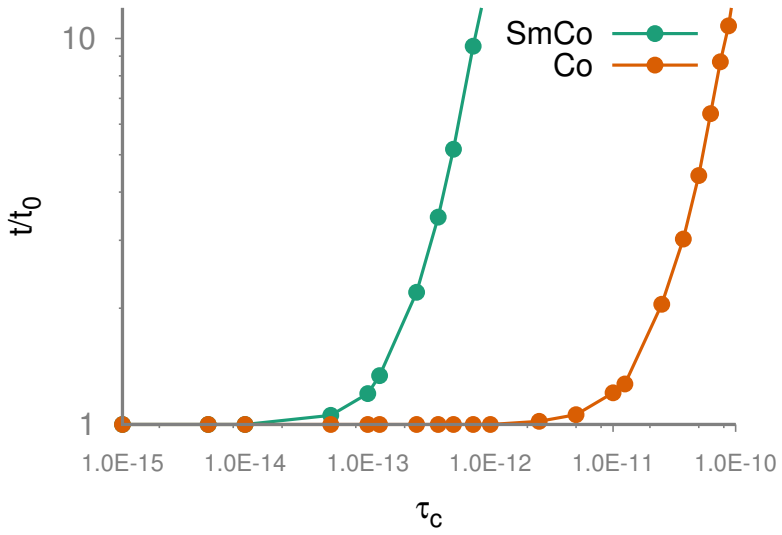

Figure 5.4: Escape time in the LLMS normalised by the uncorrelated LLG escape time for different values of the correlation time $\tau = \tau_c \gamma H_k$ and for simulations with parameters comparable to a Co and and SmCo nanoparticle.

We may scale time in the Langevin equation so that the system time is removed by taking $r = t/\tau_s$. Then we have

$$\frac{dS}{dr} = S(r) \times \overrightarrow{z} + S(r) \times \left(H_k^{-1}\bar{\eta}(r) + H_k^{-1}\chi \int_{-\infty}^{r'} dr' e^{-(r-r')\frac{\tau_s}{\tau_c}} \frac{dS(r')}{dr'}\right) \tag{5.31}$$

The autocorrelation of the noise is similarly transformed to become

$$\langle \bar{\eta}(r)\bar{\eta}(r')\rangle = \frac{\tau_s}{\tau_c}\bar{D}e^{-(r-r')\frac{\tau_s}{\tau_c}} = \frac{\bar{D}}{\tau}e^{-(r-r')/\tau} \tag{5.32}$$

where $\tau_s/\tau_c = \tau$ and $\bar{D} = D/\tau_s = \chi\tau k_B T/\mu_s$. We can then write the coupling as $\bar{\chi} = \chi/H_k$, and we absorb the H_k factor into the diffusion constant for the thermal field. Since the thermal fields are given by $\bar{\eta}(r) = \frac{\sqrt{2D}}{\tau}\int_{-\infty}^{r} K(r-r')\Gamma(r')$, the diffusion constant becomes

$$\bar{D} = \frac{\chi\tau k_B T}{\mu_s H_k^2} = \frac{\bar{\chi}\tau k_B T}{2k_u} = \frac{\bar{\chi}\tau}{2\sigma} \tag{5.33}$$

where $\sigma = k_u/k_B T$. The final expression for the Langevin equation is then

$$\frac{dS(r)}{dt} = S(r) \times \left(\overrightarrow{z} + \bar{\eta} - \bar{\chi}\int_{-\infty}^{r} dr' K(r-r')\frac{dS(r')}{dr'}\right) \tag{5.34}$$

In the case that $\tau \ll 1$ and $\tau_c \ll \tau_s$, we see that the memory kernels appearing in the noise and damping terms are reduced to delta functions. Additionally the bath coupling and the strength of the thermal fluctuations are reduced by the anisotropy field, so that in the event of a very large anisotropy the precessional dynamics of the spin dominate the thermal and damping parts. The condition that $\tau_c \gtrsim (\gamma H_k)^{-1}$ is the one that we would expect to dictate whether the effect of correlations are relevant in the system dynamics.

Figure 5.4 depicts the escape time from LLMS simulations vs the correlation time, both normalised by the Larmor frequency and the escape time normalised to the uncorrelated LLG escape. The results of these simulations are in agreement with the expectation that the Larmor precession sets the characteristic time of the system. For both sets of parameters, we see that the escape rate departs from the LLG escape rate only once the correlation time is on the order of the Larmor time, approximately $1\times10^{-13}s$ and 1×10^{-12} for the Co and SmCo respectively. In general, the higher anisotropy particle exhibits correlated behaviour at lower correlation times. As we anticipate that the bath correlation time will usually be of approximately the same order for different superparamagnets considered, we then anticipate that the higher anisotropy particles will be the more promising candidates when it comes to exhibiting non-Markovian behaviour.

5.4 INITIAL & SWITCHING CONDITIONS

When evaluating the escape time via the types of Langevin equations considered here, it is important to note that there is a degree of arbitrariness involved in the precise evaluation of the time to surmount the energy barrier. As we have stated, the general procedure

is to first initialise the spins in one of the energy minima of the problem. We must do so according to some initial condition. Naively, one might assume $S_{z,init} = 1$ for all of the spins of the problem where the positive z-direction lies antiparallel to the applied field direction. The precise choice of initial condition is an important technical point in the numerical investigation of the escape time from Langevin simulations, as point out in ref. [93] by Kalmykov *et al.*

Similarly, we must also choose some characteristic value of the magnetisation by which we judge that the spin has departed from the initial minimum and now resides in the opposite well. The amount of time, τ, taken for the spin to surpass the critical value $m_z < m_0$ gives the escape time for that spin from the initial minimum. However, this choice of the switching condition m_0 influences the final calculated escape time, as, for example, if the switching condition is taken to be the exact saddle point such that it lies along the separatrix, then there is an equal chance for the spin to enter either well. Hence, such a choice of switching condition will generally result in a smaller evaluation of the escape time when compared to an initialisation that lies deep within the well, with different choices of the switching condition giving results which may differ from each other by a factor of between 1 and 2 in the IHD regime, and may be much higher in the low damping regime.

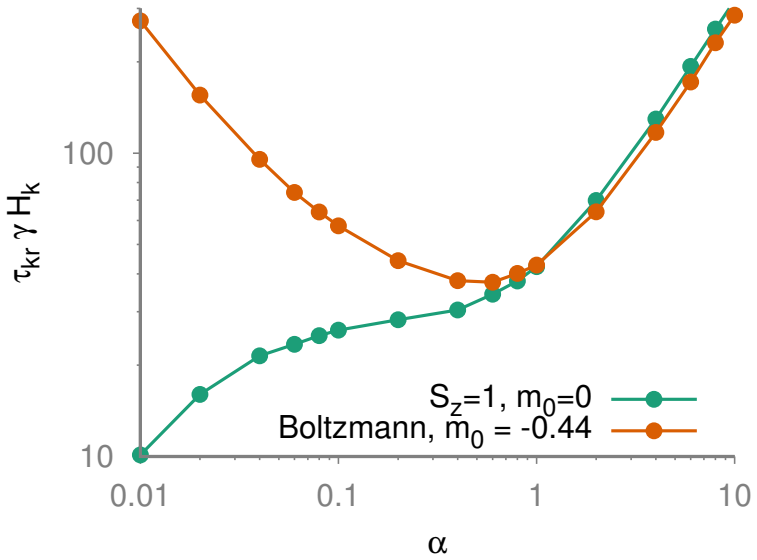

Figure 5.5: Escape time vs damping, α, for initial condition $S_z - 1$ and drawn from the Boltzmann distribution from LLG simulations.

We must also consider the choice of initial conditions when performing simulations using the LLG and LLMS equations. With the choice of initial condition $S_{z,init} = 1$ for all spins in the ensemble, we present the damping-dependence of the escape time for such an initial condition in Figure 5.6, for a reduced barrier height $\sigma = 15$, $h = 0.42$, and an angle between the applied field and easy-axis of $\psi = \pi/4$. In the intermediate-to-high damping regime, $\alpha > 1$, the numerical results from the LLG and the analytical prediction of the TST agree, and the escape time increases with increasing damping. The results of our simulations mirror those presented in ref [93], reiterating the need for great care to be taken in the simulation of the escape problem for weak damping. However, in the low damping regime the Langevin simulations show both a completely different qualitative dependence from the universal turnover and the lower-bound which is set by the TST theory, where the initial condition leads to a very fast dynamical transition between the wells without ever approaching the saddle point due to strong precession in the initial configuration.

In the IHD regime, the distribution function for the spin is everywhere the Boltzmann distribution at the bottom of the wells, with a slight deviation very close to the separatrix between the two wells. The higher damping and larger range of validity of the thermal distribution causes spins initialised along the z-axis to quickly assume the correct distribution in the well on a much shorter timescale than the timescale over which dynamical rotational escape can occur. For $\alpha < 1$ it is not longer certain that the spin approaching the barrier region from the depth of the well has the Boltzmann form, the damping and interaction with the bath is so weak that the time it takes to correctly equilibriate within the well is longer than the dynamical time over which barrier rotations may occur.

It is then generally necessary to explicitly choose different initial conditions for the spins in the wells, such that they are initialised according to the correct Boltzmann distribution inside the well, according to

$$P(\theta, \phi) = \sin\theta e^{-E(\theta,\phi)/k_B T} \tag{5.35}$$

The results of LLG simulations using this initialisation are also shown in Figure 5.6, which now produce good agreement with the TST and turnover formulas. We find a qualitatively similar difference between the low-damping behaviour in the LLMS escape rate calculations performed with both initial conditions, which we present in figure 5.5. We interpret the difference between both sets of data to be due to the same reason as for the LLG.

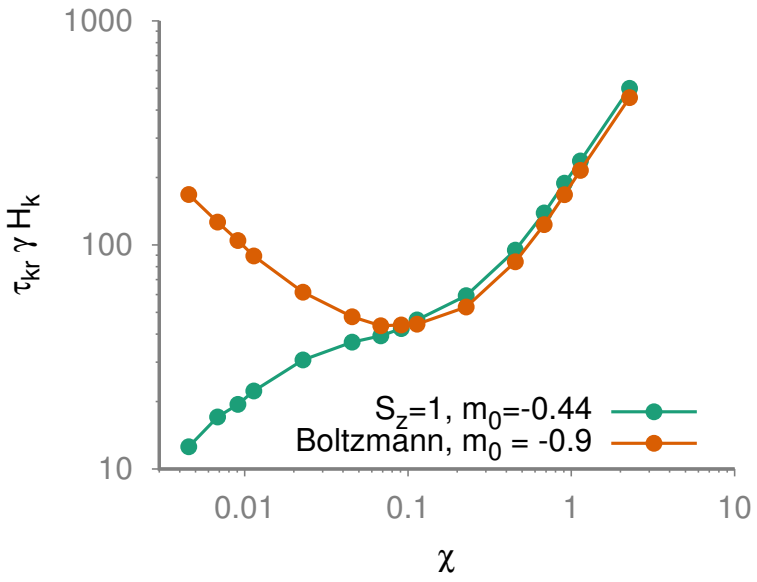

Figure 5.6: Escape time vs damping, α, for initial condition $S_z - 1$ and drawn from the Boltzmann distribution from LLMS simulations.

In general, the numerical evaluation of the switching time in the low damping regime depends crucially on the choice of initial and switching condition for both the LLG and LLMS equations. Hence, we will in general perform LLMS simulations with the initial condition also chosen according to the corresponding Boltzmann distribution, in order to give our calculations full generality and avoid any possible issues due to the thermalisation of the spins about the mimina.

5.5 LLMS: DAMPING DEPENDENCE OF THE ESCAPE TIME

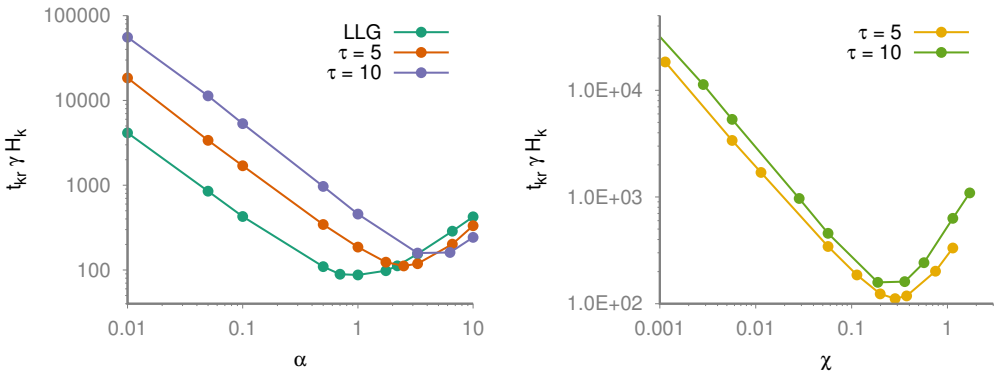

Figure 5.7: Escape time from the LLMS and LLG in the uniaxial case, $\sigma = 7.5$.

An important point of comparison between the LLMS and the LLG is the behaviour of the escape time as we vary the damping parameter of the system. An ambiguity arises in this discussion, as the LLG has a single simple phenomenological parameter determining the strength of the coupling of the spin and the thermal bath. In contrast, the LLMS is characterised by a pair of parameters, the characteristic correlation time of the bath and the strength of the coupling between the bath and the spin. In the Markovian limit, these parameters are related as $\alpha = \gamma\tau_c\chi$, as we have seen, however the phenomenological coupling α is not necessarily meaningful in the correlated problem, with the relation simply dictating how the parameters must be related in order for both descriptions to produce the same physical results.

Figure 5.7 shows the damping from LLG numerical simulations and from the LLMS with $\tau = 2, 5$ for the uniaxial problem with the reduced field $h = 0.3$. We also show the spin-bath coupling χ dependence for the LLMS simulations. These simulations have a few important implications for the Miyazaki-Seki model. Firstly, we see that the high and low damping regimes are preserved. Presumably the behaviour in both regimes is still as a result of the temperature-controlled and energy controlled diffusion regimes for the high and low damping, respectively.

As we increase the correlation time τ_c, the minimum value of the escape time generally increases, with the position of the minimum shifting to higher α as the correlation time increases. This is somewhat of an artifact of the usage of α rather than χ. In the right-hand side of the Figure, we show that behaviour vs the spin-bath coupling. The escape time again generally increases for the same value of χ with increasing correlation time, τ_c, although the exact damping-dependence and minimum appears to vary with the correlation time.

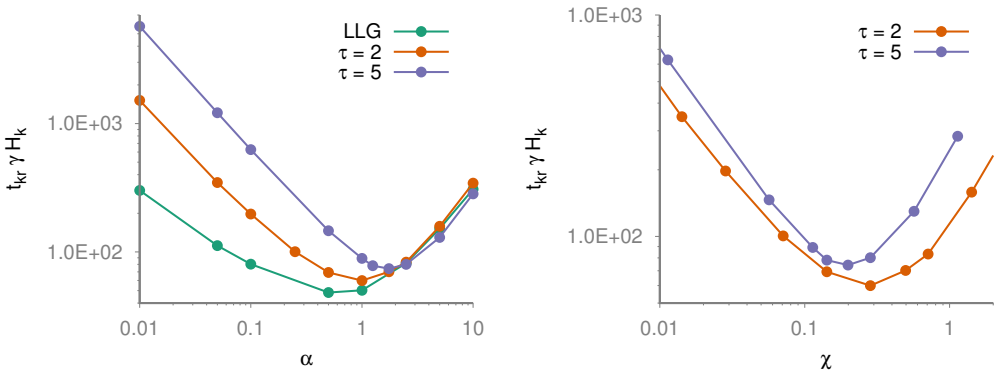

Figure 5.8: Escape time from the LLMS and LLG for $\psi = \pi/4$, $\sigma = 15$.

Figure 5.8 repeats the simulations for the non-uniaxial case, in which there is an applied field of magnitude $h = 0.3$, reduced barrier height $\sigma = 7$. The behaviour of the escape time is in general the same, with the escape time increasing in the low and high damping limit, and a precise damping dependence which is similar to the $\tau_{kr} \propto \frac{\alpha}{1+\alpha^2}$ behaviour seen from analytical consideration and LLG numerical simulations.

5.6 ESCAPE TIME: TEMPERATURE DEPENDENCE

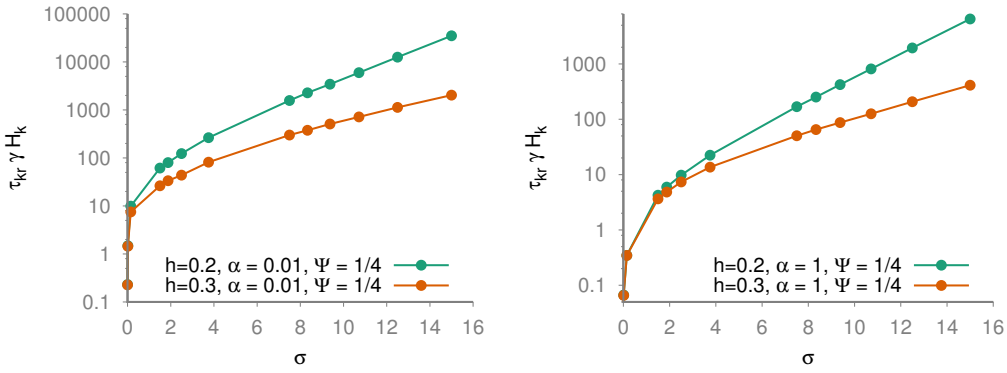

Figure 5.9: Escape time, $\tau\gamma H_k$ vs reduced barrier height, σ, from LLG numerical simulations.. **Left**: :ow damping ($\alpha = 0.01$), **Right** high damping ($\alpha = 1$).

Figure 5.9 shows the behaviour of the escape time from LLG simulations vs the reduced barrier height for both the high and low damping regimes and with different values of the reduced field, h. The most salient feature of these graph is that the behaviour of the escape time tends towards the Arrhenius exponential behaviour for larger $\sigma > 5$, as shown by

the linear appearance of the dependence. This behaviour manifests itself in all damping regimes and at all value of the field sufficient to constitute an escape problem.

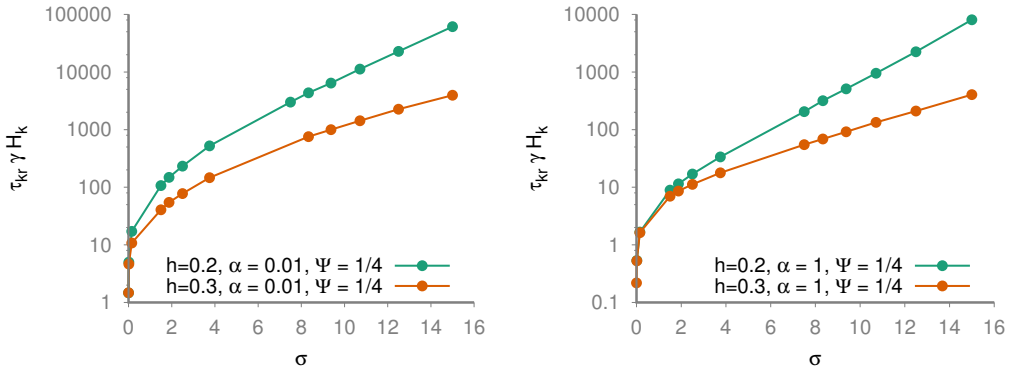

Figure 5.10: Escape time, $\tau\gamma H_k$ vs reduced barrier height, σ, from LLMS numerical simulations, with a significant correlation time of $\tau = 2$. **Left**: :ow damping ($\alpha = 0.01$), **Right** high damping ($\alpha = 1$).

Figure 5.10 repeats this analysis for LLMS simulations where we have used a correlation time that is sufficiently high that the system departs from the LLG model. These show that when the barrier is sufficiently the escape time again takes the familiar Arrhenius form, for both high and low damping and for all valid field magnitudes.

Finally, it is of interest to compare the temperature dependence of the two models directly. In the high damping case, we see that the escape rates begin to converge as the temperature tends towards 0. This result makes sense intuitively, as the transition rate between the wells becomes much longer than the bath correlation time, we would expect the detailed dynamics of the spin within the well to become less relevant.

The temperature dependence in the low damping regime is much more interesting. At low damping, the LLMS and LLG appear not to converge even at the larger barrier heights considered here, either converging very slowly as a function of σ or never actually coinciding on the same escape time. We attribute this difference to the difference in damping regimes and the physically distinct mechanisms involved in the escape process in the two regimes. The high damping regime is again reliant on thermal fluctuations to liberate the bound spin, as the thermal fluctuations become less relevant at higher σ, the two models begin to converge. In contrast, in the energy-controlled diffusion regime is characterised by the almost Newtonian motion of the particle in the well. In the highly correlated case, the simple damping is replaced with a frequency-dependent damping, an

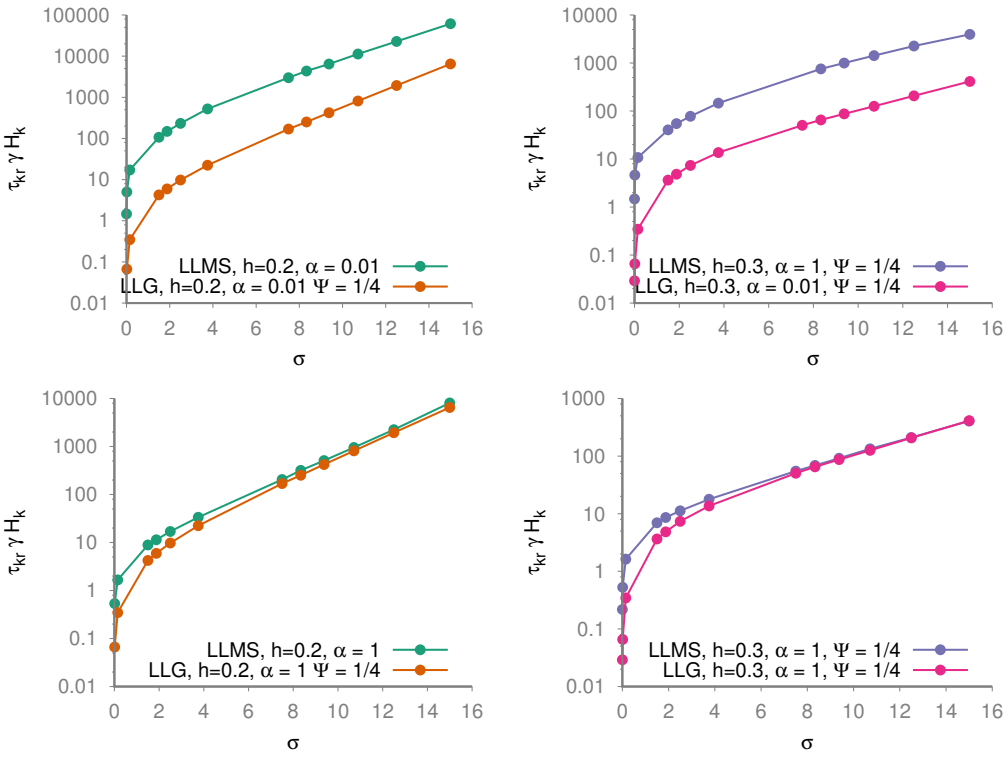

Figure 5.11: Escape time, $\tau\gamma H_k$ vs reduced barrier height, σ, from LLMS and LLG simulations. **Top Left:** Low damping, $h = 0.2$, **Top Right:** Low damping, $h = 0.3$. **Bottom Left:** High damping, $h = 0.2$, **Bottom Right:** High damping, $h = 0.3$.

effect which seems to increase the overall effective damping and inhibit the escape rate between the wells by decreasing the rate at which the spin is able to attain a trajectory with sufficient energy to leave the well.

5.7 ANGULAR VARIATION

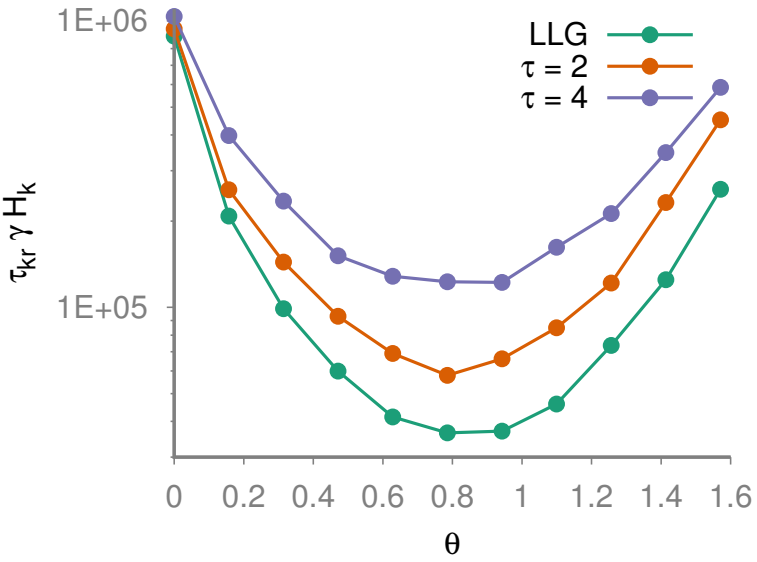

Figure 5.12: $\gamma H_k \tau_c$ vs applied field angle, Ψ, for correlation times $\tau = 2, 4$ and from the LLG. The memory effect is stronger for intermediate angles where the relaxation time is smaller.

Figure 5.12 shows the angular dependence of the escape rate for a system with $\sigma = 15$, $h = 0.2$ and $\alpha = 0.1$ between the LLG and the LLMS with $\tau = 2, 4$. The increase of the correlation time causes an increase to the escape rate at all angles, however it is interesting to note that the escape time appears to increase much faster at intermediate angles than in the uniaxial or completely transverse cases. The minimum of the escape rate is for both models, and at all values of the correlation time, near the angle $\psi = \pi/4$. It may then be the case that correlation time has greatest effect at and around this angle as the escape time is at it's lowest and hence the escape time is closer to the dynamical time range on which the correlations are relevant.

5.8 RATE EQUATIONS FOR THERMALLY-ACTIVATED MAGNETISATION REVERSAL

5.8.1 Master Equation

For an arbitrary spin Hamiltonian with N minima of the potential, the rate equation describing the dynamics of the transitions between these minima is again,

$$\frac{dn_i}{dt} = A_{ij}(t)n_j(t) \tag{5.36}$$

where n_i is a probability vector representing the probability that the system is in one of a discrete set of states, and $i, j \in N$ label those discrete states.

In the uniaxial case, the spin orientations are assumed to be restricted only to the 2 minima of the potential energy dictated by the spin Hamiltonian. For uniaxial escape with a constant external applied field, we then have constant transition rates between the wells, in contrast to the time-varying potential for the susceptibility problem. The transition matrix elements are then,

$$A_{ij} = \begin{pmatrix} -\kappa_{12} & \kappa_{21} \\ \kappa_{12} & -\kappa_{21} \end{pmatrix} \tag{5.37}$$

Where $\kappa_{1\to2} = \kappa_{12} = f_0 \exp(-\sigma(1+h)^2)$ and $\kappa_{2\to1} = \kappa_{21} = f_0 \exp(-\sigma(1-h)^2)$. The time evolution of the population of the state n_1 is again given as

$$\frac{dn_1}{dt} = -\kappa_{12}n_1 + \kappa_{21}n_2 = (\kappa_{12} + \kappa_{21})n_1 + \kappa_{21} \tag{5.38}$$

We can now write the derivative of the magnetisation as,

$$\frac{dm}{dt} = -Am(t) + B \tag{5.39}$$

where $A = \kappa_{12} + \kappa_{21}$ and $B = \kappa_{21} - \kappa_{12}$. This is the same form as the rate for the individual wells, Eq. 5.38, with the individual rate κ_{12} replaced by B. For an initial magnetisation $m_0 = n_1(t=0) - n_2(t=0)$, the magnetisation as a function of time is exponential,

$$m(t) = \frac{e^{-At}(Am_0 - B)}{A} + \frac{B}{A} \tag{5.40}$$

which tends to the value

$$\frac{B}{A} = \frac{\kappa_{21} - \kappa_{12}}{\kappa_{12} + \kappa_{21}} \tag{5.41}$$

in the long-time limit, the steady state magnetisation corresponding to the difference in the transition rates between the wells, if $\kappa_{2\to1} > \kappa_{1\to2}$, the transition rate into well 1 is

greater than the rate out, then we have a positive magnetisation, as expected. We note that we can also solve this equation by Laplace transform, as this will give us some basis for comparison to the non-Markovian case. The Laplace transform of Eq. 5.40 for the initial magnetisation m_0 is

$$\omega m(\omega) - m_0 = -Am(\omega) + \frac{B}{\omega} \tag{5.42}$$

Giving a frequency-space expression for the magnetisation,

$$m(\omega) = \frac{m_0}{\omega + A} + \frac{B}{A\omega + \omega^2} \tag{5.43}$$

the inverse transform of which is again the exponentially decaying solution of Eq. 5.40.

5.8.2 Relaxation: Generalised Master Equation

We may again study the behaviour of the rate equations by extending the transition rates in Eq. 5.36 to a set of memory kernels, resulting in an integro-differential expression for the rate of change of the well populations,

$$\frac{dn_i}{dt} = \int_0^\infty M_{ij}(t-\tau)n(\tau)d\tau \tag{5.44}$$

And the transition rates are simplified to

$$M_{ij}(t) = \frac{e^{-t/\Theta}}{\Theta} A_{ij} = K(t)A_{ij} \tag{5.45}$$

where A_{ij} are the same constant transition rates considered in the Markovian master equations, now modified by a simple exponential kernel over the recent population of the well. The integro-differential expression for the magnetisation then becomes

$$\frac{dm}{dt} = -A\int_0^\infty K(t-\tau)m(\tau)d\tau + B\int_0^\infty K(t-\tau)d\tau \tag{5.46}$$

Where we note that for the exponential kernel, $K(t) = \frac{e^{-t/\Theta}}{\Theta}$, the uncorrelated form of the master equation is recovered in the limit of vanishing correlation time, $\lim_{\Theta\to 0} K(t) = \delta(t)$.

The Laplace transform of this equation is

$$\omega m(\omega) - m_0 = -AK(\omega)m(\omega) + \frac{B}{\omega}K(\omega) \tag{5.47}$$

where $K(\omega) = \mathcal{L}(K(t))$ is the Laplace transform of the memory kernel, which we note now multiplies all of the terms in comparison to the Markovian case in Eq. 5.42. The transform of the kernel is

$$K(\omega) = \frac{\Theta^{-1}}{\omega + \Theta^{-1}} = \frac{1}{1 + \Theta\omega} \tag{5.48}$$

we then have

$$m(\omega) = \frac{\frac{B}{\omega}K(\omega) + m_0}{\omega + AK(\omega)} \tag{5.49}$$

After inserting the expression for the Laplace transform of the kernel we find

$$m(\omega) = \frac{\frac{B}{\omega} + m_0(1 + \Theta\omega)}{\Theta\omega^2 + \omega + A} \tag{5.50}$$

5.8.3 Solution from Formal Expression

We may also arrive at this expression by utilising a formal expression, derived in Appendix 1, relating the solutions of the Markovian master equation to the master equation with a specified memory kernel [94],

$$m(\omega) = \frac{1}{K(\omega)} f(\frac{\omega}{K(\omega)}) \tag{5.51}$$

where $f(\omega)$ is the uncorrelated solution, which we have noted previously takes the form $\frac{m_0}{\omega+A} + \frac{B}{A\omega+\omega^2}$. Inserting the Laplace transform of the memory kernel into this expression we have

$$\begin{aligned} m(\omega) &= (1 + \Theta\omega)\Big(\frac{m_0}{\omega(1 + \Theta\omega) + A} \\ &+ \frac{B}{A\omega(1 + \Theta\omega) + \omega^2(1 + \Theta\omega)^2}\Big) \\ &= \frac{\frac{B}{\omega} + m_0(1 + \Theta\omega)}{\Theta\omega^2 + \omega + A} \end{aligned} \tag{5.52}$$

which agrees with the expression derived from the explicit Laplace transform. Upon taking the $\Theta \to 0$ limit, the two terms proportional to Θ drop out and we have the uncorrelated expression for $m(\omega)$.

5.8.4 Relaxation

Finally we solve for the time-dependence of the magnetisation by taking the inverse Laplace transform,

$$m(t) = \mathcal{L}^{-1}\Big[\frac{\frac{B}{\omega} + m_0(1 + \Theta\omega)}{\Theta\omega^2 + \omega + A}\Big] = \frac{\phi(t)(Am_0 - B)}{A} + \frac{B}{A} \tag{5.53}$$

we note that this bears a strong resemblance to the Markovian expression, Eq. 5.40, with the exponential being replaced by the function $\phi(t)$, which is

$$\phi(t) = \frac{1}{2\beta}\Big((\beta - 1)e^{-t(1+\beta)/2\Theta} + (\beta + 1)e^{-t(1-\beta)/2\Theta}\Big) \tag{5.54}$$

where $\beta = \sqrt{1-4A\Theta}$. We note that in the limit $t \to \infty$, the limiting value of the magnetisation is again $\frac{B}{A}$. To see that this agrees with the uncorrelated solution for small correlation times, we may expand β in Θ for small Θ, hence $\beta = 1-2A\Theta$. The exponential factors become

$$\frac{1+\beta}{2\Theta} = \frac{2A\Theta}{2\Theta} = A \tag{5.55}$$

and

$$\frac{1-\beta}{2\Theta} = \frac{2-2A\Theta}{2\Theta} = \frac{1}{\Theta} - A \tag{5.56}$$

The time-evolution function is then,

$$\begin{aligned} \phi(t) &= \frac{\beta-1}{2\beta}e^{-t/2\Theta}e^{At} + \frac{(\beta+1)}{2\beta}e^{-At} \\ &= \frac{2A\Theta}{1-2A\Theta}e^{-t/2\Theta}e^{At} + \frac{1}{2}\Big(1+\frac{1}{1-2A\Theta}\Big)e^{-At} \end{aligned} \tag{5.57}$$

Taking the small correlation time limit of the factors multiplying each exponential term,

$$\begin{aligned} \lim_{\Theta\to 0}\Big[\frac{2A\Theta}{1-2A\Theta}\Big] &= 0 \\ \lim_{\Theta\to 0}\Big[\frac{1}{2}\Big(1+\frac{1}{1-2A\Theta}\Big)\Big] &= 1 \end{aligned} \tag{5.58}$$

As $\Theta \to 0$, only the exponentially-decaying term in the magnetisation survives, $\phi(t) = e^{-At} \to m(t) = \frac{e^{-At}(Am_0-B)}{A} + \frac{B}{A}$, so the small correlation time limit of the spin evolution agrees with the non Markovian master equation.

Finally, we note that the solution for the magnetisation breaks down into two regimes. First, we note that the expression for β depends only on the product of the correlation time, Θ, and the rate A, and not on their specific individual values. We may then discuss the behaviour of the model in terms of only the ratio parameter $R = A\Theta = \Theta/A^{-1}$, which gives the ratio of the well correlation time to the escape time. Rewriting the expression for the spin vs time,

$$\begin{aligned} m(t) &= \frac{(Am_0-B)}{A}\Big((e^{-t/2\Theta}([e^{\beta t/2\Theta} - e^{-\beta t/2\Theta}]/2\beta \\ &+ [e^{-\beta t/2\Theta} + e^{\beta t/2\Theta}]/2)\Big) + \frac{B}{A} \end{aligned} \tag{5.59}$$

which may be simplified in terms of hyperbolic trigonometric functions,

$$\begin{aligned} m(t) &= \frac{(Am_0-B)}{A}\Big(e^{-t/2\Theta}(\frac{\sinh(\beta t/2\Theta)}{\beta} + \cosh(\beta t/2\Theta))\Big) + \frac{B}{A} \\ &= \frac{(Am_0-B)}{A}\Big(e^{-t/2\Theta}\Big[\frac{\sinh(\sqrt{1-4R}t/2\Theta)}{\sqrt{1-4R}}\Big] + \cosh(\sqrt{1-4R}t/2\Theta))\Big) + \frac{B}{A} \end{aligned} \tag{5.60}$$

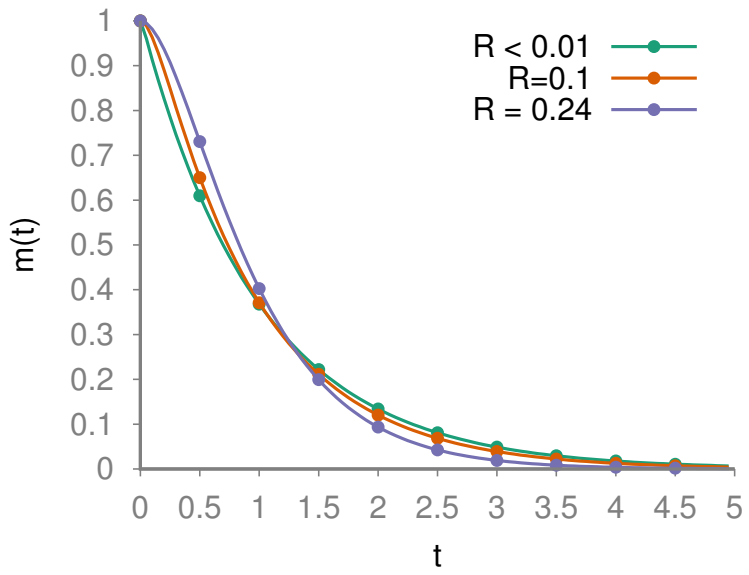

Figure 5.13: $n_1(t)$ vs t, for $R = 0.5, 1, 2$, under the initial condition $n_1 = 1$, with transition rates $\kappa_{12} = 1$, $\kappa_{21} = 0$. The population of particles in the individual wells may assume negative values at these correlation times.

For smaller $R < \frac{1}{4}$, we have a real value of $\beta = \sqrt{1 - 4R}$, and the time-dependence of the spin corresponds to Eq. 5.61. In Figure 5.13, we plot the time-evolution for values of $R < \frac{1}{4}$ with a correlation time of $\Theta = 1s$ and $m_0 = 1$. Once the correlation time is some sizable fraction of the escape time, the behaviour begins to depart from the simple exponential behaviour predicted in the Markovian system. At early times the magnetisation decays more slowly than the exponential decay and at later times it decays more quickly, while the timescale over which the decay occurs, A, remains the same. The overall effect of the increasing correlation time is to cause a slower decay at earlier times and decaying more rapidly at later times, an effect which corresponds in the shift of the decay process to lower frequencies.

In the case that $R > \frac{1}{4}$, we have an imaginary argument to sinh and cosh, we then have an expression for $m(t)$

$$m(t) = \frac{(Am_0 - B)}{A}\Big(e^{-t/2\Theta}\big(\frac{\sin(bt/2\Theta)}{b} + \cos(bt/2\Theta)\big)\Big) + \frac{B}{A} \tag{5.61}$$

where $b = \sqrt{4R - 1}$. We note that the solutions take the form of damped oscillations which tends toward the equilibrium value of the magnetisation. However, these solutions may cause the occupation in individual wells to become less than 0, as shown in Figure 5.14. It is not obvious whether or not the interpretation of the probability to find a particle

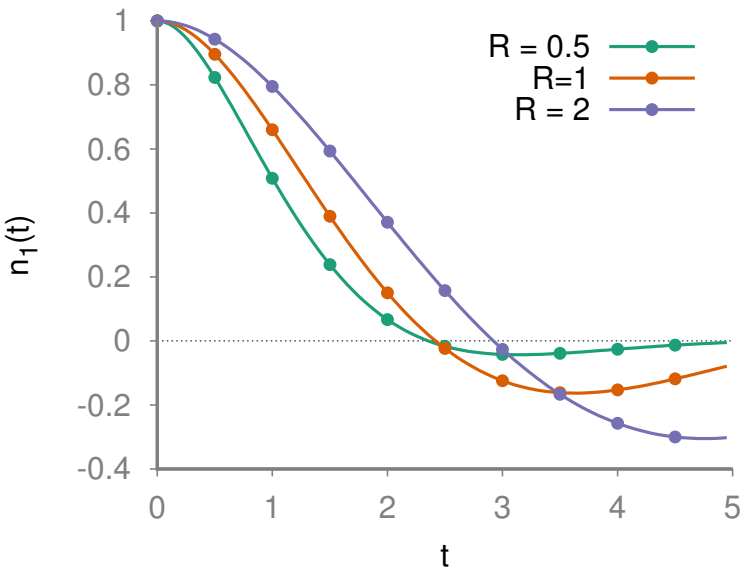

Figure 5.14: $n_1(t)$ vs t, for $R = 0.5, 1, 2$, under the initial condition $n_1 = 1$, with transition rates $\kappa_{12} = 1$, $\kappa_{21} = 0$. The population of particles in the individual wells may assume negative values at these correlation times.

in a well should be modified in order to interpret the generalised master equation for very high Θ, as the total magnetisation stays in the bounds $(-1, 1)$ for all values of Θ.

However, it may be that such solutions are unphysical, as for longer correlation times the generalised master equation will overestimate the population in each well and generate a time evolution which will continue to reduce the population of a well, even when that well is presently empty. We also note that it is not obvious what it would even mean for the correlation time of the well population to exceed or be on the order of the overall escape time, as this would imply that the timescale over which the spin population is correlated exceeds the overall escape time for the system, which is itself determined by changes in the individual well populations.

Regardless of the meaning of these solutions to the non-Markovian rate equation, we note that in the implementation of correlations in the Langevin equation via the lLMS, increasing correlation time is generally accompanied by an increase in the transition rate between the wells, as seen in the escape rate calculations, and so we expect that the value of the rate parameter is fixed to be quite low by this fact and $R < 1/4$ in general.

5.9 RELAXATION: LLMS SIMULATIONS

We may now compare the predictions of the generalised rate equation to numerical simulations of the LLMS. Any comparison between the two approaches is by nature qualitative, as the master equation approach assumes some fixed escape rate $A = 2f_0e^{-q}$ with a correlation time for the well population relative to this rate. In contrast, the LLMS approach results in changes in this escape rate for variations in the damping and correlation time. There is no way to incorporate the effect of damping into the master equation models, in contrast to the LLG and LLMS where damping is an important input parameter which effects the observed rates and other properties of the system.

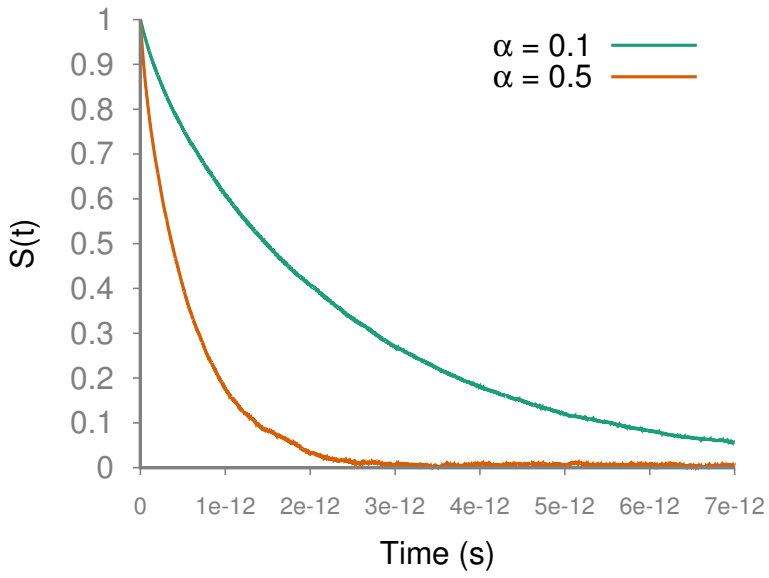

Figure 5.15: Total spin vs time for SmCo with reduced barrier height $\sigma = 1.5$, for different values of the damping, with correlation time $\tau < 0.01$ (LLG simulations).

Figure 5.15 depicts the spin vs time from the LLG with parameters chosen close to those of a SmCo nanoparticle, with a magnetic moment $\mu_s = 6.4\times10^{-18}$, anisotropy energy $k_u = 2.16 \times 10^{-16}$ and with different spin-bath couplings. The qualitative prediction of the discrete orientation model is reflected in the exponential profile of the spin's time-evolution, e^{-At} with the exact value of A varying with the damping. It is important that in general the profile of the spin relaxation may be different from exponential, even in the LLG, as the escape follows from the set of nonvanishing eigenvalues of the Fokker-Planck operator corresponding to the system. However, it is frequently sufficient to consider

only the inverse of the smallest nonvanishing eigenvalue. This is the case for the spin Hamiltonians and parameters used here, as we see the behaviour is dominated by the lowest eigenvalue and hence is exponential.

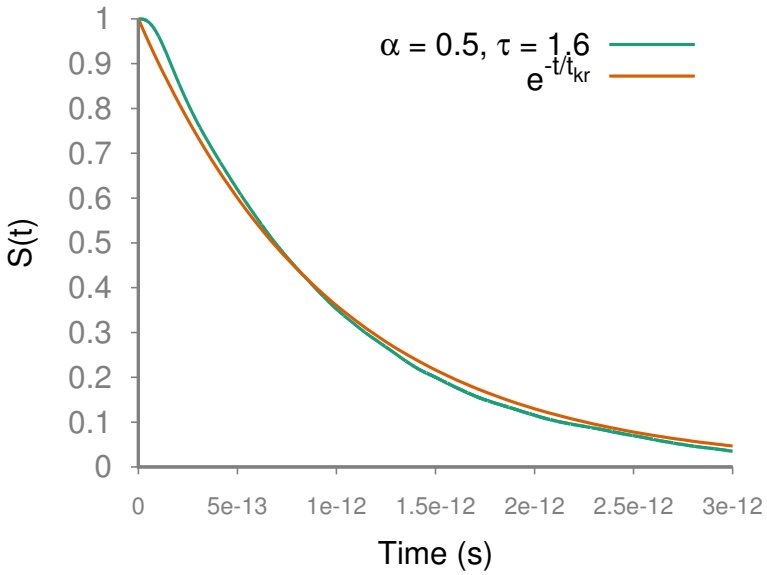

Figure 5.16: Biexponential behaviour in the LLMS for $\tau = 1.6$, $\sigma = 1.5$

As the correlation time increases and non-Markovian effects become more relevant, this increasing escape rate is accompanied by a departure from the simple exponential behaviour predicted by the master equation. Figure 5.16 depicts the time profile of the magnitude of the spin for correlation time $\tau = 1.6$ with a relatively low barrier height of $\sigma = 2$. The LLMS simulations have a similar profile to that predicted by the generalised master equation, with the distinctive biexponential behaviour causing the spin to decay more slowly at earlier times and faster at later times in comparison to a naive exponential using the Kramers escape time, $e^{-t/t_{kr}}$.

The qualitative agreement of both models implies that the correlation of the individual well population occurs on some similar timescale to the increased escape time. However, we stress that the master equation correlation time is distinct from the one that occurs in the LLMS, with one representing the timescale over which the well populations are correlated, while the LLMS correlation time reflects the frequency shift in the damping and thermal spectrum for the Langevin equation.

5.10 MEMORY KERNELS IN THE GENERALISED MASTER EQUATION

The memory kernels which occur in the generalised master equation are equivalent to assuming a specific form of the waiting time distribution for the hopping probability in the continuous-time-random-walks (CTRW) which underlie the original formulation of the problem. The waiting time distributions refer to the probability that a walker in a CTRW will still be at a given site after a certain duration of time has elapsed. If we think of the 2-well spin problem as a simple CTRW with 2 edges, then the assumption of a waiting time distribution is the same as assuming a form of the time-dependence of the total spin.

The relationship between the memory kernel used in the GME and the distribution takes the form

$$K^*(\omega) = \frac{\omega\psi^*(\omega)}{1-\psi^*(\omega)} \tag{5.62}$$

where the notation $f^*(\omega)$ denotes the Laplace transform of the time function $f(t)$, K is the memory kernel and ψ is the associated waiting time distribution.

5.10.1 Exponential Waiting Time

For an exponential waiting time and hence spin decay, $\psi(t) = e^{-At}$, we have $\psi^*(\omega) = \frac{A}{A+\omega}$. The resulting memory kernel is then

$$K^*(\omega) = \frac{\omega\frac{A}{A+\omega}}{1-\frac{A}{A+\omega}} = \frac{A\omega}{\omega} = A \tag{5.63}$$

Hence the Laplace transform of the memory kernel corresponding to exponential decay is a constant. The inverse Laplace transform, $K(t) = \mathcal{L}^{-1}[A](t) = 2A\delta(t)$. So we see that the assumption of exponential decay implies a δ-function memory kernel and hence an ordinary Markovian master equation.

5.10.2 Biexponential Waiting Time

A general waiting-time distribution of the form,

$$\psi(t) = 2a\frac{1}{\sqrt{\lambda^2-4a}}e^{-\lambda t/2}\sinh(\frac{1}{2}t\sqrt{\lambda^2-4a}) \tag{5.64}$$

under the condition that $\lambda^2 > 4a$ results in the memory kernel

$$K(t) = ae^{-\lambda t} \tag{5.65}$$

Hence the fact that the time profile of the magnetisation exhibits a biexponential form is not too surprising, since the use of an exponential kernel is equivalent to assuming that the waiting time distribution is the sum of two exponentials. The condition that $\lambda^2 > 4a$ results in the limitation on the rate variable $R < 1/4$, as the CTRW will begin to exhibit the type of unphysical behaviour that arises in the spin system from the argument to the hyperbolic function turning negative.

5.11 CONCLUSIONS

We have implemented the LLMS Langevin equation to model the escape problem in the context of superparamagnetic nanoparticle which are generally admissible for modelling as a single large magnetic moment. In the low correlation time limit, we find that the LLG and the LLMS predict the same damping dependence for the escape time, and that both models agree with the analytical prediction of the escape time from Kramer's theory.

In general, departure from white noise behaviour occurs when the bath correlation time exceeds the characteristic time of the system. For a bound superparamagnetic nanoparticle, we predict that the dynamical timescale of the system is set by the Larmor precession time, hence we anticipate stronger correlations in systems with higher magnetic anisotropy energy. We observe that the increase of the correlation time in the high and low damping limits persists in the correlated case, with increasing correlation time also generally increasing the escape time, while the difference in the physics of the escape problem at low and high damping predicting that the high damping escape converges on the LLG escape time with increasing barrier height, while for low damping the predicted escape rates differ.

Finally, at intermediate barrier height, $\sigma > 1$, we see that the LLMS predicts a characteristic biexponential time profile for the spin dependence, indicative of a generalized rate equation description of the well population dynamics.

Chapter 6

Conclusions & Further Work

6.1 NON-MARKOVIAN EFFECTS IN MAGNETIC SYSTEMS

In this work we have examined the effects of non-Markovian extensions to the models currently used to investigate the dynamics of magnetic moments. In particular, we relate our numerical investigations to the possible implications for superparamagnetic nanoparticles, and to the properties which could be seen to be indicative of the presence of coloured noise in such systems.

6.1.1 System Time & Coloured Noise

The LLMS Langevin equation provides the more fundamental incorporation of non-Markovian behaviour into the physics of magnetism, being a realisation of a generalized Langevin equation with the appropriate fluctuation-dissipation theorem for a magnetic system, and therefore should be applicable for any system of magnetic moments where it is the case that the system timescale and the bath timescale are not widely separated and that the system must be expected to equilibriate through the interaction with the bath. It is of wide potential applicability, having already been applied outside the context of superparamagnetism in the context of atomistc spin dynamics. [24]

In general for coloured noise effects, we expect that the noise departs from Markovian behaviour when the system and bath are on or near the same timescale. For the LLMS specifically, the system timescale is related to the magnitude of the magnetic fields in the Hamiltonian. The energy involved in these processes sets the timescale of the spins' precessional motion, and so the effects of coloured noise are inherently linked for any magnetic system to the Larmor precession frequency.

The fact that the coloured noise effects become evident as the system time increases implies that for any finite characteristic bath time, departure from the LLG will become inevitable for sufficiently high applied fields. The need to understand the physical regimes under which such departure will occur, and the precise differences in the physics predicted by the LLG and the LLMS motivates much of this work. In general, it is beneficial to understand the coloured noise regime as it is the more fundamental approach to the thermal interactions of magnetic moments than the LLG.

6.1.2 Superparamagnets & Magnetic Anisotropy

In the context of superparamagnetic particles which are confined by magnetic anisotropy energy to specific orientations due to the energy potential, we see that this timescale is generally dictated by the Larmor precession time about the anisotropy field. This allows us to predict that this relevant system timescale is set by the magnitude of the magnetic anisotropy energy of the particle. This is borne out by explicit numerical investigations using the LLMS, according to which both the qualitative properties in terms of the decay profile, and the quantitative escape rate begin to depart from the LLG predictions when the bath correlation time, $\tau_c \geq (\gamma H_K)^{-1}$ exceeds a significant fraction of the inverse of the Larmor precession time about the anisotropy field.

If we anticipate that the correlation time of the thermal bath for different nanoparticles are at least of the same order of magnitude, then it also implies that spins with large magnetic anisotropy energy will be more promising candidates for coloured noise effects.

6.2 COLOURED NOISE & THERMAL ESCAPE

In terms of the Kramers escape problem under the influence of coloured noise, the results of our simulations have some important implications. Firstly, we see that there appears to be a very similar structure to the damping-dependence for any fixed correlation time, wherein there exists both a low-damping and a high-damping regime, The escape time increases with the damping parameter, χ, in the limit of both decreasing and increasing damping, with the minimum occurring at similar values of the damping with increasing correlation time for similar values of the barrier height, applied field and angle between the applied field and easy-axis. Additionally, for a fixed damping we see that the escape time tends to increase with increasing correlation time.

An additional similarity between the coloured noise approach and the LLG is the

observation that as the temperature decreases the escape rate tends toward the familiar Arrhenius form. An interesting result with respect to the escape time is that, for a fixed α, we see that the escape rate for high damping seems to converge on the LLG solution as the inverse barrier parameter increases. This makes some sense intuitively, since we might anticipate that the Markovian and non-Markovian models should make similar predictions when the escape time becomes much larger than timescale over which the particle motion is correlated. In contrast, and perhaps surprisingly, for low damping the simulations predict there is a persistent difference in the escape rate even as the barrier height grows.

We stress that the precise implication of this is not readily apparent, as the LLG phenomenological parameter α is only meaningful in the context of the LLMS when we take the limit of vanishing correlation time, in which case the relationship $\alpha = \gamma\chi\tau_c$ guarantees correspondence between the two models. In the case that we have genuinely correlated bahaviour, $\gamma H_k \approx \tau_c$, we in fact have two parameters to quantify the nature of the spin-bath coupling, both of which effect the escape rate of the system. We cannot, in general, increase the correlation time and hold α fixed, since this will cause a corresponding decrease in the spin-bath coupling. It is for this reason that plotting the escape time as a function of the spin-bath coupling, χ, is the more natural way to investigate the damping properties of the coloured noise system.

Overall, we anticipate that this difference in the escape at high barriers for the low and high damping regimes is due to the difference in physics between the regimes, which we anticipate is still an energy-controlled diffusion at low damping, and a direct thermal escape at high damping. However, the physics of both regimes and their escape properties in the correlated coloured noise regime merits further investigation, using both numerical and analytical techniques.

6.3 GENERALISED MASTER EQUATION

The generalsed master equation provides an alternative means of incorporating non-Markovian effects into the physics of superparamagnetic particles. Under this approach the memory effect is reflected directly in correlation of the bath population over a characteristic timescale, Θ. It is important to note that the correlation time thus represented in the GME is quite distinct from the LLMS correlation time, where one is the correlation between well populations, and the other is the timescale of correlation between spin orientations.

As is the case in its Markovian equivalent, the discrete orientation model can only indirectly incorporate the effect of damping through the choice of interwell transition rates, and thus the predictions of the model will generally be of a qualitative nature.

6.3.1 Frequency-Dependent Diamagnetic Susceptibility

An important prediction of the GME model is the observation of a negative in-phase susceptibility for sufficiently high frequencies at any fixed nonzero correlation time. LLMS simulations make extremely qualitative predictions to the GME across a range of parameters. The observed transition from paramagnetic to diamagnetic behaviour occurs for similar values of the frequency, $\omega \approx \gamma H_k$ in both models, while the variation of the susceptibility with inverse barrier height is also extremely qualitatively similar and the profile of the susceptibility for increasing correlation time is broadly similar between both models. This qualitative similarly leads us to anticipate that a frequency-dependent transition to diamagnetic susceptibility could be an indication of the presence of coloured noise in magnetic systems.

6.3.2 Biexponential Decay

A second qualitative prediction of the GME approach is the biexponential time profile of the relaxation profile of the magnetisation for a superparamagnetic problem. On a physical basis, this is not necessarily indicative of coloured noise in the way that the diamagnetic susceptibility is, since from experimental observations a decay profile which differs from the simple exponential behaviour could be attributed to the detailed energy structure of the nanoparticles, whereby the spin relaxation is generally determined by the eigenvalues of the Fokker-Planck operator, which is generally dominated by the lowest eigenvalue and hence often results in a single exponential timescale for the decay, but could in general result from a nontrivial energy dependence through the Fokker-Planck operator.

However, as we find that the LLMS predicts biexponential behaviour where similar parameters in the LLG predict a decay which is largely dominated by the exponential term, is interesting since it does provide another possible indication for those systems which we would strongly anticipate to be dominated by a single decay time. It is also an additional qualitative similarity between the non-Markovian master equation and coloured noise approach.

When taken in the context of the negative susceptibility predicted by both models,

it suggests that an interesting future direction of work may be to ascertain whether the Fokker-Planck of the single spin is similar to the GME expression, at least for some range of parameters.

Abbreviations

AC Alternating Current

DC Direct Current

DFT Density Functional Theory

FMR Ferromagnetic Resonance

FPE Fokker-Planck Equation

GLE Generalised Langevin Equation

GME Generalised Master Equation

LLB Landau-Lifshitz-Bloch

LLG Landau-Lifshitz-Gilbert

LLMS Landau-Lifshitz-Miyazaki-Seki

OU Ornstein-Uhlenbeck

References

[1] Georgia C. Papaefthymiou. Nanoparticle magnetism. *Nano Today*, 4(5):438447, Oct 2009.

[2] Manuel Benz. Superparamagnetism : Theory and applications.

[3] Wahajuddin and Arora. Superparamagnetic iron oxide nanoparticles: magnetic nanoplatforms as drug carriers. *IJN*, page 3445, Jul 2012.

[4] M. Zeisberger D. Schler U. Heyen I. Hilger R. Hergt, R. Hiergeist and W. A. Kaiser. Magnetic properties of bacterial magnetosomes as potential diagnostic and therapeutic tools. *J. Magn. Magn. Mater.*, 2005.

[5] Ingrid Hilger, Rudolf Hergt, and Werner A. Kaiser. Towards breast cancer treatment by magnetic heating. *Journal of Magnetism and Magnetic Materials*, 293(1):314319, May 2005.

[6] Silvio Dutz, Joachim H. Clement, Dietmar Eberbeck, Thorsten Gelbrich, Rudolf Hergt, Robert Mller, Jana Wotschadlo, and Matthias Zeisberger. Ferrofluids of magnetic multicore nanoparticles for biomedical applications. *Journal of Magnetism and Magnetic Materials*, 321(10):15011504, May 2009.

[7] M. O. A. Ellis, R. F. L. Evans, T. A. Ostler, J. Barker, U. Atxitia, O. Chubykalo-Fesenko, and R. W. Chantrell. The landaulifshitz equation in atomistic models. *Low Temp. Phys.*, 41(9):705712, Sep 2015.

[8] Jr. Brown, William Fuller. *Micromagnetics*. New York: Wiley, 1963.

[9] R.C. Merton. Theory of rational option pricing. *The Bell Journal of Economics and Management Science*, 4:141–183, 1973.

[10] Daniel T. Gillespie. The chemical langevin equation. *J. Chem. Phys.*, 113(1):297, 2000.

[11] G. Kallianpur and Robert L. Wolpert. Weak convergence of stochastic neuronal models. *Stochastic Methods in Biology*, page 116145, 1987.

[12] H.A Dijkstra, L.M Frankcombe, and A.S von der Heydt. A stochastic dynamical systems view of the atlantic multidecadal oscillation. *Philosophical Transactions of the Royal Society A: Mathematical, Physical and Engineering Sciences*, 366(1875):25432558, Jul 2008.

[13] J. Daunizeau, K.J. Friston, and S.J. Kiebel. Variational Bayesian identification and prediction of stochastic nonlinear dynamic causal models. *Physica D: Nonlinear Phenomena*, 238(21):20892118, Nov 2009.

[14] Lawrence Murray and Amos J Storkey. Continuous time particle filtering for fmri. In J. C. Platt, D. Koller, Y. Singer, and S. T. Roweis, editors, *Advances in Neural Information Processing Systems 20*, pages 1049–1056. Curran Associates, Inc., 2008.

[15] Don S. Lemons. Paul langevins 1908 paper on the theory of brownian motion [sur la theorie du mouvement brownien, c. r. acad. sci. (paris) 146, 530533 (1908)]. *American Journal of Physics*, 65(11):1079, 1997.

[16] J. L. Doob. The brownian movement and stochastic equations. *The Annals of Mathematics*, 43(2):351, Apr 1942.

[17] Daniel T. Gillespie. Exact numerical simulation of the ornstein-uhlenbeck process and its integral. *Phys. Rev. E*, 54(2):20842091, Aug 1996.

[18] Daniel Campos and Vicenc Mendez. Two-point approximation to the kramers problem with coloured noise. *J. Chem. Phys.*, 136(7):074506, 2012.

[19] B U Felderhof. On the derivation of the fluctuation-dissipation theorem. *Journal of Physics A: Mathematical and General*, 11(5):921927, May 1978.

[20] A Crisanti and F Ritort. Violation of the fluctuationdissipation theorem in glassy systems: basic notions and the numerical evidence. *Journal of Physics A: Mathematical and General*, 36(21):R181R290, May 2003.

[21] E. Beaurepaire, J.-C. Merle, A. Daunois, and J.-Y. Bigot. Ultrafast spin dynamics in ferromagnetic nickel. *Physical Review Letters*, 76(22):42504253, May 1996.

[22] I. Radu, K. Vahaplar, C. Stamm, T. Kachel, N. Pontius, H. A. Drr, T. A. Ostler, J. Barker, R. F. L. Evans, R. W. Chantrell, and et al. Transient ferromagnetic-like state mediating ultrafast reversal of antiferromagnetically coupled spins. *Nature*, 472(7342):205208, Mar 2011.

[23] T.A. Ostler, J. Barker, R.F.L. Evans, R.W. Chantrell, U. Atxitia, O. Chubykalo-Fesenko, S. El Moussaoui, L. Le Guyader, E. Mengotti, L.J. Heyderman, and et al. Ultrafast heating as a sufficient stimulus for magnetization reversal in a ferrimagnet. *Nat Comms*, 3:666, Feb 2012.

[24] U. Atxitia, O. Chubykalo-Fesenko, R. W. Chantrell, U. Nowak, and A. Rebei. Ultrafast spin dynamics: The effect of colored noise. *Physical Review Letters*, 102(5), Feb 2009.

[25] Ioannis Karatzas and Steven Shreve. *Brownian motion and Stochastic Calculu.* Springer, New York, 1998.

[26] J. L. Garcia-Palacios. Introduction to the theory of stochastic processes and brownian motion problems.

[27] Scott Hottovy. The fokker-planck equation.

[28] van Kampen. *Stochastic Processes in Physics and Chemistry.* Elsevier Science B. V., 1992.

[29] Zinn-Justin. *Quantum Field Theory and Critical Phenomena.* Oxford University Press, 1997.

[30] Hannes Risken. The Fokker-Planck equation. *Springer Series in Synergetics*, 1989.

[31] Bernt K ksendal. *Stochastic Differential Equations: An Introduction with Applications.* Springer, Berlin, 0003.

[32] The euler-heun method.

[33] Endre Sli and David Mayers. *An Introduction to Numerical Analysis.* Cambridge University Press, 0003.

[34] P. Hänggi and P. Jung. Colored noise in dynamical systems. *Adv. Chem. Phys.*, 89:239, 1995.

[35] Ming Chen Wang and G. E. Uhlenbeck. On the theory of the brownian motion ii. *Rev. Mod. Phys.*, 17(2-3):323342, Apr 1945.

[36] Robert Zwanzig. *Nonequilibrium Statistical Mechanics*. Oxford University Press.

[37] L. Chotorlishvili, Z. Toklikishvili, V. K. Dugaev, J. Barna, S. Trimper, and J. Berakdar. Fokker-Planck approach to the theory of the magnon-driven spin seebeck effect. *Physical Review B*, 88(14), Oct 2013.

[38] L. Stella, C. D. Lorenz, and L. Kantorovich. Generalized langevin equation: An efficient approach to nonequilibrium molecular dynamics of open systems. *Physical Review B*, 89(13), Apr 2014.

[39] Eric Lutz. Fractional langevin equation. *Phys. Rev. E*, 64(5), Oct 2001.

[40] Ryogo Kubo. Statistical-mechanical theory of irreversible processes. i. general theory and simple applications to magnetic and conduction problems. *Journal of the Physical Society of Japan*, 12(6):570586, Jun 1957.

[41] E. C. Stoner and E. P. Wohlfarth. A mechanism of magnetic hysteresis in heterogeneous alloys. *Philos. Trans. R. Soc. London, Ser. A*, 240:599, 1948.

[42] B.D.Cullity. *Introduction to Magnetic Materials*. AddisonWesley Publishing Co, 1973.

[43] P. Bean and J.D. Livingstone. Superparamagnetism. *, J. Appl. Phys.*, 30:120, 1959.

[44] M. Knobel., W. C. Nunes., L. M. Socolovsky, E. De Biasi, J. M. Vargas, and J. C. Denardin. Superparamagnetism and other magnetic features in granular materials: A review on ideal and real systems. *J. Nanosci. Nanotechnol.*, 8(6), 2008.

[45] S. K. Jones Q. A. Pankhurst, J. Connolly and J-Dobson. Applications of magnetic nanoparticles in biomedicine. *J. Phys. D: Appl. Phys.*, pages R167–R181, 2003.

[46] L. Landau and Lifshitz E.M. On the theory of the dispersion of magnetic permeability in ferromagnetic bodies. *Phys. Z. Soviet Union*, 8(153), 1935.

[47] L. Landau and Lifshitz E.M. Reprint. On the theory of the dispersion of magnetic permeability in ferromagnetic bodies. *Ukr. J. Phys.*, 53(14), 2008.

[48] William T. Coffey, Yuri P. Kalmykov, and Serguey V. Titov. Magnetization reversal time of magnetic nanoparticles at very low damping. *Physical Review B*, 89(5), Feb 2014.

[49] M.A. Wongsam and R.W. Chantrell. The equations of motion of micromagnetics in hamiltonian form. *Journal of Magnetism and Magnetic Materials*, 152:234–242, 1995.

[50] T Bose and S. trimer. Lagrangian approach and dissipative magnetic systems. *Physics Letters A*, 375:2452–2455, 2011.

[51] E Minguzzi. Rayleighs dissipation function at work. *European Journal of Physics*, 36(3):035014, 2015.

[52] Gilbert T. A. Phenomenological theory of damping in ferromagnetic materials. *IEEE Trans. Magn.*, 40:3443, 2004.

[53] T. A Gilbert. Lagrangian formulation of the gyromagnetic equation of the magnetic field. *Phys. Rev.*, 100:1243, 1955.

[54] M. LAKSHMANAN. The fascinating world of the landaulifshitzgilbert equation: an overview. *Phil. Trans. R. Soc. A*, 369:1280–300, 2011.

[55] S.IIDA. The difference between gilbert's and landau-lifshitz's equations. *J. Phys, Chem. Solids.*, 24:625, 1962.

[56] J.C. Mallinson. On damped gyromagnetic precession. *IEEE Transactions on Magnetics*, 23:2003, 1987.

[57] W.T Brown.. Thermal fluctuations of a single-domain particle. *Phys. Rev.*, 130:1677, 1963.

[58] W.T Brown.. Thermal fluctuation of fine ferromagnetic particles. *IEEE Transactions on Magnetics*, 15(5):1196–1208, 2003.

[59] Camille Aron, DanielG Barci, LeticiaF Cugliandolo, ZochilGonzlez Arenas, and GustavoS Lozano. Magnetization dynamics: path-integral formalism for the stochastic landaulifshitzgilbert equation. *Journal of Statistical Mechanics: Theory and Experiment*, 2014(9):P09008, 2014.

[60] Kunimasa Miyazaki and Kazuhiko Seki. Brownian motion of spins revisited. *J. Chem. Phys.*, 108(17):7052, 1998.

[61] Robert Zwanzig. Memory effects in irreversible thermodynamics. *Physical Review*, 124(4):983992, Nov 1961.

[62] K Kawasaki. Simple derivations of generalized linear and nonlinear langevin equations. *Journal of Physics A: Mathematical, Nuclear and General*, 6(9):12891295, Sep 1973.

[63] J L Garca-Palacios, J B Gong, and F Luis. Equilibrium susceptibilities of superparamagnets: longitudinal and transverse, quantum and classical. *Journal of Physics: Condensed Matter*, 21(45):456006, 2009.

[64] M. Baanda. AC susceptibility studies of phase transitions and magnetic relaxation: Conventional, molecular and low-dimensional magnets. *Acta Physica Polonica A*, 124(6):964976, Dec 2013.

[65] U MARCONI, A PUGLISI, L RONDONI, and A VULPIANI. Fluctuationdissipation: Response theory in statistical physics. *Physics Reports*, 461(4-6):111195, Jun 2008.

[66] W. Coffey, Y.P. Kalmykov, and J.T. Waldron. *The Langevin Equation: With Applications to Stochastic Problems in Physics, Chemistry, and Electrical Engineering.* EBL-Schweitzer. World Scientific, 2004.

[67] Masatsugu Sei Suzuki and Itsuko S. Suzuki. Lecture note on solid state physics ac magnetic susceptibility.

[68] H.B.G. Casimir and F.K. du Pr. Note on the thermodynamic interpretation of paramagnetic relaxation phenomena. *Physica*, 5(6):507511, Jun 1938.

[69] J. L. Garca-Palacios. On the statics and dynamics of magnetoanisotropic nanoparticles. *Advances in Chemical Physics*, page 1210.

[70] W. T. Coffey and Y. P. Kalmykov. Thermal fluctuations of magnetic nanoparticles: Fifty years after brown. *J. Appl. Phys.*, 112:121301, 2012.

[71] I. Klik and C. R. Chang. Thermal relaxation in arrays of coupled ferromagnetic particles. *Phys. Rev. B*, 52:3540–3545, 1995.

[72] P. Svedlindh, T. Jonsson, and J.L. Garca-Palacios. Intra-potential-well contribution to the AC susceptibility of a noninteracting nano-sized magnetic particle system. *Journal of Magnetism and Magnetic Materials*, 169(3):323334, May 1997.

[73] D. V. Berkov and N. L. Gorn. Susceptibility of the disordered system of fine magnetic particles: a langevin-dynamics study. *J. Phys. :Condensed Matter*, 13:9369–9382, 2001.

[74] D. A. Garanin, V. V. Ishchenko, and L. V. Panina. Dynamics of an ensemble of single-domain magnetic particles. *Theor Math Phys*, 82(2):169179, Feb 1990.

[75] I. Klik and Y. D. Yao. Magnetization reversal by a field pulse. *J. Magn, Magn. Mat.*, 186:233–238, 1998.

[76] C. R. Chang I. Klik and H. L. Huang. Field-dependent prefactor of the thermal relaxation rate in single-domain magnetic particles. *Phys. Rev. B*, 48:15823, 1993.

[77] Sergio Sierra-Bermdez, Lorena P. Maldonado-Camargo, Franois Orange, Maxime J.-F. Guinel, and Carlos Rinaldi. Assessing magnetic nanoparticle aggregation in polymer melts by dynamic magnetic susceptibility measurements. *Journal of Magnetism and Magnetic Materials*, 378:6472, Mar 2015.

[78] X. Yan I. Klik, Y. D. Yao and C. R. Chang. Magnetic viscosity effect in ac susceptibility measurements. *Phys. Rev. B*, 57:92–95, 1998.

[79] José Luis García-Palacios and Francisco J. Lázaro. Langevin-dynamics study of the dynamical properties of small magnetic particles. *Phys. Rev. B*, 58(22):14937–14958, dec 1998.

[80] R. Kiihne and P. Reineker. Nakajima-zwanzig's generalized master equation: Evaluation of the kernel of the integro-differential equation. *Z. Physik B*, 31:105–110, 1978.

[81] M. M. Kosek-Dygas, B. J. Matkowsky, and Z. Schuss. Colored noise in dynamical systems. *SIAM Journal on Applied Mathematics*, 48(2):425441, Apr 1988.

[82] Jong-Soo Rhyee, J. B. Peng, C. T. Lin, and S. M. Lee. Anisotropic magnetization and dynamic susceptibility sign change in single-crystal na 0.85 Coo 2. *Physical Review B*, 77(20), May 2008.

[83] V. G. Veselago. The electrodynamics of substances with simultaneously negative values of ϵ and μ. *Soviet Physics Uspekhi*, 10:509–514, 1968.

[84] R. Hergt, S. Dutz, R. Müller, and M. Zeisberger. *J. Magn. Magn. Mat.*, 18:S2919–S2934, 2008.

[85] M. M. Klosek-Dygas, B. J. Matkowsky, and Z. Schuss. Colored noise in activated rate processes. *Journal of Statistical Physics*, 54(5-6):13091320, Mar 1989.

[86] Wenjie Chen, Shufeng Zhang, and H. Neal Bertram. Energy barriers for thermal reversal of interacting single domain particles. *Journal of Applied Physics*, 71(11):5579, 1992.

[87] P.E Jönsson, J.L Garcıa-Palacios, M.F Hansen, and P Nordblad. Relaxation in interacting nanoparticle systems. *Journal of Molecular Liquids*, 114(1-3):131135, September 2004.

[88] U. Atxitia. *Modeling of ultrafast laser-induced magnetization dynamics within the Landau-Lifshitz-Bloch approach.* PhD thesis, Universidad Autnoma de Madrid, 2012.

[89] Peter Hängg, Peter Talkner, and Michal Borkovec. Reaction-rate theory: fifty years after kramers. *Rev. Mod. Phys.*, 62(2):251341, Apr 1990.

[90] U. Nowak. Thermally activated reversal in magnetic nanostructures. In *Annual Reviews of Computational Physics IX*. World Scientific, 2001.

[91] Yuri P. Kalmykov, William T. Coffey, Unai Atxitia, Oksana Chubykalo-Fesenko, Pierre-Michel Djardin, and Roy W. Chantrell. Damping dependence of the reversal time of the magnetization of single-domain ferromagnetic particles for the nel-brown model: Langevin dynamics simulations versus analytic results. *Physical Review B*, 82(2), Jul 2010.

[92] P.M. Dejardin, D.S.F. Crothers, W.T. Coffey, and D.J McCarthy. Interpolation formula between very low and intermediate-to-high damping kramers escape rates for single-domain ferromagnetic particles. *Phys. Rev. E.*, 63:021102, 2001.

[93] Yuri P. Kalmykov, William T. Coffey, Unai Atxitia, Oksana Chubykalo-Fesenko, Pierre-Michel Djardin, and Roy W. Chantrell. Damping dependence of the reversal time of the magnetization of single-domain ferromagnetic particles for the nel-brown model: Langevin dynamics simulations versus analytic results. *Physical Review B*, 82(2), Jul 2010.

[94] I. M. Sokolov. Thermodynamics and fractional Fokker-Planck equations. *Phys. Rev. E*, 63(5), Apr 2001.